UNIVERSITY OF SOUTHAMPTON

FACULTY OF NATURAL AND ENVIRONMENTAL SCIENCES

Ocean and Earth Sciences

The effect of ocean acidification on the organic complexation of iron and copper

by

Lizeth Avendaño Ceceña

Thesis for the degree of Doctor of Philosophy

December 2014

UNIVERSITY OF SOUTHAMPTON

ABSTRACT

FACULTY OF NATURAL AND ENVIRONMENTAL SCIENCES

Ocean and Earth Sciences

Thesis for the degree of Doctor of Philosophy

THE EFFECT OF OCEAN ACIDIFICATION ON THE ORGANIC COMPLEXATION OF IRON AND COPPER

by Lizeth Avendaño Ceceña

Trace metal biogeochemistry is projected to be affected by ocean acidification. The understanding of the effects is of particular interest, as trace metals such as Fe and Cu are known for their significant biological roles. Dissolved Fe and Cu in seawater occur predominantly in the form of metal organic complexes. This thesis has investigated the influence that ocean acidification may have on the chemical forms (speciation) of dissolved Fe and Cu in seawater, focusing on their organic complexation, in order to provide a first insight into the possible future changes in their cycling and bioavailability. Competitive Ligand Exchange Adsorptive Cathodic Stripping Voltammetry (CLE-ACSV) was used as an analytical technique throughout this PhD work to determine Fe and Cu organic binding ligand characteristics. Organic Fe complexation was determined at current seawater pH in the high latitude North Atlantic (HLNA), which is an area of climate interest due to the importance of iron limitation on phytoplankton productivity and hence the carbon cycle. Main findings indicate that iron biogeochemistry in surface and subsurface waters of the HLNA is controlled by a combination of phytoplankton iron uptake and microbial iron binding ligand production, whilst in deep waters ligand saturation was evident, suggesting that additional Fe would be removed by scavenging or precipitation. The effect of ocean acidification on organic complexation of Fe and Cu was determined in the northwest European shelf seas, during the first UK Ocean Acidification consortium programme research cruise. Results suggested that a decrease in surface ocean pH will potentially result in a reduction of the free and inorganic metal fraction (Fe'), and also in an increase in the organically complexed iron fraction. Direct impacts on Fe bioavailability, however, are difficult to quantify, as the overall iron solubility, and hence its bioavailability, is controlled by the interrelationship between inorganic solubility, organic complexation, redox chemistry, and phytoplankton-trace metal feedback mechanisms. No significant effects were observed of a decrease in pH on the organically complexed Cu (II) fraction, or on the overall free and inorganically bound fraction (Cu'). Consequently, it is not clear so far whether Cu ligand production will be affected by ocean acidification, or the possible effects on its toxicity. In addition, surface water trace metal distribution in the northwest European shelf seas was assessed. Dissolved metal concentrations of Cd, Cu, Fe, Ni and Zn appeared to be significantly influenced by riverine inputs in the study area; whereas surface seawater pH was not evident as a controlling factor. The diversity of the chemical and biological processes controlling Fe and Cu biogeochemistry, and the way in which they will be altered by ocean acidification, is likely to be complex.

List of contents

List of tables

List of figures

Declaration of authorship

I, Lizeth Avendaño Ceceña declare that the thesis entitled "The effect of ocean acidification on the organic complexation of iron and copper" and the work presented in it are my own and have been generated by me as the result of my own original research. I confirm that:

- this work was done wholly while in candidature for a research degree at this University;
- where any part of this thesis has previously been submitted for a degree or any other qualification at this University or any other institution, this has been clearly stated;
- where I have consulted the published work of others, this is always clearly attributed;
- where I have quoted from the work of others, the source is always given. With the exception of such quotations, this thesis is entirely my own work;
- I have acknowledged all main sources of help;
- where the thesis is based on work done by myself jointly with others, I have made clear exactly what was done by others and what I have contributed myself;
- this work has not been wholly or partly published.

Signed:.....

Date:.....

Acknowledgements

A special gratitude to the National Council for Science and Technology in Mexico (CONACYT), for wholly funding this PhD work. I am also grateful to the NERC funded UK Ocean Acidification D366 research cruise, for giving me the opportunity to participate as part of the scientific crew.

I am very grateful to my supervisors, P. Eric Achterberg, and Dr Martha Gledhill, for their guidance and support. Thank you both for sharing your knowledge and for helping me develop my research skills. I am especially grateful to Dr Martha Gledhill, for going far beyond a supervisor's duties. Martha, your constant encouragement and guidance were the propeller that kept me on the move. I am also grateful to my panel chair, Doug Connelly, for his advice and support throughout this whole process.

I am grateful to all the people in the Ocean and Earth Science Graduate School and the National Oceanography Centre, Southampton, whom in one way or another helped me with this work. My laboratory work and data analysis would not have been produced with the help and advice of several people. A special mention to Dr Khairul N. Mohamed, for his guidance and help with the CLE-ACSV analyses; to Dr Sebastian Steigenberger, for providing me with the dissolved metal data of the HLNA region, and to Christian Schloesser, for his guidance and help with the analysis of the dissolved metal data in the northwest European shelf seas. I am also very grateful to Dr Micha Rijkenberg, for his guidance and for providing me with the R progamming code for the calculation of the metal ligand characteristics throughout this PhD work.

My warmest thanks to all my family. I thank my parents, my brother and sister, for always being at my side, encouraging and supporting my projects. To Pete, for being the most caring and supporting partner throughout the whole writing process of this thesis. To Paulina, for being my faithful witness throughout this whole enterprise. Thank you for motivating my efforts and guide my sailing.

Finally, special thanks also to all the people that helped me with babysitting Paulina while in this path; I could have not done it without your precious help.

Definitions and Abbreviations

CLE-ACSV	Competitive Ligand Equilibration – Adsorptive Cathodic Stripping Voltammetry
CTD	Conductivity, temperature, depth
Chl	Chlorophyll
DOC	Dissolved organic carbon
DIC	Dissolved inorganic carbon
DSOW	Denmark Strait Overflow Water
EPS	Exopolysaccharides
EZSEM	Effective Zero Salinity End Member
FEP bottle	Fluorinated ethylene propylene bottle
HLNA	High Latitude North Atlantic
HNLC	High Nutrient Low Chlorophyll
HS	Humic substances
HR-ICPMS	High Resolution - Inductively coupled plasma mass spectrometry
ID-ICPMS	Isotope Dilution - Inductively coupled plasma mass spectrometry
IPCC	Intergovernmental Panel on Climate Change
ISOW	Iceland-Scotland Overflow Water
ISW	Irminger Sea Water
kDa	Dalton
LDPE/HDPE	Low/high density polyethylene bottle
LSW_e	Labrador Sea Water in the Iceland Basin
LSW_w	Labrador Sea Water in the Irminger Basin
Milli-Q	Ultrapure water
NOCS	National Oceanographic Centre, Southampton
NEAW	Northeast Atlantic Water
NAC	North Atlantic Current
NACW	North Atlantic Central Water
NEADW	Northeast Atlantic Deep Water

OES	Optical emission spectroscopy
OTE bottle	Ocean Test Equipment bottle
ODV	Ocean Data View
ppm	Parts per million
RRS	Royal Research Ship
TA	Total Alkalinity
UpA	Ultrapure acid

CHEMICAL TERMINOLOGY/FORMULAS

AgCl	Silver chloride
AL	Added ligand
α'	Side reaction coefficient for inorganic complexation and complexation by added ligand
$\alpha_{Me'}$	Side reaction coefficient for inorganic complexation of Me^{n+}
$\alpha_{Me(AL)x}$	Side reaction coefficient for complexation of a metal by an added ligand
$\beta'_{Fe(TAC)2}$	Conditional stability constant for the formation of $Fe(TAC)_2$
β_i	Conditional stability for ligand addition
C_L	Total organic ligand concentration
C_{Fe}	Total iron concentration
(C_{TAC})	Total concentration of TAC
$[C_i]$	Total ion concentration
(C_i)	Free ion activity
CO_2	Carbon dioxide
CO_3^{2-}	Carbonate ion
Cu^{2+}	Cupric ion
eL_i	Excess ligand
Fe^{3+}	Ferric ion
Fe'	Inorganic iron
FeL	(Organic) iron ligand complex
$Fe(TAC)_2$	Iron complexed by TAC

Fe_{labile}	Labile iron
Fe(II), Fe(III)	Ferrous, ferric ion
$FeCO_3$	Carbonate iron species
$Fe(OH)_3$	Hydroxide iron species
$Fe(OH)_2^+$	Hydrolysis iron species
HCl	Hydrochloric acid
HL	Protonated ligand
HNO_3	Nitric acid
HMDE	Hanging mercury drop electrode
i_p	Current
KCl	Potassium chloride
K'_{FeL}	Conditional stability constant for the formation of the FeL complex
L_1	Strongest Fe organic ligand class
L_2	Weakest Fe organic ligand class
$[L,_{Fe}]$	Organic Fe (III) binding ligand concentration
$[L,_{Cu}]$	Organic Cu (II) binding ligand concentration
M-AL	Metal-added ligand complex
M^{n+}	Divalent/trivalent metal
ML_i	Metal ligand compound
N_2	Nitrogen gas
NO_3^-/NO_2^-	Nitrate/nitrite ion
PO_4^{-3}	Phosphate ion
S	Sensitivity
SiO_4^{-4}, SiO_3^{-2}	Silicate ion
SO_4^{-2}	Sulphate ion
TAC	Thiazolylazo-p-cresol
y_i	Total activity coefficient
SA, H_2SA	Salicylaldoxime
NN, HNN	1-nitroso-2-naphthol
eL_i	excess ligand

Chapter 1: Introduction

1.1 General

Ocean acidification has been generally tagged as "the other CO_2 problem" (Henderson, 2006; Doney *et al*., 2009), as it is the additional concern to that of CO_2 induced climate change, and has only been recognised in the past decade. Despite being the apparent "secondary problem", the threat it poses to the marine environment is of a considerable significance. The chemical processes involved when atmospheric CO_2 is absorbed by the ocean and dissolves in seawater, are very well established. However, much less is known about the potential impacts of ocean acidification on the biological and chemical processes in the oceans. Trace metals form an important chemical component of the life cycle in the world's oceans, and their cycling is predicted to be affected by ocean acidification. The scientific community's understanding on the specific effects of ocean acidification on the chemical speciation of trace metals, especially on organic metal interactions, is poor. The understanding of these effects are of special concern, as trace metals such as iron and copper are known for their significant biological roles. This work attempts to provide an insight into the effects of ocean acidification on iron and copper speciation, focusing on their organic metal interactions.

1.2 Justification

The increase in the uptake of anthropogenic CO_2 by the world's oceans and the consequent decrease in surface ocean pH predicted for the end of this century represents a change in sea surface chemistry that has not been experienced over at least the past 420,000 years. The rate of this change is at least 100 times faster than the experienced over this period of time. This considerable rate of change will inevitably affect marine organisms. The base of the marine food chain consists of photosynthetic organisms, which play a major ecological role as they are responsible for >99% of the ocean's primary productivity; their products are used by heterotrophic organisms. Most of the organic matter produced by primary producers is consumed by other microorganisms, establishing the base of the marine food webs. Marine primary productivity accounts for almost half of the earth's primary production. The vast majority of

primary producers occur in the surface oceans as free-floating microscopic phytoplankton. Recent research suggests that ocean acidification will have important but minor effects on the rate of photosynthesis, cell composition or growth of phytoplankton, with most significant effects related to resource allocation. Nevertheless significant impacts have been predicted for phytoplankton iron uptake rates as a result of changes in iron availability, as a result of changes in the ocean's carbonate system.

The main concerns about changes in metal speciation is that a decrease in surface ocean pH could increase the proportion of the free dissolved forms of toxic metals (as is projected in the case of Cu (II)), and that essential trace metals could feature a decrease in their bioavailable forms (as is projected in the case of Fe (III)).

The impact of pH induced seawater changes on trace metal speciation in the ocean is difficult to determine. The role of trace metals in ocean biogeochemistry along with metal bioavailability are topics of continuous research. However, changes in metal speciation, especially involving their organic complexation, represents a challenge for the scientific community due to the complexity of the controlling processes and the analytical challenges that the current metal speciation methods represent.

1.3 Objectives and structure

The overall aim of this PhD research is to assess the effect of ocean acidification on the speciation of iron and copper, focusing on their organic complexation. To achieve this goal, the dissertation approaches the topic in terms of organic ligand characteristics for both metals. Thus, the assessment of the influence of ocean acidification on the organic complexation of these metals has the following objectives: (i) analyze the trends in organic iron ligand concentrations throughout the water column, at the current seawater pH; (ii) analyze the effect of a decrease in pH on the iron and copper speciation; (iii) analyze the horizontal distribution of several dissolved trace metals, including iron and copper, in order to determine the main processes influencing their sources and spatial variabilities, focusing on the influence of pH and salinity. From a broad perspective, this thesis seeks to raise awareness on the potential impacts of ocean acidification on the bioavailability of trace metals.

This thesis is organized in 6 chapters. Chapter 2 gives an insight into the current knowledge of the potential biological and chemical effects of ocean acidification. Chapter 3 comprises a description of the organic ligand characteristics for iron at the current seawater pH in an understudied region of the ocean, the high latitude North Atlantic, in the Iceland and Irminger Basins and the vicinity of Greenland. The results presented in chapter 3 were obtained during the RRS Discovery cruise D354 in summer 2010, and they lead to the conclusion that uncomplexed Fe ligand concentrations in surface and subsurface waters in the study area are controlled by a combination of phytoplankton iron uptake and microbial ligand production. The analysis of iron ligand characteristics also shows that iron is likely to be removed by precipitation and scavenging in deep waters of the high latitude North Atlantic. Chapter 4 assesses the effects of ocean acidification on iron and copper speciation. This chapter's results suggests that a decrease in surface ocean pH will potentially result in a reduction of the free and inorganic metal fraction (Fe'), and also in an increase in the organically complexed iron fraction. Conditional stability constants for the organic iron complexes also appear to increase with a decrease in pH. In the case of copper, this study did not find changes in the overall free and inorganically complexed form (Cu'). Furthermore, chapter 5 assesses the distribution of total dissolved metals on surface waters of the northwest European shelf, as part of the results obtained during cruise Discovery 366 – the first of the UK Ocean Acidification consortium, which took part during the summer of 2011, and during which the iron and copper ligand characteristics at different pH levels were obtained (Chapter 4). During this study, trace metal distributions seemed to be strongly influenced by riverine inputs. The highest metal concentrations were observed off the east coast of Ireland, in the Irish Sea, and also in the southern North Sea, where the Dover Strait is one of the main inputs of trace metals, along with significant riverine inputs. Conclusions and future work are included as a synthesis in chapter 6.

Chapter 2: The rise in atmospheric CO_2 concentrations and its effects on surface ocean pH

The present chapter provides an introduction to the currently supported research field of ocean acidification. This chapter also provides an insight into the potential effects of ocean acidification on iron and copper speciation and their bioavailability, in agreement with the principles of thermodynamic equilibrium theory.

2.1 Introduction

Atmospheric CO_2 concentrations have oscillated between 200 and 280 parts per million (ppm) over the 400,000 years before the Industrial Revolution. Today, CO_2 concentrations have reached 400 ppm as a consequence of human activities (Feely *et al.*, 2004) (Figure 2.1). This means that CO_2 concentrations are now about 30% higher than they were a few hundred years ago, and they are projected to increase up to 800 ppm by the end of this century (Houghton, 2001; Doney, 2006). Since the beginning of the Industrial Revolution, about 40-50% of the CO_2 released by burning of fossil fuels and land use changes has remained in the atmosphere. About 30% has been taken up by the oceans and 20% by terrestrial biosphere (Sabine *et al.*, 2004; Doney, 2006). The rise in atmospheric CO_2 concentrations over the past two hundred years has led to an enhanced CO_2 uptake by the oceans (Feely *et al.*, 2004) causing significant changes in ocean carbonate chemistry (Wolf-Gladrow *et al.*, 1999).

When CO_2 dissolves in seawater it lowers the pH, making the ocean more acidic (Caldeira and Wickett, 2003). This phenomena has been termed as “ocean acidification” by the scientific community (Orr *et al.*, 2005a; Orr *et al.*, 2005b; Doney, 2006; Doney *et al.*, 2009; Feely *et al.*, 2009; Millero *et al.*, 2009; Shi *et al.*, 2010). It also changes the balance of the carbonate species (Doney, 2006), leading to a decrease in the carbonate ion concentration and to an increase in the bicarbonate and aqueous CO_2 concentrations (Zeebe and Wolf-Gladrow, 2001; Orr *et al.*, 2005a).

The rise in atmospheric CO_2

The capacity of the ocean's carbonate buffer to restrict pH changes diminishes proportionally to the amount of CO_2 absorbed by the oceans (Royal Society, 2005).

The absorption of CO_2 from human activities has already caused the pH of today's surface ocean to be about 0.1 units lower than preindustrial values (Caldeira and Wickett, 2003)(Figure 2.1).

If CO_2 absorption continues according to current trends, a decrease in pH of about 0.3-0.5 units by the year 2100 in the surface oceans is projected, which corresponds to a three-fold increase in the concentration of hydrogen ions from pre-industrial times (Brewer, 1997; Zeebe and Wolf-Gladrow, 2001; Feely *et al.*, 2004; Orr *et al.*, 2005a; Orr *et al.*, 2005b; Doney, 2006). By approximately 2300, this CO_2 absorption could lead to a pH reduction of about 0.7 units from its current value of 8.1 to 7.4. This predicted change in ocean pH would be greater than any experienced over the past 300 million years (Caldeira and Wickett, 2003). Absorbed CO_2 is slowly transferred to the deep ocean by mixing, where it is gradually titrated by dissolution of limestone sedimentary rocks. Therefore, the greatest pH change is seen in surface waters, where the changes are faster (Royal Society, 2005).

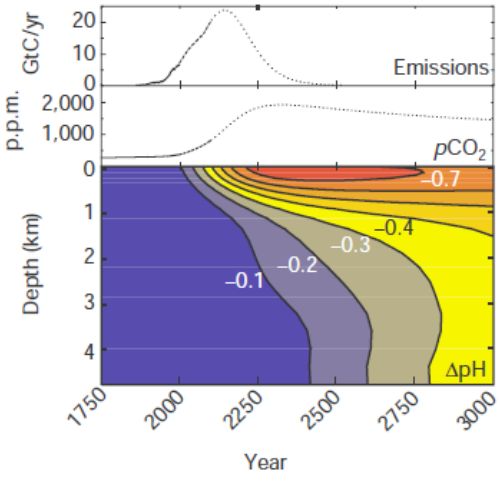

Figure 2.1 Atmospheric CO_2 emissions, historical atmospheric CO_2 levels and projected CO_2 concentrations from business as usual scenario, together with changes in ocean p. Source: Caldeira and Wickett (2003).

2.2 Potential impacts of ocean acidification

2.2.1 Biological impacts

Along with the increase in hydrogen ions, carbonate ion concentrations will decrease and are expected to drop by half over this century, making it more difficult for marine calcifying organisms to form biogenic calcium carbonate ($CaCO_3$) shells, and to maintain their external skeletons due to increased dissolution of the calcified structures (Riebesell *et al.*, 2000; Caldeira and Wickett, 2003; Orr *et al.*, 2005a). Both processes could affect the amount of carbon that is produced in surface waters and sequestered into the deep oceans (Royal Society, 2005).

These changes in ocean chemistry could cause strong impacts on marine ecosystems, even under future scenarios in which most of the remaining fossil fuel CO_2 is not released (Kleypas *et al.*, 1999; Riebesell *et al.*, 2000; Caldeira and Wickett, 2003; Langdon *et al.*, 2003). Some of the life-forms that have been shown to slow down calcification are coccolithophorids, foraminifera, pteropods, corals, coralline algae, and certain molluscs, which build up their shells out of aragonite, calcite or magnesium calcite (Kleypas *et al.*, 1999; Riebesell *et al.*, 2000; Zondervan *et al.*, 2001; Feely *et al.*, 2004; Orr *et al.*, 2005a; Doney, 2006; Young *et al.*, 2014).

2.2.2 Chemical impacts

Several studies have also suggested that continued release of CO_2 to the atmosphere may result in undersaturation of the surface ocean with respect to the calcium carbonate minerals (calcite and aragonite) in the near future. The Southern Ocean surface waters will begin to become undersaturated with respect to aragonite by the year 2050. Based on IPCC 2000, by 2100, this undersaturation could extend throughout all the Southern Ocean and into the subarctic Pacific Ocean. Aragonite undersaturation is followed by calcite undersaturation (Feely *et al.*, 2004; Caldeira and Wickett, 2005; Orr *et al.*, 2005a). In addition to changes in carbonate saturation state, other changes to ocean chemistry are also possible. Trace metal biogeochemistry is strongly influenced by their chemical speciation, which in turn can be influenced by both carbonate ion and hydrogen ion concentrations.

The rise in atmospheric CO_2

2.2.3 The effect on the bioavailability of trace metals – iron and copper

There are only a few studies that have considered the effect of ocean acidification on the speciation and/or bioavailability of trace metals to marine organisms (Turner *et al.*, 1981; Byrne *et al.*, 1988; Byrne, 2002; Sunda and Huntsman, 2003; Millero *et al.*, 2009; Shi *et al.*, 2010; Campbell *et al.*, 2014; Gledhill *et al.*, submitted).

In the surface ocean, the trace metals that have a significant biological role for phytoplankton are manganese, iron, cobalt, copper, zinc and cadmium (Brand *et al.*, 1983; Bruland *et al.*, 1991; Morel and Price, 2003). These metals are necessary for the growth and survival of photosynthetic organisms (Price and Morel, 1990; Morel and Price, 2003). As a result of their low solubilities and effective removal from the water column by phytoplankton, most of these essential trace metals are depleted at the surface (Bruland, 1989; Rue and Bruland, 1995; Morel and Price, 2003).

The chemical forms of an element in seawater (its speciation) are affected by the presence of other ions with which it may interact. Among these are the hydrogen ions. Consequently, a decrease in surface ocean pH can alter the speciation of these trace elements, and may affect the availability of micronutrients and toxins to marine organisms. In some cases essential nutrients act as toxins when present at high concentrations; examples are the trace elements copper, zinc and cadmium (Brand *et al.*, 1986; Morel and Price, 2003; Millero *et al.*, 2009).

The toxicity and availability of trace metals are controlled by their free metal ion concentration. A decrease in pH generally increases the fraction of free ionic forms (Millero *et al.*, 2009), especially of those metals that form strong complexes with OH^- and CO_3^{-2} ions (e.g., Cu (II) and Fe (III), Figure 2.2) (Millero *et al.*, 2009). These anions are expected to decrease in surface waters by 82% and 77% by the year 2100, respectively. These changes in speciation will also increase the thermodynamic and kinetic activity of the metals (Millero *et al.*, 2009).

2.2.3.1 Iron

Phytoplankton is responsible for about half of the photosynthetic carbon fixation (primary production) on earth (Morel and Price, 2003). Their growth

rates are known to be limited by iron availability over at least 30% of the world's ocean (Boyd *et al*., 2000). The low availability of some metals such as Fe controls the rate of photosynthesis in parts of the oceans and the transformation and uptake of major nutrients such as nitrogen (Martin and Fitzwater, 1988; Boyd *et al*., 2000; Morel and Price, 2003).

A decrease in pH from 8.1 to 7.4 will increase the solubility of Fe (III) by about 40%, which could have a large impact on biogeochemical cycles (Morel and Price, 2003; Millero *et al*., 2009). Although a decrease of pH could increase Fe (III) solubility, a recent study (Shi *et al*., 2010) has shown that the bioavailability of dissolved Fe to marine phytoplankton may decline because of ocean acidification, which could in turn reduce the ability of the ocean to take up atmospheric CO_2 (Sunda, 2010). Shi *et al.* (2010) also demonstrated that the effect of a lower pH on iron availability is a consequence of a pH-linked changes in iron chemistry. The decrease in pH within the range expected to occur in surface seawater by 2100 decreased iron uptake by a diatom species by 10 to 20%. By itself, this finding suggests that a lowering of the ocean water pH may decrease iron availability to phytoplankton, thereby affecting the biological carbon pump (Sunda, 2010).

In some areas of the oceans (such as the subtropical ocean gyres), photosynthesis is not limited directly by the availability of iron, but by the availability of nitrogen. As iron plays an important role in di-nitrogen fixation by diazotrophs, it indirectly influences the ocean's biological pump by influencing the supply of nitrogen (Moore *et al*., 2009).

Thus, any processes that reduce the availability of iron to phytoplankton should restrict the ocean's biological pump, thereby increasing atmospheric CO_2 concentrations and global warming, hence providing a positive climate feedback.

But when we consider other complicating factors, the implications are less clear. The role of organic ligands in maintaining soluble Fe concentrations is a key factor to be considered when studying the effects of a lower ocean pH on iron speciation. Several studies have demonstrated that the majority of the dissolved concentrations (mostly >99%) of metals such as Fe, Co, Cu, Zn and Cd are in the form of metal organic complexes (Hering *et al*., 1987; Sunda and Hanson, 1987; Coale and Bruland, 1988; Donat and van den Berg, 1992;

The rise in atmospheric CO_2

Gledhill and van den Berg, 1994; Rue and Bruland, 1995). This is evidence that these metals are bound to strong organic ligands. The best documented case of the presence of strong ligands is the production of siderophores by marine bacteria (Mawji *et al.*, 2008). Organic complexation directly influences the bioavailability of metals in surface seawater (Gledhill and Buck, 2012).

The hydroxide ion and organic chelators compete for binding of Fe (III) so that a decrease in pH affects the extent of organic chelation of Fe and hence its availability to marine organisms. At the same time that a decrease in pH may affect the availability of Fe to phytoplankton, an increase in pCO_2 may change their Fe requirements (Rost *et al.*, 2003; Shi *et al.*, 2010). As a result, Fe uptake by phytoplankton largely depends on the extent of Fe (III) complexation, as well as on the nature of the complexing ligands (Maldonado and Price, 2001; Shaked *et al.*, 2005; Kustka *et al.*, 2007; Shi *et al.*, 2010) .

Although it is thought that a decrease in pH by 0.3 units should slightly increase iron's solubility in seawater (Shi *et al.*, 2010), this decrease in pH may also decrease the bioavailability of this metal to an extent dictated by the acid-base chemistry of the chelating ligands (Shi *et al.*, 2010).

The effectiveness of natural ligands in maintaining Fe in solution might be increased at low pH and may result in a slower Fe loss via the formation of Fe oxyhydroxide precipitates (Shi *et al.*, 2010) (Figure 2.2).

2.2.3.2 Copper

As mentioned above, complexes of copper with organic ligands (e.g., naturally-present and/or antropogenically-induced) have been shown to be the dominant forms (usually as much as 99%) of dissolved copper in oceanic and coastal waters.

Cu (II) has been shown to be toxic at concentrations as low as 10^{-12} M to marine phytoplankton (Brand *et al.*, 1986). Complexation of a metal cation by organic ligands can decrease its toxicity by decreasing the metal's free ion concentration (Donat *et al.*, 1994). However, a pH decrease may reduce copper binding by organic ligands through enhanced competition for ligand binding sites between protons and copper, therefore making copper more bioavailable and consequently toxic to marine organisms. It has been predicted that the increase for the free form of copper under a scenario reaching pH 7.5 will be

as high as 30% (Millero *et al.*, 2009). It is also thought that Cu II will be more toxic in estuarine waters (Millero *et al.*, 2009), due to the much lower pH that these environments will experience (Hofmann *et al.*, 2009) .

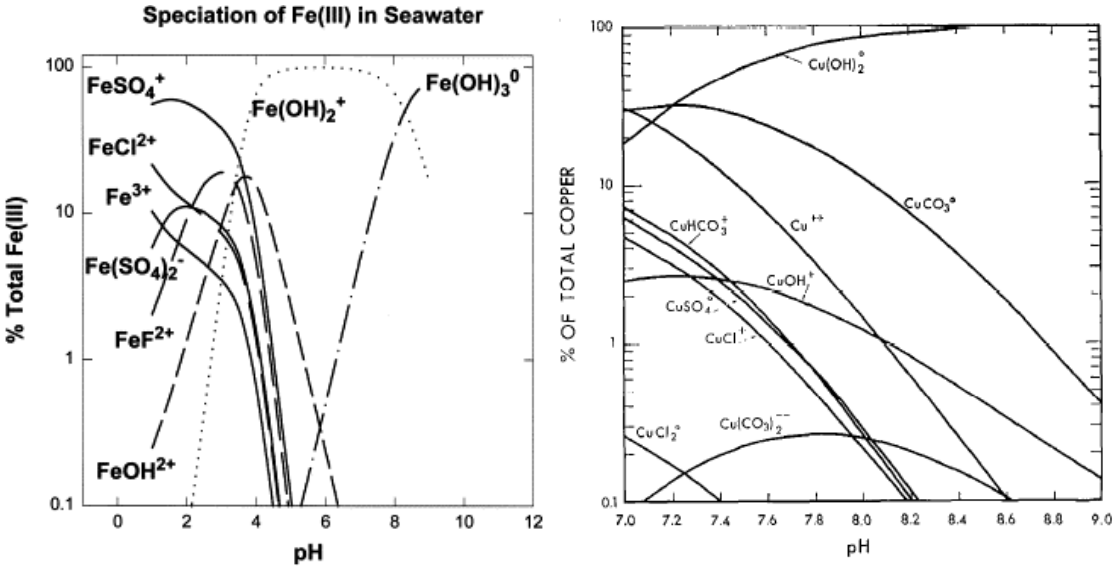

Figure 2.2 Distribution of the chemical species in seawater as a function of pH at 1 atm and 25°C: a) iron (Millero, 1998), b) copper (Zirino and Yamamoto, 1972).

2.2.4 Importance of complexation on metal solubility – natural ligands

Regardless of their source, organic ligands seem to control dissolved iron and copper concentrations and iron bioavailability in the marine environment (Buck and Bruland, 2007; Gledhill and Buck, 2012; Semeniuk *et al.*, 2015).

There is strong evidence supporting the idea of a biological source of both Fe and Cu binding ligands in seawater (Moffett and Brand, 1996; Gledhill and Buck, 2012). An example are some incubation experiments that have shown production of Fe-binding ligands along with diatom growth under Fe-limiting conditions (Buck *et al.*, 2010).

Similar stability constant values of ligands produced by phytoplankton and bacteria to those found in seawater also support the notion of a biological source of organic Fe and Cu binding ligands (Rue and Bruland, 1995; Witter *et al.*, 2000). These ligands may be compounds such as siderophores, humic substances and porphyrins (Gledhill and Buck, 2012).

The rise in atmospheric CO_2

At the current pH of surface seawater (e.g. ca. pH 8.1), Fe (III) is at its minimum solubility. Fe (III) solubility is strongly influenced by organic ligands at pH near 8 (Liu and Millero, 2002). The Fe solubility is much higher in natural than in artificial seawater due to the formation of strong organic complexes (Liu and Millero, 2002). As pH decreases, solubility increases. A decrease in pH from 8.1 to 7.4 will increase the solubility of Fe (III) by about 40%.

It is known that the extent of complexation of trace metals by dissolved organic material is a strong function of pH. This relationship is due to the presence of phenolic and carboxylic functional groups present on organic material that may be responsible for the chelation of metals.

Louis *et al*. (2009) determined the effect of pH on the L_1 ligand class. They observed that the concentration of this ligand class decreased by 25%, when seawater pH fell below 8.

2.3 Metal complexation – the basic principles of equilibrium theory

The form or speciation of a metal in natural waters directly influences its kinetic and thermodynamic properties (Millero, 2001). It is well known that the interactions between marine biota and trace metals (essential micronutrients) are directly dependent on the chemical speciation of the constituents. For example, the toxicity of many trace metals to phytoplankton (such as copper and zinc) is determined by their free ion activities, and not their total concentrations (Millero *et al*., 2009). The speciation of a metal also strongly influences its solubility. For example, Fe (II) is soluble in aqueous solutions, while Fe (III) is nearly insoluble.

The majority of trace elements in seawater are present as organic complexes (Hering *et al*., 1987; Sunda and Hanson, 1987; Coale and Bruland, 1988; Donat and van den Berg, 1992; Gledhill and van den Berg, 1994; Rue and Bruland, 1995), and these complexes increase the total soluble concentration of these elements.

Ionic interaction models have been used to determine the activity and speciation of divalent and trivalent metals in seawater. These models have also

been used to determine the effect of pH on metal speciation (de Baar *et al.*, 2008; Millero *et al.*, 2009).

Although the coordination chemistry of complexation is well developed, the determination of trace element speciation is analytically difficult to undertake.

The general expressions for ligand equilibrium reactions are:

1. Addition of a ligand:

$M^{n+} + L \rightarrow ML_i$, and its conditional stability:

$\beta_i = [ML_i]/[M][L]^i$

2. Addition of a protonated ligand:

$M^{n+} + HL \rightarrow ML_i + H^+$, and its conditional stability:

$\beta_i = [ML_i][H^+]/[M][HL]^i$

2.3.1 Complexation in natural waters

Metal-ligand interactions can be of an electrostatic or covalent nature, or both. When the reaction is primarily electrostatic and the reactants retain some hydration water between them, the product is called an ion pair or an outer sphere complex. In natural waters this type of interaction is particularly important amongst the major ions of high ionic strength systems such as seawater.

When the reaction of a metal with a ligand involves coordination at several positions, it is called a chelation reaction. Such a reaction requires the combination of a metal with a coordination number greater than one (i.e., more than one site for coordination), and a multidentate ligand, an organic compound with several reactive functional groups. These organic compounds are called chelators or chelating agents (Stumm and Morgan, 1981).

The different types of chemical complexes in natural waters are briefly described (adapted from Stumm and Morgan (1981)):

The rise in atmospheric CO_2

1. *Ion pairs of major constituents*

The seven major aquatic constituents that can be considered in seawater are: Na^+, Ca^{2+}, Mg^{2+}, K^+, Cl^-, SO_4^{2-}, CO_3^{2-}.

Interactions amongst major ions are divided into two types: long-range electrostatic interactions (single ion activity coefficients), and specific complex formation (formation constants for the ion-pairs).

All electrostatic interactions among ions, including ion pair formation, can be considered as non-ideal interactions. In this approach a total activity coefficient, y_i, is defined for each ion as the ratio of the free ion activity to the total ion concentration:

$$y_i^T = [C_i]/(C_i)_T$$

These total activity coefficients are dependent on the ionic composition of the system, and they must be determined for each different system. These total activity coefficients are easier to determine experimentally, and they are the better approach to use when trying to obtain valid thermodynamic interactions amongst major constituents in seawater.

2. *Inorganic complexes of trace elements*

Minor ion-interactions can be viewed independently of other constituents, unlike with major ion-interactions, where they depend on all species. This is because the important complexes are formed with constituents in large excess whose free concentrations (activities) are unaffected by complexation with a trace element.

The most important inorganic ligands considered to form complexes with a divalent or trivalent trace metal (M^{n+}) in natural waters are: OH^-, Cl^-, SO_4^{2-}, CO_3^{2-}, S^{2-}.

The speciation of metals that form important carbonate (e.g. Cu^{2+}) or hydroxide (e.g. Fe^{3+}) complexes is a strong function of pH. In the case of hydroxide complexes, for example, their formation is thought to be due to the dissociation of the weakly acidic hydrated metal ions, as seen with ferric hydroxide precipitation.

Apart from the hydroxides, there are relatively few inorganic complexes of trace metals that are expected to be dominant in oxic waters. The major exceptions are the carbonate complex of copper in sufficiently alkaline systems and the chloride complexes of cadmium, silver, and mercury in the presence of high chlorinity.

3. Organic complexes

Aquatic organic ligands can be organized into three categories:

1) Ligands of known composition that have been measured to form a sizable fraction of the DOC (e.g. amino acids).
2) Other ligands produced by phytoplankton present at trace concentrations, but with high affinities for metals.
3) Humic substances isolated from a variety of aquatic systems and whose coordination properties have been characterized.

2.3.2 Chemical characterization of organic ligands

Characterization of organic ligands in seawater represents a challenge due to the unknown ligand structures, the complexity of their chemical nature and their presence at very low concentrations in the marine environment (Gledhill and Buck, 2012).

However, the strengths and concentrations of the ligands measured with the current available electrochemical techniques indicate that ambient ligands have a high affinity for iron (Gledhill and van den Berg, 1994; Rue and Bruland, 1995; van den Berg, 1995; Wu and Luther, 1995). The recent progress made in the improvement of sensitivity, mass accuracy and robustness of analytical techniques such as mass spectrometry have resulted in the detection of specific iron organic chelators such as siderophores by HPLC-ESI-MS (High Performance Liquid Chromatography - Electrospray Ionization Mass Spectrometry) (Gledhill *et al.*, 2004; Mawji *et al.*, 2008), and other complex organic fractions associated with iron by FFFF-ICP-MS (Flow Field Flow Fractionation - Inductively Coupled Plasma Mass Spectrometry (Stolpe *et al.*, 2010; Stolpe and Hassellov, 2010).

Other studies have also suggested that these detected ligands have very similar binding strengths to the ones produced by phytoplankton and bacteria,

The rise in atmospheric CO_2

and may include compounds such as siderophores and porphyrins (Witter *et al.*, 2000; Macrellis *et al.*, 2001).

In the case of copper, evidence shows that the strongest ligands found in seawater are produced by cyanobacteria and heterotrophic bacteria to alleviate Cu toxicity by complexing Cu extracellularly (Moffett and Brand, 1996; Gordon *et al.*, 2000; Semeniuk *et al.*, 2015), while eukaryotes produce weaker ligands (Croot *et al.*, 2000).

Although the structures of the strong in situ Cu binding ligands remain unknown, the ligands may contain thiol and amino functional groups (Ross *et al.*, 2003), and could be phytochelatins, phytochelatin precursors (e.g., glutathione and cysteine), humic and fulvic acids, or other low molecular weight compounds (Leal and van den Berg, 1998; Laglera and van den Berg, 2003; Tang *et al.*, 2004; Dupont *et al.*, 2006; Yang and van den Berg, 2009).

2.3.2.1 Common functional groups

The most common functional groups that are known to serve as iron and copper chelators identified so far are: i) carboxylic acids, such as EDTA, which are chelators with acidic binding groups not protonated at the pH of seawater; ii) amino groups, which are amongst the simplest chelating agents; iii) catechols, such as azotochelin, which are chelators protonated at the pH of seawater and are known to serve as strong ligands for Fe (III) and have been identified as components of the organic matter presumptively responsible for the chelation of Fe in the surface ocean (Macrellis *et al.*, 2001); iv) hydroxamates, such as DFB (desferri-ferrioxamine B), which are amongst the principal functional groups in strong chelators like siderophores (Maldonado and Price, 2001; Shaked *et al.*, 2005), and v) thiols, which are known to be part of the Cu binding ligand pool and which have also functional groups not protonated at the pH of seawater and hence form negative ions via deprotonation, as in the case of carboxylic acids. The structures of some of the common functional groups are shown in Figure 2.3.

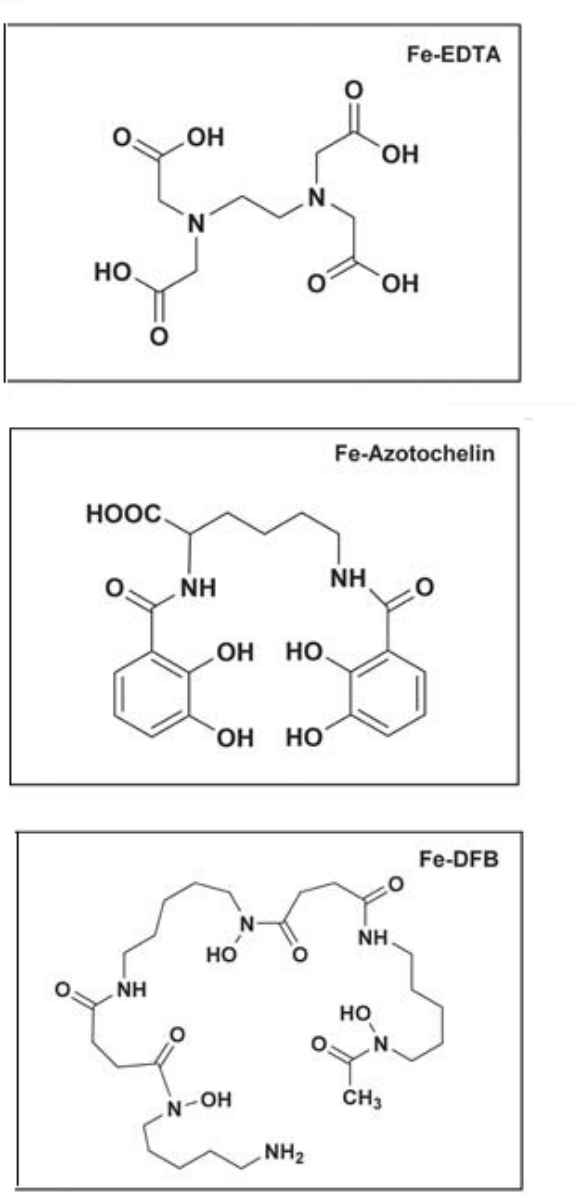

Figure 2.3 Structures of common functional groups for Fe chelation. The amino carboxylate EDTA (ethylenediaminetetraacetic acid), the catechol azotochelin, and the hydroxamate DFB (desferri-ferrioxamine B). Modified from Shi *et al.* (2010).

2.3.2.2 Specific chelators

Amino acids

These are the major class of the identified organic compounds with sizable complexation affinities for metals. The presence of both a carboxyl and an amino group gives all amino acids the ability to coordinate metals at two positions. Fe and Cu are amongst the most reactive with amino acids (Stumm and Morgan, 1981).

The rise in atmospheric CO_2

Siderophores

Even though little is known about the origin and nature of in situ produced Fe (III) organic ligands in seawater, they have Fe-binding functional groups and conditional stability constants typical of siderophores (Rue and Bruland, 1995; Johnson *et al.*, 1997; Macrellis *et al.*, 2001; Maldonado *et al.*, 2005).

Siderophores are Fe-specific, low molecular weight organic ligands, released by marine bacteria (heterotrophic and cyanobacteria) and fungi to enhance Fe acquisition under Fe-limiting conditions (Raymond *et al.*, 1984; Granger and Price, 1999; Mawji *et al.*, 2008). However, it has been observed that siderophores may only be produced in significant amounts where organic carbon concentrations are high enough to support significant bacterial productivity (Mawji *et al.*, 2011), but where dissolved iron is depleted. Siderophores seem to play an important role in increasing the availability of Fe for marine bacteria (Gledhill and Buck, 2012), and also in the solubilisation of particulate and colloidal Fe. Siderophores may be associated with these fractions in the surface ocean (Gledhill and Buck, 2012).

Humic substances (HS) and exopolysaccharides (EPS)

Humic substances (humic and fulvic acids, HS) and exopolysaccharides (EPS) are typically found in the colloidal fraction (Gledhill and Buck, 2012), and their associated Fe and Cu is available to phytoplankton (Hassler *et al.*, 2011). Humic substances include a complex mixture of carboxylated and fused alicyclic structures, which are expected to constitute strong ligands for metal binding (Hertkorn *et al.*, 2006).

High excess ligand concentrations (Boye *et al.*, 2003; Buck *et al.*, 2007; Kondo *et al.*, 2007) found in coastal waters may be humic substances which may be an important component of the ligand pool for dFe in margin environments (Laglera *et al.*, 2007; Batchelli *et al.*, 2009; Laglera and van den Berg, 2009), and especially in coastal and deep waters (Batchelli *et al.*, 2009).

Porphyrins

Porphyrins are thought to be closely related to cellular metabolic components (Hunter and Boyd, 2007). They have also been suggested to be part of the Fe-

binding pool (Witter *et al.*, 2000; Hunter and Boyd, 2007); although good evidence of this still has to be produced (Gledhill and Buck, 2012).

Glutathione and cysteine

Thiols like glutathione and cysteine are common in the marine water column and are known to form such stable complexes with copper (I) that they preclude the presence of copper (II) (Leal and van den Berg, 1998).

Chapter 3: Organic Fe (III) complexation in the high latitude North Atlantic Ocean

The concentrations and conditional stability constants of organic iron complexing ligands are presented in this chapter, obtained during a research cruise in the North Atlantic Ocean on-board RRS *Discovery* (D354) in 2010, along with a general description of other physical and chemical oceanographic features such as dissolved iron and inorganic nutrients concentrations, and water masses. This cruise was conducted in the high latitude North Atlantic Ocean (HLNA), including the Iceland and Irminger Basins and waters off Greenland. The main objective of this work is to compare the results of iron binding ligand characteristics from this cruise, in the context of oceanographic conditions, with the results obtained by Mohamed *et al.* (2011) during a previous cruise conducted in the same study area.

3.1 Introduction

An analysis of Fe (III) organic binding ligand characteristics is presented in this chapter from the results obtained from the RRS *Discovery* 354 cruise during summer 2010, as part of the High Latitude North Atlantic Fe limitation project, as an attempt to understand better the Fe cycles in this marine ecosystem. To achieve this goal, this chapter has the following objectives: i) determination of the Fe (III) binding ligand concentrations and their associated stability constants in the HLNA region, especially in the Irminger and Iceland Basins; ii) comparison of these results with previous data from the Iceland Basin and other ocean regions; and iii) analysis of trends in organic ligand concentrations throughout the water column in terms of excess ligand concentrations and L/dFe ratios.

3.2 Literature review

3.2.1 Biogeochemical cycle

3.2.1.1 Fe limitation

Iron availability controls the productivity and species composition of phytoplankton communities in large regions of the ocean (Sunda and Huntsman, 1995b; Johnson *et al.*, 1997; Hunter and Boyd, 2007).

Iron is required for the synthesis of chlorophyll and several photosynthetic electron transport proteins, and the reduction of CO_2, SO_4^{-2} and NO_3^- during the photosynthetic production of organic compounds (Martin and Fitzwater, 1988; Hudson and Morel, 1990; Raven *et al.*, 1999). Iron is therefore of great importance to the global carbon cycle.

It has been demonstrated that Fe deficiency limits phytoplankton growth in high nitrate low chlorophyll (HNLC) waters such as the equatorial and subarctic Pacific, and the Southern Ocean (Martin and Fitzwater, 1988; Boye *et al.*, 2005; Boyd *et al.*, 2007). Dissolved Fe concentrations in these HNLC surface waters are on the order of 0.02 to 0.05 nM (Bruland, 2001). HNLC waters make up around 25% of the world ocean (de Baar *et al.*, 2005), and along with the nutrient-poor-low latitude waters where Fe helps to regulate nitrogen fixation (Moore *et al.*, 2009), Fe controls productivity in half of the world's oceans (Boyd and Ellwood, 2010).

The HLNA plays an important role in the oceanic biological carbon cycle (Sarmiento and Toggweiler, 1984; Sanders *et al.*, 2005). A pronounced spring bloom is observed in this region, and after this significant drawdown of macronutrients occurs along with high rates of export production, as observed in the Irminger Basin (Sanders *et al.*, 2005). Furthermore, regions of the HLNA are sites of deep water formation (North Atlantic Deep Water; (Pickart *et al.*, 2003)) which is important for atmospheric CO_2 sequestration (Sarmiento and Toggweiler, 1984).

It was previously assumed that iron limitation did not exist in the HLNA due to sufficient supply of atmospheric Fe containing aerosols derived from the Sahara (Martin *et al.*, 1993), and therefore this region differed from the high

latitude HNLC regions such as the Southern Ocean and the North Pacific. However recently, it has been demonstrated that iron limits phytoplankton primary production in some of the HLNA areas (e.g. the Iceland Basin and the central Irminger Basin) (Moore *et al.*, 2005; Nielsdottir *et al.*, 2009). In situ measurements in the Iceland Basin have shown low surface water dissolved iron concentrations ([dFe] <0.001 to 0.22 nM) (Measures *et al.*, 2008; Nielsdottir *et al.*, 2009). Amended experimental bottles (with Fe additions) have shown an increase in photosynthetic efficiency compared to the controls (Nielsdottir *et al.*, 2009). Iron availability thus seems to be a significant determinant of phytoplankton productivity in the North Atlantic.

3.2.1.2 Fe sources

The three most important sources of Fe to the ocean are: atmospheric deposition, fluvial (riverine) inputs and sea floor processes such as hydrothermal venting, sediment resuspension and diffusive release of Fe from reducing sediments (Ussher *et al.*, 2004)(Figure 3.1). Most of the iron from these sources is either particulate or colloidal in size (Hunter and Boyd, 2007). However, in many ocean regions (e.g. Kerguelen Plateau and Ona Basin in the Southern Ocean) Fe supply by both winter mixing and diapycnal mixing can provide the main source of dFe to surface waters (Blain *et al.*, 2008; Frants *et al.*, 2013). Sometimes the combined effect of the two processes can consistently supply sufficient iron to sustain phytoplankton blooms in these regions.

Atmospheric deposition is highly important because it is considered to be the main iron source in remote offshore regions (Spokes *et al.*, 2001), although important uncertainties remain about the solubility and bioavailability of iron in dust (Hunter and Boyd, 2007).

Fluvial inputs are an important source of iron throughout the coastal zone. Almost all of this iron is in the form of colloidal hydroxides and oxides which are largely removed by scavenging/flocculation in estuaries (Ussher *et al.*, 2004; Hunter and Boyd, 2007). It is not well known how much of this iron is transported into the open ocean.

Hydrothermal vents are known to have very high iron concentrations (~ 1mM), although it has been seen that the majority of the dissolved iron precipitates in

the nearby sediments (Ussher *et al.*, 2004). Recent work has however indicated that the iron from hydrothermal vents makes a significant contribution to the dFe inventory of the deep ocean (Bennett *et al.*, 2008; Tagliabue *et al.*, 2010; Hawkes *et al.*, 2013).

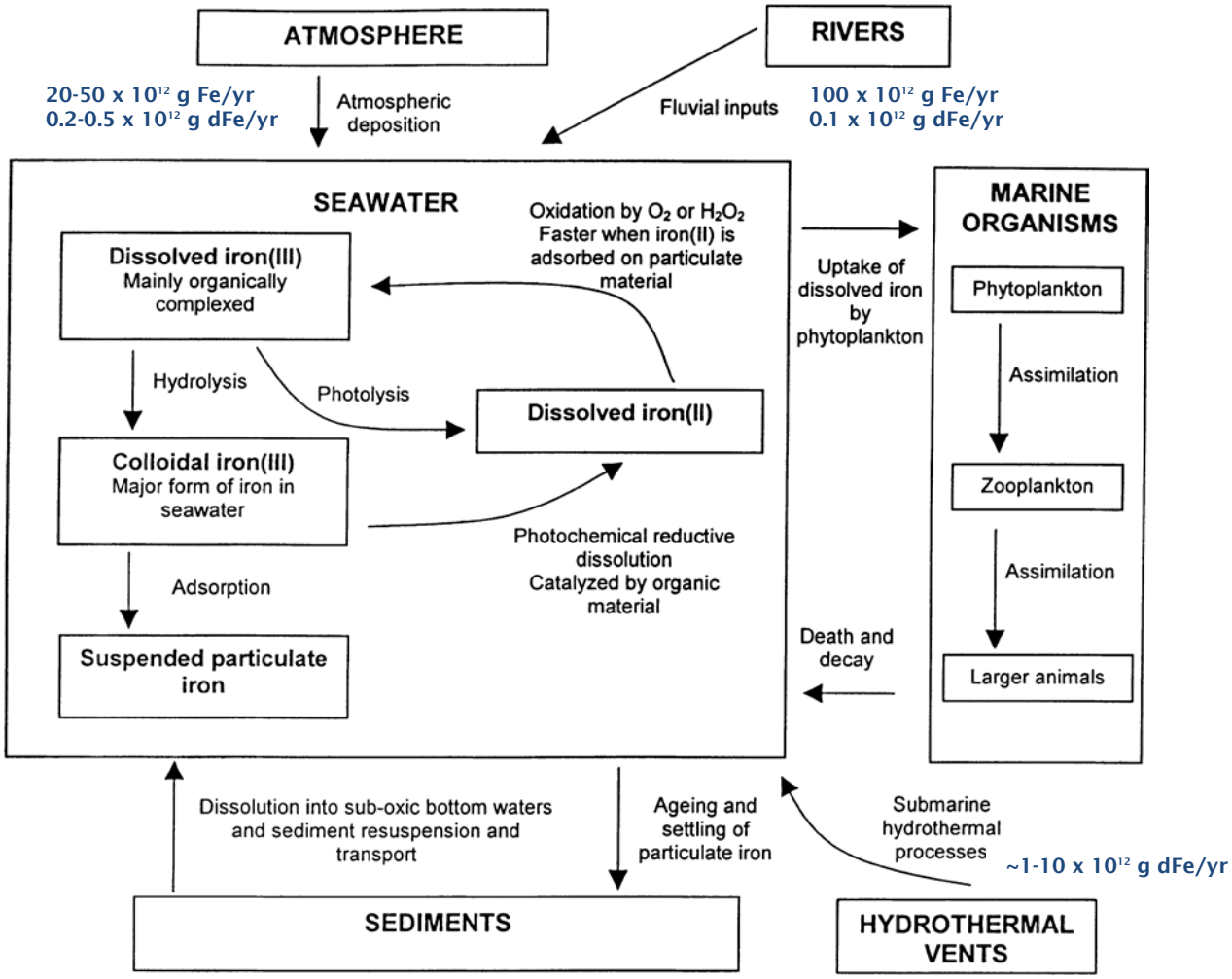

Figure 3.1 The biogeochemical iron cycle in the ocean, and approximate particulate iron (Fe) and dissolved iron (dFe) annual fluxes to the ocean (g/year). Riverine flux is estimated on the basis of 90% loss from estuarine mixing. Dissolved inputs from sediments are considered within the hydrothermal vents dissolved inputs, as they are only important in anoxic areas, in areas where there is a significant degree of turbidity, or if there is a gradual release of iron in a chemically stabilized form. Sources: Achterberg *et al.* (2001); Ussher *et al.* (2004).

Also, iron-rich bottom shelf waters and shelf sediments can influence surface [dFe] through resuspension processes where vertical mixing through the water

column is important, or by release of Fe(II) from reducing sediments (Buck and Bruland, 2007).

The iron sources to the HLNA are spatially and temporally variable due to episodic dust inputs, seasonal biological activity and hydrographic features which includes deep winter mixing (Jickells, 2001; Rijkenberg *et al.*, 2008; Nielsdottir *et al.*, 2009).

3.2.1.3 Fe concentrations

Dissolved iron concentrations are controlled by a balance between Fe stabilisation by organic complexes and removal by biological uptake and scavenging, involving adsorption and precipitation of Fe onto particles (Johnson *et al.*, 1997; Liu and Millero, 2002).

Particulate forms of Fe in HNLC regions can exist at concentrations higher than dFe (Price and Morel, 1998). In contrast, some regions of the surface ocean such as the oligotrophic gyre of the central North Pacific show [dFe] between 0.02 and 0.4 nM and typically exceed particulate Fe concentrations (Bruland *et al.*, 1994).

Dissolved iron concentrations generally resemble the shape of the major nutrient profiles, indicating its biological role (Martin and Gordon, 1988). Removal by biological uptake occurs in the surface waters (low concentrations) and remineralisation processes occur throughout the water column increasing its concentration at depth (Boyd and Ellwood, 2010).

In coastal waters, surface dFe can reach up to 10 nM (Wu and Luther, 1996; Bruland *et al.*, 2001), due to high source strengths. Particulate iron in these coastal waters is also very high and variable (Wu and Luther, 1996).

3.2.1.4 Fe speciation

Physicochemical speciation of dissolved Fe in seawater plays an important role in its solubility and bioavailability to phytoplankton (Maldonado *et al.*, 2005; Buck *et al.*, 2007).

The chemical form of iron is defined by physical size fractions separated on the basis of filtration methods (Bruland, 2001), hence these forms are operationally defined. The size fractions comprise particulate (>0.2 μm),

colloidal (>0.02 µm and <0.2 µm) and soluble (<1kDa or <0.02 µm), where the colloidal and soluble fractions make up the total dissolved fraction. The colloidal fraction is determined from the difference between the dissolved (<0.2 µm) and soluble (<1kDa or <0.02 µm) fractions (Schlosser and Croot, 2008; Gledhill and Buck, 2012).

It has been shown that a significant portion of the dFe pool is colloidal in size (Wu *et al.*, 2001; Cullen *et al.*, 2006; Bergquist *et al.*, 2007; Hunter and Boyd, 2007; Schlosser and Croot, 2008; Boye *et al.*, 2010; Gledhill and Buck, 2012). These organic colloids formed in surface seawater are scavenged rapidly throughout the water column (Wu *et al.*, 2001; Cullen *et al.*, 2006; Bergquist *et al.*, 2007; Kondo *et al.*, 2008; Schlosser and Croot, 2008; Boye *et al.*, 2010; Thuroczy *et al.*, 2010); but despite this and the question about how much Fe in this portion is truly exchangeable, it is thought that this fraction has a great impact on the overall Fe cycle.

Chemical species are defined chemical constituents within a particular form or size fraction of the metal. In the case of dissolved iron, these species comprise Fe (II) and Fe (III), either within a variety of soluble complexes with inorganic and organic ligands, or in a variety of colloidal and/or particulate forms (Bruland, 2001). These fractions cycle in different ways in the environment (Kuma *et al.*, 1996; Maldonado *et al.*, 2005; Hunter and Boyd, 2007; Boyd and Ellwood, 2010).

The relative proportions of dissolved Fe (III) and Fe (II) in surface seawater is dependent on the relative rates of reduction and oxidation by various mechanisms (Waite, 2001) and by the extent of stabilization of the oxidized and reduced iron by inorganic and organic complexation (Bruland, 2001) (Figure 3.1).

It has been demonstrated that most of the dFe in surface seawater and throughout the water column (>99%) is present as complexes formed with natural organic ligands whose nature and origin has just begun to be understood (Gledhill and van den Berg, 1994; Rue and Bruland, 1995; van den Berg, 1995; Rue and Bruland, 1997; Witter and Luther, 1998; Thuroczy *et al.*, 2010; Mohamed *et al.*, 2011). Organic Fe binding ligands are present in the entire ocean, from surface to deep waters and from coastal to open ocean (Gledhill and Buck, 2012). There is only one study so far about organic ligands

in the HLNA (Mohamed *et al.*, 2011), even though several studies on dFe distribution in this area have been reported (Martin *et al.*, 1993; Measures *et al.*, 2008; Nielsdottir *et al.*, 2009).

Fe (II) speciation

It has been estimated that ~76% of Fe (II) is hydrated Fe^{2+} at pH 8.00 (Millero *et al.*, 1995); the rest being $FeCO_3$ species. However, Fe^{2+} oxidizes very slowly, and Fe(II) oxidation is controlled instead by the trace Fe(II) species ($Fe[OH]^2_0$, $Fe[CO_3]^{-2}_2$] that oxidize much faster (Roy *et al.*, 2008).

Traditionally, it was thought that Fe (II) species have a trace and ephemeral presence. However, it has been recently demonstrated that Fe(II) concentrations in near surface waters are related with a photochemical (rather than a biological) source and that Fe(II) can account for up to 50% of the total dFe pool in sunlit waters such as the subarctic Pacific (Roy *et al.*, 2008).

Fe (II) also comprises an important fraction of the total Fe reservoir in systems such as hydrothermal vents and oxygen minimum zones (Gledhill and Vandenberg, 1995; Ussher *et al.*, 2007; Roy *et al.*, 2008; Sarthou *et al.*, 2011), hence its importance in the overall Fe biogeochemistry in these regions, even though little is known about the role of Fe (II) for eukaryotic phytoplankton.

Fe (III) speciation

The inorganic speciation of Fe (III) is dominated by iron hydroxide complexes in the pH range of most natural waters (Millero *et al.*, 1995; Kuma *et al.*, 1996). However, the importance of the $Fe(OH)_3$ species on the solubility of Fe (III)' is still uncertain (Millero, 1998).

3.2.1.5 Bioavailability

Iron availability in seawater is mainly determined by the solubility of Fe(III) (Johnson *et al.*, 1997), which is both temperature and pH dependant (Liu and Millero, 2002). Organic ligands in seawater only affect Fe(III) solubilities in the pH range from 7 to 9, and within this pH range, organic ligands may increase iron solubilities up to 0.3-0.5 nM; the resulting concentrations are much higher compared to the values in 0.7 M NaCl (0.011 nM) at 25 °C (Liu and Millero, 2002).

Organic Fe complexation in the HLNA

The low temperature and pH of ocean deep waters may be responsible for the higher Fe (III) solubilities found in these waters (Johnson *et al.*, 1997).

Iron uptake by phytoplankton has typically been related with free, hydrated Fe^{3+} concentrations. However, it was later realized that hydrolysis species comprising Fe (III)' (such as $Fe(OH)^{+}_{2}$), which are more abundant and labile, are the ones that actually control uptake rates of inorganic iron (Hudson and Morel, 1990).

Prokaryotes and also some eukaryotes such as diatoms are able to utilize some of the complexed iron (Price *et al.*, 1994; Hutchins *et al.*, 1998; Price and Morel, 1998; Hutchins *et al.*, 1999). Two major mechanisms have been described for the Fe acquisition from organic Fe complexes for phytoplankton: siderophore mediated acquisition (Soria-Dengg *et al.*, 2001) and the reductive Fe uptake pathway (Maldonado and Price, 2001; Shaked *et al.*, 2005). It is to date known that the latter mechanism is the most prevalent form of Fe acquisition strategy amongst phytoplankton (Shaked and Lis, 2012). Both prokaryotes and eukaryotes can access chelated Fe(III) by using cell surface-bound reductases to reduce the chelated Fe(III) to Fe(II) which then dissociates and is subsequently transported into the cell either as Fe(II)' or after re-oxidation, as Fe(III)' (Maldonado and Price, 1999).

Particulate and colloidal iron can also be utilized by the microbial and planktonic community, either through solubilisation of colloidal iron (in the case of protozoan grazers; (Barbeau *et al.*, 1996), or by remineralisation and reuse as regenerated iron (Hutchins and Bruland, 1994). The latter has been found to be an important uptake mechanism used by microorganisms in the euphotic zone of the equatorial Pacific (Price and Morel, 1998). Phytoplankton *Ochromonas* can obtain iron directly in particulate form by ingesting bacteria (Maranger *et al.*, 1998).

The chemical characteristics of the organic colloids is probably a determinant for the biological availability of the colloidal Fe (Kuma and Matsunaga, 1995). Also important is the capability of the organisms to extract Fe from the colloids (Gledhill and Buck, 2012).

Some of the iron that is not directly available may be recycled by various mechanisms (e.g. photochemical reduction and biologically mediated

reduction) and at various rates into biologically available forms (Wells *et al.*, 1995) (Figure 3.1).

It has been observed that both bioreduction of organically bound iron and photochemistry are the most important mechanisms to enhance the dissociation of iron from organic ligands (Maldonado *et al.*, 2005). Photochemistry in surface waters of some regions of the Southern Ocean probably plays a significant role in Fe uptake by plankton from the dissolved organic Fe pool (Maldonado *et al.*, 2005) (Figure 3.1).

3.2.1.6 CLE-ACSV technique

Organic iron complexation is traditionally measured in seawater with the Competitive Ligand Equilibration-Adsorptive Cathodic Stripping Voltammetry (CLE-ACSV) method (Gledhill and van den Berg, 1994; Rue and Bruland, 1995; Croot and Johansson, 2000). CLE-ACSV is a highly sensitive indirect electrochemical method that relies on the adsorption of a metal-added ligand complex (M-AL) onto a hanging mercury drop electrode (HMDE) followed by a voltammetric scan where the analytical signal comes from the resultant reduction current as the Fe (III) in the adsorbed complex is reduced during the cathodic stripping step (Gledhill and van den Berg, 1994; Bruland, 2001). The complexation of Fe by natural ligands is determined after a competing equilibrium has been established between added Fe (III)', a well-characterized added ligand (AL), and the naturally-occurring Fe (III)-binding organic ligands (Bruland, 2001).

A seawater titration with iron is carried in presence of the AL with the following procedure: aliquots of a seawater sample to which the AL and a pH buffer have been added are spiked with increasing amounts of iron. These aliquots are then left overnight to allow the added iron to equilibrate with the natural ligands and the AL. The current (i_p) produced by reduction of iron complexed with the added ligand in each aliquot is measured by ACSV at a HMDE. The i_p values are plotted against the total iron concentration (Donat and van den Berg, 1992). The titration data are linearly transformed using the van den Berg/Ruzic (1982) method (van den Berg and Kramer, 1979; Ruzic, 1982; van den Berg, 1982a), or can be treated with a non-linear transformation method described by Gerringa *et al.* (1995), in order to calculate the concentration of

organic Fe-binding ligands in the sample (L) and their conditional stability constants (log K'_{FeL}) (Rue and Bruland, 1995; Gledhill and Buck, 2012).

Usually the ligand concentrations determined by this technique are described as "ligand classes" (L_i) defined by the associated conditional stability constant (Gledhill and Buck, 2012). In most cases, only one ligand class is identified in Fe speciation measurements using this method (Gledhill and Buck, 2012).

Despite being the most widely used method to determine organic complexation by metals in seawater, it has some limitations caused by assumptions made in the data interpretation, which have been recently reviewed. The two main assumptions are: i) raw titration data is interpreted assuming that ambient ligands are coordinated with dFe in a 1:1 ratio, and ii) all of the dFe in a given sample is in an exchangeable form with respect to the added competitive ligand (AL) (Gledhill and Buck, 2012).

3.2.2 Organic ligands

3.2.2.1 External sources

Atmospheric inputs have been suggested to be an external source of ligands for surface waters of the North Atlantic (Gerringa *et al.*, 2006). Also, river plumes and sediment resuspension on shelves appear to be a source of both dFe and Fe-binding ligands to the marine water column, especially in coastal waters (Croot and Johansson, 2000; Buck *et al.*, 2007; Gerringa *et al.*, 2008).

In the presence of organic Fe complexes, incubation experiments with phytoplankton have demonstrated that biomass increases in response to the addition of the Fe complexes, suggesting a biological source (Maldonado *et al.*, 2005).

The chemical characterization of organic ligands is described in section 2.3.2 of this document.

3.2.2.2 Ligand types (L_1 and L_2)

Studies have shown the presence of at least two chemical classes of dissolved organic ligands (L_1 and L_2) in the waters of the North Pacific and North Atlantic (Buck and Bruland, 2007; Hunter and Boyd, 2007), present in both the soluble (<0.02 µm) and colloidal (0.02 to 0.4 µm) size fractions (Wu *et al.*, 2001).

Generally, L_1 is used to be referred to the strongest binding ligand class (log K'_{FeL} >22) found mainly in the upper water column; whilst L_2 is a weaker ligand class (log K'_{FeL} =21-22) found throughout the water column (Rue and Bruland, 1995; Rue and Bruland, 1997; Boye *et al.*, 2006; Cullen *et al.*, 2006; Hunter and Boyd, 2007). Both classes are most likely a mixture of a wide variety of ligands with similar stability constants.

L_1 type

There is evidence that the L_1 class is siderophore-like and is specifically generated by marine bacteria (i.e. heterotrophic and cyanobacteria) (Hunter and Boyd, 2007). The L_1 ligand class presents the same class of log K'_{FeL} values (log K'_{FeL} >22) as siderophore type ligands measured by CLE-ACSV (Rue and Bruland, 1995; Witter *et al.*, 2000; Buck *et al.*, 2010).

As siderophores are produced by marine microorganisms to access Fe from their surrounding environment under Fe limiting conditions, the large excess of L_1 observed at very low (<0.2 nM) [dFe] supports the possibility of some fractions of the L_1 ligand pool being siderophores (Buck and Bruland, 2007).

However, it is not clear whether the excess L_1 type ligands generally seen in low Fe waters are due to L_1 production under Fe-depleted conditions or due to Fe being removed from the FeL_1 complexes as a result of uptake by organisms (Maldonado and Price, 2001; Buck and Bruland, 2007).

L_2 type

It is considered that the weaker L_2 ligand pool is mainly formed from the remineralisation of sinking biological particles, and therefore should have higher concentrations in the subsurface and deep waters (Hunter and Boyd, 2007).

Other important sources of weaker Fe-binding ligands include the grazing and bacterial remineralisation of organic matter. They are thought to be an important component of the dissolved Fe-binding ligand pool in some coastal and deep waters (Laglera and van den Berg, 2009).

Organic Fe complexation in the HLNA

Both L_1 and L_2

Shelf sediments can be a source of both L_1 and L_2 ligand types, and may remain associated with colloids throughout the water column (Buck and Bruland, 2007).

3.2.2.3 Excess ligands – link to biological activity

Excess ligand concentrations [eL_i] are used as an approximation of ligand undersaturation, when compared to total ligand concentration (Wu and Luther, 1995; Witter *et al.*, 2000; Boye *et al.*, 2001; Tian *et al.*, 2006; Rijkenberg *et al.*, 2008; Thuroczy *et al.*, 2010), and this term is more or less independent of the iron concentration used in ligand calculations (Gledhill and Buck, 2012). Total ligand concentration includes stable inorganic colloidal Fe and other Fe inert components that affect the measured values (Gledhill and Buck, 2012).

Excess ligand concentrations have shown to be related with high productivity in Fe-depleted waters (Boye *et al.*, 2003; Gerringa *et al.*, 2006; Buck and Bruland, 2007; Gledhill and Buck, 2012). Higher eL_i within a profile are generally found in the upper water column (Rue and Bruland, 1995; van den Berg, 1995; Boye *et al.*, 2001; Boye *et al.*, 2006; Gerringa *et al.*, 2006; Rijkenberg *et al.*, 2008; Thuroczy *et al.*, 2010; Mohamed *et al.*, 2011), and mostly in the soluble size fraction (Cullen *et al.*, 2006; Kondo *et al.*, 2008; Boye *et al.*, 2010; Thuroczy *et al.*, 2010). These high [eL_i] are often associated with the fluorescence or chlorophyll biomass maxima (Boye *et al.*, 2006; Gerringa *et al.*, 2006; Buck and Bruland, 2007; Wagener *et al.*, 2008), possibly being the remnants of a previous bloom (Sato *et al.*, 2007). In most of the ocean, organic ligand concentrations exceed [dFe] (Gledhill and Buck, 2012).

3.2.2.4 Acquisition mechanisms

It has been demonstrated that bacteria have a more efficient mechanism for acquisition of organically bound Fe than phytoplankton (Granger and Price, 1999; Maldonado *et al.*, 2005), possibly reflecting higher Fe requirement of marine heterotrophic (Tortell *et al.*, 1996) and autotrophic (Brand, 1991) bacteria relative to eukaryotic phytoplankton (Brand, 1991; Sunda and Huntsman, 1995b). However, observed rapid Fe uptake rates by bacterioplankton from organically bound Fe do not indicate whether they are

accessing organic Fe directly or they are utilizing the inorganic Fe liberated from these complexes (Maldonado *et al.*, 2005).

At low concentrations of inorganic Fe, eukaryotic phytoplankton are able to access Fe bound within strong organic Fe complexes (Hutchins *et al.*, 1999; Maldonado and Price, 1999; Maldonado and Price, 2001; Buck and Bruland, 2007). It has been demonstrated that these organisms possess inducible reductases at the cell surface that mediate the reduction of organically bound Fe (III) and subsequent dissociation of Fe from the ligand (Maldonado and Price, 2001). Once dissociation occurs, the cells internalize the inorganic Fe via inorganic Fe transporters at the cell surface (Hudson and Morel, 1990; Sunda and Huntsman, 1995b; Maldonado *et al.*, 2005).

It is thought that another mechanism that allows phytoplankton to acquire iron from organic Fe complexes involves photoreduction (Barbeau *et al.*, 2001). Some studies have shown that light enhances the rates of Fe uptake from all organic complexes studied so far.

It has also been proposed that the denticity of the ligands (the number of donor groups from a given ligand attached to the same central Fe atom) could also determine the bioavailability of the organic Fe complexes (Boukhalfa and Crumbliss, 2002; Maldonado *et al.*, 2005).

3.3 Materials and methods

3.3.1 Sampling

Water column samples were collected in the High Latitude North Atlantic Ocean (Figure 3.2, Table 3.1), during the RRS Discovery 354 in July-August 2010. Profile sampling was carried out using a titanium CTD frame, which was fitted with trace metal clean 10 L OTE (Ocean Test Equipment) sampling bottles (Steigenberger, 2010). Samples for Fe-binding ligands were collected at 15 stations, up to 15 depths on each (Table 3.1). Samples were filtered through a 0.2 µm pore size cartridge filters (Sartobran P-300, Sartorious) under slight positive pressure (oxygen-free N_2), and collected into 125 ml low density polyethylene (LDPE, Nalgene) bottles for dissolved Fe analysis, and into 250 ml high density polyethylene (HDPE, Nalgene) bottles for the Fe-binding ligand determination.

Organic Fe complexation in the HLNA

Sampling bottles were cleaned according to the standard protocol described by Achterberg *et al.* (2001), with slight modifications: LDPE and HDPE bottles were immersed in 5% detergent bath (Decon, Merck BDH) for 1 week. Bottles were then rinsed filling them with deionised water (MilliQ, Millipore, >18.2 MΩ cm^{-1}; the same quality used for all the cleaning steps) 6 times or until there was no trace of detergent, and immediately immersed in 6M analytical grade HCl bath (1 week, AnalaR grade, BDH Merck). Bottles were then rinsed filling them with deionised water 3 times, and immersed into 3M analytical grade HNO_3 bath (1 week, AnalaR grade, BDH Merck). Bottles were then rinsed filling them with deionised water 3 times, and then filled with deionised water and acidified to pH 2 with 1 ml UpA Q-HCl (9M) in a clean air (class-100) laboratory. Bottles were then put inside double plastic bags, sealed and stored inside a larger plastic bag within a plastic box until sample collection.

Table 3.1 Location and number of samples collected on each CTD cast during cruise D354 in summer 2010.

Location	Date	CTD	Lat (°N)	Long (°W)	# of samples
Iceland Basin	11/07/2010	002	60°00	19°58	12
	12/07/2010	004	60°02	19°55	12
	13/07/2010	005	61°48	21°05	14
	14/07/2010	006	60°02	19°55	12
Reykjanes Ridge	16/07/2010	008	60°02	29°00	13
Irminger Basin	18/07/2010	009	60°02	35°00	15
Greenland Slope	18/07/2010	011	59°59	41°35	11
	19/07/2010	012	59°59	41°59	6
	19/07/2010	014	59°59	42°39	8
Irminger Basin	22/07/2010	015	63°00	34°59	13
	23/07/2010	016	63°00	34°58	10
	24/07/2010	017	62°59	29°54	6
Iceland Shelf	02/08/2010	024	63°25	23°35	4
	02/08/2010	025	63°09	23°47	6
Reykjanes Ridge	03/08/2010	026	61°47	24°27	8

Seawater samples for dissolved Fe determination were filtered and acidified to pH~2 using nitric acid (Romil UpA) within twelve hours of collection (Steigenberger, 2010). Sample bottles for Fe-binding ligand analysis were rinsed thoroughly with deionised water and then with seawater before

collection. These samples were immediately frozen at -20°C (not acidified) for analysis on land. Samples were thawed just prior to analysis.

Samples for inorganic nutrients (nitrite+ nitrate, silicate and phosphate) were collected on Niskin bottles from the CTD's. These samples were analyzed onboard by Mark Stinchcombe, NOCS, using standard colourimetric methods (Grasshoff *et al.*, 1999).

3.3.2 Chemicals

All chemicals were prepared in a clean electrochemistry laboratory under a Class 100 laminar flow bench at room temperature (20°C), and using deionised water. A 0.02 M TAC (thiazolylazo-p-cresol; Sigma Aldrich) solution was prepared in triple quartz distilled methanol. The borate buffer solution (pH ~8.05) was prepared using boric acid in 0.3 M ammonia (Suprapur, Merck). Borate buffer was cleaned from iron contamination using the following procedure: after adjusting the pH, a TAC concentration of 10 µM was added to the borate solution and left to equilibrate overnight (~15 h). The buffer was then passed through a previously activated C_{18} SepPack column (Whatman) (activation by 10 ml of methanol, 10 ml of MQ and 10 ml of HCl) with the help of a small peristaltic pump, until the solution was clear.

Iron standard solutions were prepared using a 1000 mg/L Fe ICP-MS stock solution (Fisher Scientific).

3.3.3 Determination of dissolved iron (dFe)

Dissolved iron analysis was determined by Sebastian Steigenberger (NOCS), using the isotope dilution approach followed by HR-ICPMS detection (high resolution magnetic sector inductively coupled mass spectrometry) following the methods described in Milne *et al.* (2010). Certified Reference Materials, detection limits and blank values used for the dissolved trace metal determination for the samples collected during the D354 research cruise are provided in Appendix A.

3.3.4 Determination of Fe (III) organic binding ligand concentrations [$L_{,Fe}$]

Fe (III)-binding ligand concentrations [$L_{,Fe}$] were determined using the CLE-ACSV method with TAC as the competing ligand (Croot and Johansson, 2000).

200 ml of seawater was buffered to pH 8.05 (5 mM Borate buffer) and subsequently TAC solution was added to a final concentration of 10 µM. After 1-2 hr equilibration, an aliquot of 15 ml of the sample was pipetted to a set of 12 x 30 ml preconditioned Teflon FEP bottles. Iron (5 x 10^{-7} M Fe (III) standard solution) was added to all but 2 of these bottles, yielding concentration additions from 0 to 8 nM, and then allowed to equilibrate overnight (>15 h) at room temperature (~20°C).

The samples were analyzed next day after equilibration using an electrochemical system consisting of a potentiostat (µAutolab Echochemie, Netherlands) with a static mercury drop electrode (Metrohm, 663 VA stand), a KCl reference electrode (Ag/AgCl in 3 M KCl saturated with AgCl) and a counter electrode of glassy carbon. The TAC-Fe analysis was performed using the following procedure: 1) removal of oxygen for 5 min with nitrogen (oxygen free grade) gas, after which 5 fresh mercury drops were formed, 2) a deposition potential of -0.40 V applied for 120 s whilst the solution was stirred, and 3) at the end of the adsorption period the stirrer was stopped and the potential was scanned from -0.3 to -0.65 V using the differential pulse method. The stripping current (peak height) from the reduction of the adsorbed $Fe(TAC)_2$ complex was recorded.

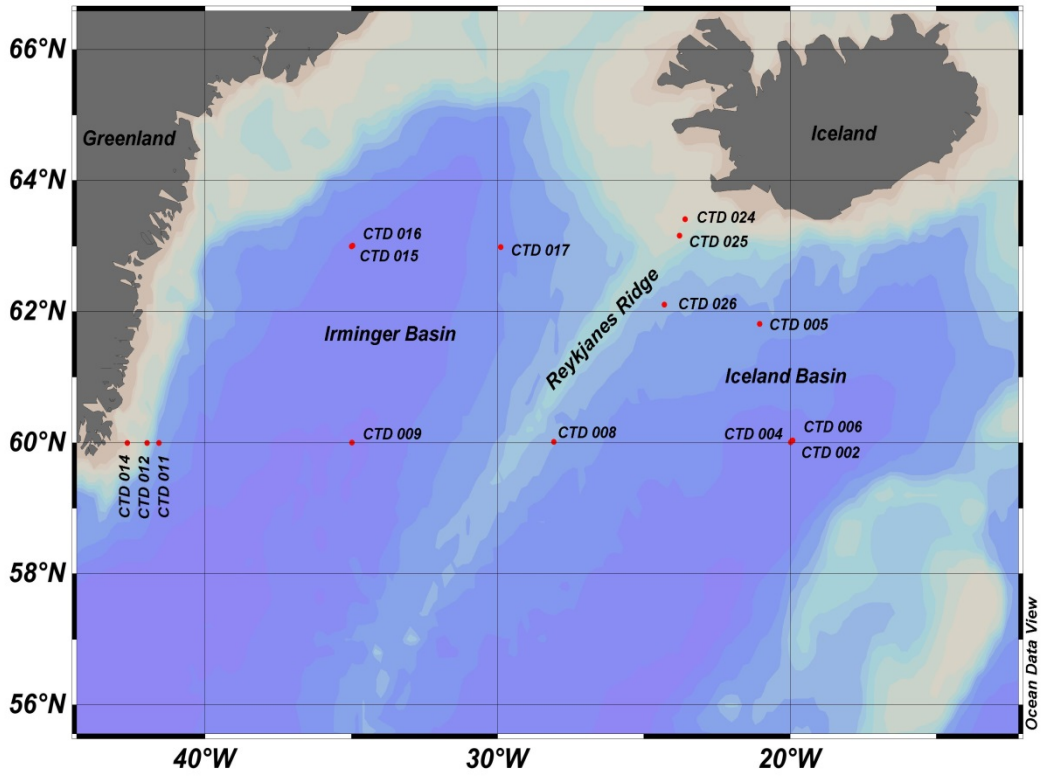

Figure 3.2 CTD casts during RRS Discovery 354 (summer 2010).

3.3.5 Theoretical considerations

The theoretical considerations for the calculation of ligand concentration from titration data for labile metal concentrations have been widely described (van den Berg and Kramer, 1979; Ruzic, 1982; van den Berg, 1982a). A synthesis of the method for the calculation of [$L_{,Fe}$], using TAC as the competing ligand, is as follows:

The equilibrium equation for the association between Fe^{3+} and one class of natural organic ligands L is:

$$[Fe^{3+}] + [L'] \leftrightarrow [FeL] \qquad (3.1)$$

where [Fe^{3+}] is the free ferric ion concentration, and [L'] is the concentration of L not complexed by Fe (free [L'] and complexes of L with the major cations, protons and maybe other trace metals).

The equilibrium expression for this equation is:

$$K'_{FeL} = [FeL]/[Fe^{3+}][L'] \qquad (3.2)$$

where K'_{FeL} is the conditional stability constant for the formation of the FeL complex, and is conditional upon the seawater composition (salinity, pH and competing trace metals).

The total ligand concentration (free and complexed species) in a given sample is represented by C_L:

$$C_L = [L'] + [FeL] \quad (3.3)$$

Equations (3.2) and (3.3) form the basis of the linear relationship between $[Fe^{3+}]$ and [FeL].

By substituting [L'] from equation (3.3) into equation (3.2), the following relationship is obtained (see Appendix B):

$$\frac{[Fe^{3+}]}{[FeL]} = \frac{[Fe^{3+}]}{C_L} + \frac{1}{K'_{FeL}\,[C_L]} \quad (3.4)$$

A plot of $[Fe^{3+}]/[FeL]$ as a function of $[Fe^{3+}]$ produces a straight line, assuming a simple model of 1:1 complex formation (Fe^{3+} complexation by only one type or class of organic ligand; Ruzic (1982); van den Berg (1982a)).

During this study, the plots produced were linear. The reason for the linearity is the limited range of the iron concentration covered by the titration and detection of only a certain group of natural ligands (L_i) determined by the ACSV detection window (which is dependent on the type and concentration of the added ligand used (TAC in this study)).

Data for the calculation of the complexing ligand concentration were obtained from a titration of each seawater sample with iron. The FeL concentration at each point of the titration is calculated from the total dissolved Fe concentration C_{Fe}:

$$[FeL] = C_{Fe} - [Fe_{labile}] \quad (3.5)$$

where C_{Fe} equals to the iron concentration initially present in the sample augmented by that added during titration. The labile Fe concentration is that which reacts and equilibrates with the added ligand (TAC), and includes all inorganic Fe and the Fe released from complexes with L upon addition of TAC.

C_{Fe} was obtained using the isotope dilution approach followed by HR-ICPMS detection (high resolution magnetic sector inductively coupled mass

spectrometry) following the methods described in Milne *et al.* (2010), by Sebastian Steigenberger, NOCS (dissolved Fe analysis), along with the Fe added at each point of the sample titration.

In the presence of TAC, equation (3.5) becomes:

$$C_{Fe} = [Fe'] + [Fe(TAC)_2] + [FeL] \quad (3.6)$$

where [Fe'] is the concentration of inorganic Fe (not complexed by TAC or natural organic complexing ligands, but either free or complexed with inorganic ligands), and [$Fe(TAC)_2$] is the concentration of Fe complexed by TAC.

Substitution of equation (3.6) into equation (3.5) gives the following expression for labile Fe concentration:

$$[Fe_{labile}] = [Fe'] + [Fe(TAC)_2] \quad (3.7)$$

The CSV peak height (i_p) is related to the labile Fe concentration via the sensitivity:

$$i_p = S[Fe_{labile}] \quad (3.8)$$

Where S is obtained from the slope of the titration curve at high concentration of total (and labile) iron where all organic ligands (L) are saturated (high end of the titration).

[Fe^{3+}] is directly related to the labile Fe concentration by α', which is the overall α-coefficient (Ringbom and Still, 1972) for inorganic complexation and complexation by TAC (excluding complexation by L):

$$[Fe^{3+}] = [Fe_{labile}]/\alpha' \quad (3.9)$$

Substitution for Fe^{3+} from equation (3.9) into equation (3.4) gives:

$$\frac{[Fe_{labile}]}{[FeL]} = \frac{[Fe_{labile}]}{C_L} + \frac{\alpha'}{K'_{FeL}[C_L]} \quad (3.10)$$

This equation is more convenient to use for the van den Berg/Ruzic plots, as it is the labile Fe concentration which is measured by ACSV rather than Fe^{3+}.

α' is calculated from:

$$\alpha' = \alpha_{Fe'} + \alpha_{Fe(TAC)2} \quad (3.11)$$

where $\alpha_{Fe'}$ is the α-coefficient for inorganic complexation of Fe^{3+} (log $\alpha_{Fe'}$=10 is the value used in this study and was calculated by Hudson *et al.* (1992), and $\alpha_{Fe(TAC)2}$ is the α-coefficient for complexation of Fe by TAC.

$$\alpha_{Fe(TAC)2} = \beta'_{Fe(TAC)2}[TAC]^2 \quad (3.12)$$

and the conditional stability constant $\beta'_{Fe(TAC)2}$ is defined by:

$$\beta'_{Fe(TAC)2} = [Fe(TAC)_2]/[Fe^{3+}][TAC']^2 \quad (3.13)$$

where [TAC'] is the concentration of TAC not complexed by iron.

As $C_{TAC} >> C_{Fe}$, the total concentration of TAC (C_{TAC}) was used in this study.

A value of log $\beta'_{Fe(TAC)2}$ = 12.4 (or in Fe^{3+} notation of log $\beta'_{Fe(TAC)2}$ = 22.4) was used in this work following Croot and Johanson (2000). Values for $\alpha_{Fe(TAC)2}$ were then calculated from log $\beta'_{Fe(TAC)2}$ along with the final TAC concentration in each sample (10 µM).

The values for $[Fe_{labile}]$ in equation (3.10) were obtained directly from the ACSV current as $[Fe_{labile}] = i_p/S$, and the concentration of [FeL] from equation (3.5).

Values of C_L and K'_{FeL} are calculated by least squares linear regression from the slope^{-1} and α'/(y-intercept x C_L) of the plot $[Fe_{labile}]/[FeL]$ as a function of $[Fe_{labile}]$.

Values of log K'_{FeL} are referred in terms of Fe^{3+} throughout this whole chapter.

Linearisation plots

Examples of the titration curves obtained for the samples in this study are shown in Figure 3.3 (left side plots). The curvature at low total iron concentrations indicates the presence of complexing ligands (e.g. CTD 004-03 in this Figure). The corresponding linear transformation plots for each titration curve are shown in the right side of Figure 3.3.

Iron ligand parameters were obtained employing the theoretical considerations above mentioned, along with the non-linear approach described in Chapter 4. The calculations were made with a script code in the R programming language. An example of graphic results obtained with the R programme is shown in Appendix C. Further details are presented in chapter 4.

CTD 004-03, Iceland Basin

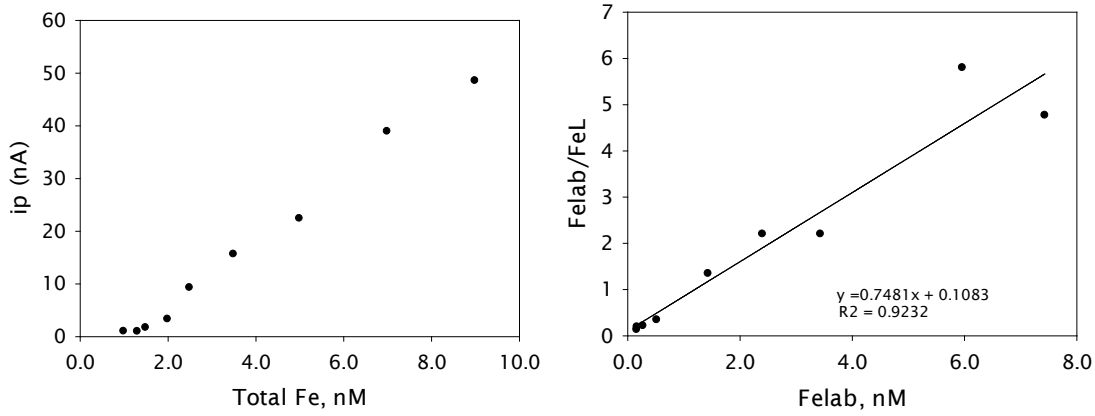

CTD 002-08, Iceland Basin

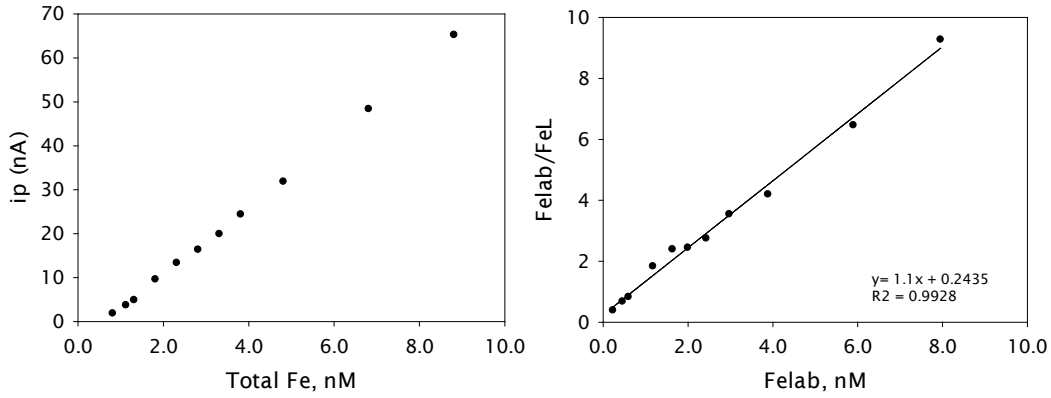

CTD 009-13, Irminger Basin

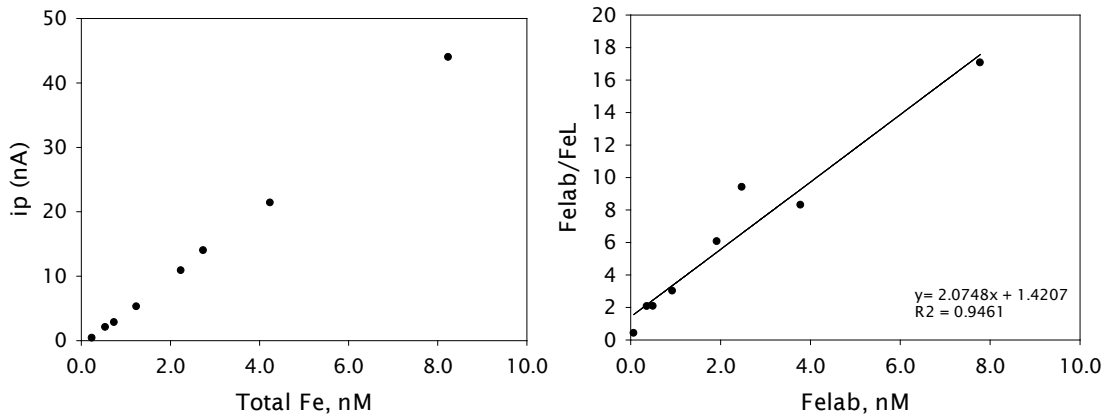

Figure 3.3 Examples of iron titration curves (left plots) with respective linear transformation plot (right plots).

Organic Fe complexation in the HLNA

Excess ligands

Results in this study are described as a function of excess ligand concentrations [eL_i]:

$$eL_i = C_L - [dFe]$$

3.4 Results and discussion

3.4.1 Study area

The high-latitude North Atlantic Ocean has climatic importance because the Nordic Seas and the Labrador and Irminger basins are regions where cold, dense waters are formed (Curry and Mauritzen, 2005). During these processes, atmospheric CO_2 is sequestered, and residual nutrients are transferred to the deep ocean.

3.4.1.1 Water masses

The sampling stations visited during this study are shown in Figure 3.2. Water mass definitions by Fogelqvist *et al.* (2003) are used here to describe the physical properties of the study area.

Iceland basin

During cruise D354, Northeast Atlantic Water (NEAW) with a salinity of 35.26-35.31 and a potential temperature between 8.11-9.03 ˚C was observed in the subsurface and mid-depth waters of the Iceland Basin, from around 45 to 750 m depth (Figure 3.4). It had been observed in previous studies that this water mass dominates the northern Iceland Basin and Reykjanes Ridge region (Read, 2001).

The North Atlantic Current (NAC) is one of the two main branches of the Gulf Stream extension (Sy, 1988). It flows northwards through the Iceland and Irminger Basins (Read, 2001). A significant number of eddies occur within the Iceland Basin which aid the transfer of water across the barrier of the NAC.

North Atlantic Central Water (NACW) was also evident at mid-depth waters in the Iceland Basin and Reykjanes Ridge region, with salinities from ~35.10-35.22 and potential temperatures from ~7.5 – 10 ˚C.

In deep waters of the Iceland Basin (as observed in CTD 004), from ~1770-2060 m, the potential temperature decreased to 3.2-3.4 ˚C with a salinity of ~34.91, indicating the presence of Labrador Sea Water (LSW_e; Figure 3.4). LSW_e and LSW_w are the notations used for Labrador Sea Water in the Iceland Basin and in the Irminger Basin, respectively, as this water mass has different characteristics in each basin.

Northeast Atlantic Deep Water (NEADW) was present at the bottom layer of the Iceland Basin (CTD 004), from ~2380-2720 m, with salinities around 34.95-34.99 and a potential temperature of 2.60-2.98˚C (Figure 3.4). The NEADW is characterised by high oxygen and tracer values (halocarbons CFC-11, CFC-12 and CFC-113), and low silicate contents.

According to Fogelqvist *et al*. (2003), the Iceland-Scotland Overflow Water (ISOW) is situated from around 850 m to a depth about 2300 m in the Iceland Basin, mixing with the overlying water masses along its pathway. However, ISOW was not evident in the Iceland Basin during this study probably due to the fact that our stations were sufficiently far removed from the overflow regions and the mixing that this water mass experiences with NEAW, LSW_e and NEADW during its subduction to deeper waters had removed its distinct signature.

Irminger Basin

Irminger Sea Water (ISW) is an Atlantic water mass that is mainly supplied by the Irminger Current, and is mainly found in the northern Irminger Basin (Krauss, 1995; Fogelqvist *et al*., 2003). ISW was evident in the mid-depth layers of the northern part of the Irminger Basin (from ~300-400 m depth in CTD 016), with potential temperatures between 5.59-6.14 ˚C and salinities from 35.02-35.05 (Figure 3.4).

The deep water masses that were present in the Irminger Basin during this study were ISOW, LSW_w and Denmark Strait Overflow Water (DSOW).

ISOW was present during this study in the Irminger Basin from ~1690-1750 m in CTD 009, and from 2260-2370 m in CTD 015, with salinities ~34.92 and potential temperatures from 2.73-2.90 ˚C.

LSW_w was observed with salinities from 34.89-34.90 and potential temperatures from 1.9-2.5 ˚C at around 2400 m in CTD 015, and from 2900-3100 m in CTD 009 (Figure 3.4).

The characteristics of LSW in the Irminger Basin have indicated in previous studies that the water is of very recent origin, thus confirming that cold, fresh intermediate (depth) water spreads northwards from the Labrador Sea directly into the Irminger Basin and crosses the Mid Atlantic Ridge south of 54 ºN to spread northwards into the Iceland Basin and Rockall Trough (Talley and Mccartney, 1982).

DSOW was present at the bottom waters of the Irminger Basin from ~2630-2670 m, with potential temperatures from 1.2-1.7˚C and salinities of ~34.9 (Figure 3.4).

3.4.1.2 Inorganic nutrients

Inorganic nutrient concentrations (nitrite + nitrate, phosphate and silicate) displayed strong gradients in the study area during D354, with increasing surface water concentrations moving from east to west; therefore higher nutrient concentrations were observed in the Irminger Basin compared to the Iceland Basin. In the Irminger Basin, increasing surface nitrite + nitrate concentrations from east to west were observed and ranged ca. between 2-5.5 µM (Figure 3.5). Phosphate and silicate concentrations showed the same spatial pattern as for nitrite + nitrate, with surface phosphate concentrations from around $\geq$ 0.2-0.45 µM (Figure 3.6), and silicate concentrations from around 2-4 µM (Figure 3.7). The opposite trend was observed in the Iceland Basin: nitrite + nitrate concentrations were generally lower than 0.1 µM, whereas phosphate concentrations were lower than 0.18 µM and silicate concentrations $\leq$ 1.5 µM (data from D354 cruise report by Stinchcombe (2010)).

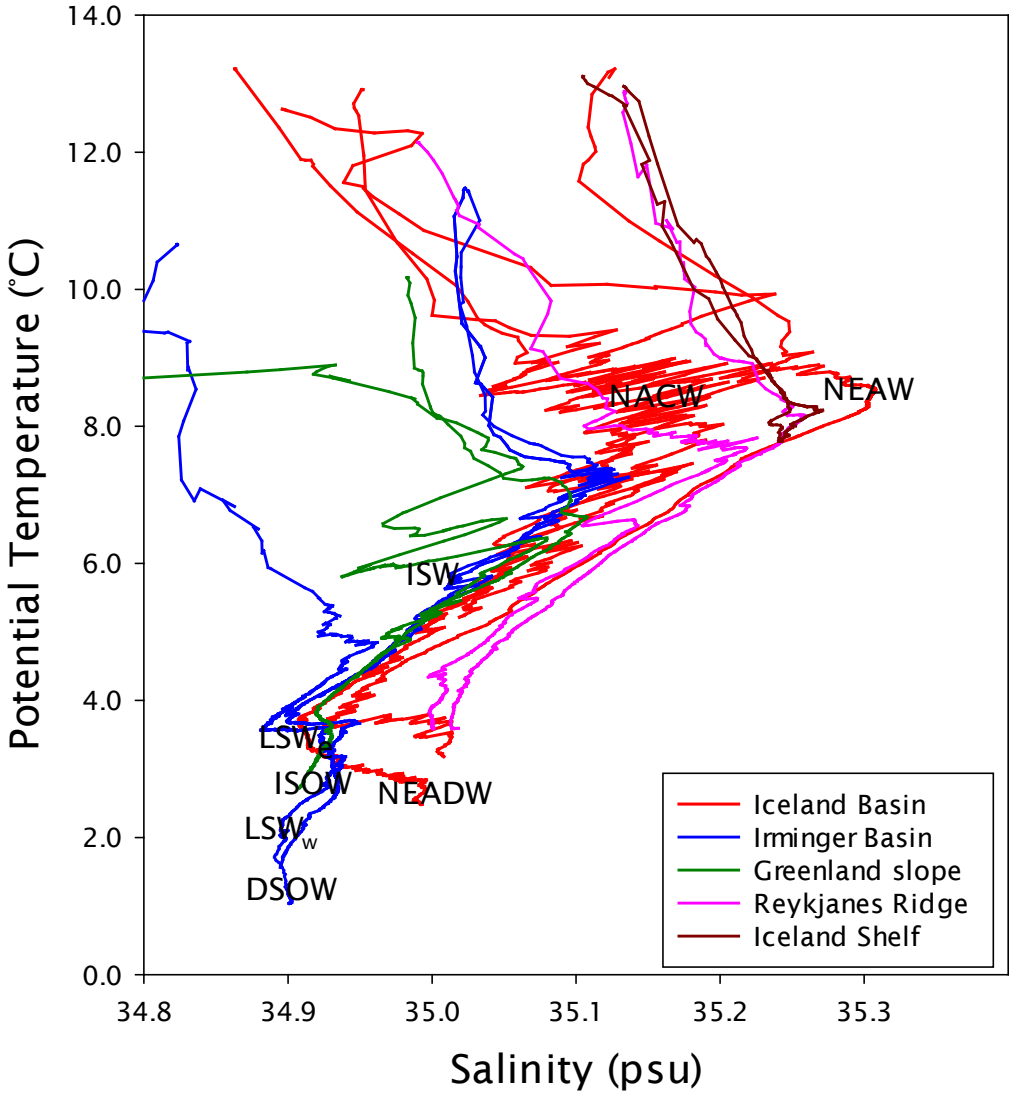

Figure 3.4 TS diagram for the study area during D354 2010 cruise.

The high nutrient concentrations in the Irminger Basin indicated that production failed to exhaust the nutrient stocks due to Fe limitation (Ryan-Keogh *et al.*, 2013), as inferred from the very low dissolved iron concentrations in surface waters of this basin (< 0.1 nM in the upper 20 m for CTD 009 and CTD 015). These residual nutrients concentrations are similar to those that have been observed in HNLC regions such as the Southern Ocean (Steigenberger, 2010).

A nutrient profile in the Iceland Basin (CTD 002) was compared to one in the Irminger Basin (CTD 016). Although all of the inorganic nutrient concentrations are very similar at depth, there are significant differences in the upper water column (~10 m). In the CTD 002 profile, both phosphate and nitrite + nitrate

concentrations were lower than 0.1 µM, whilst silicate concentrations were below 1 µM. In the CTD 016 profile, nitrite + nitrate concentrations were >4 µM, >0.3 µM for phosphate and ~2 µM for silicate (data from D354 cruise report by Stinchcombe (2010)).

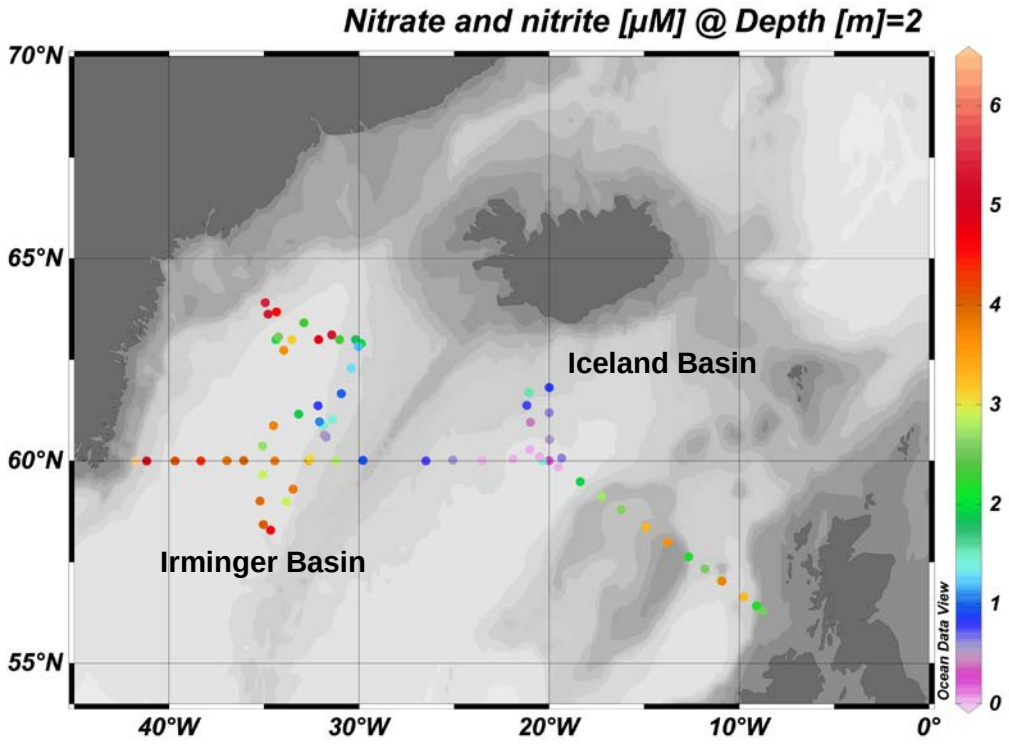

Figure 3.5 Surface nitrite NO_2^- + nitrate NO_3^- (µM) from the underway nutrient data during the D354 research cruise.

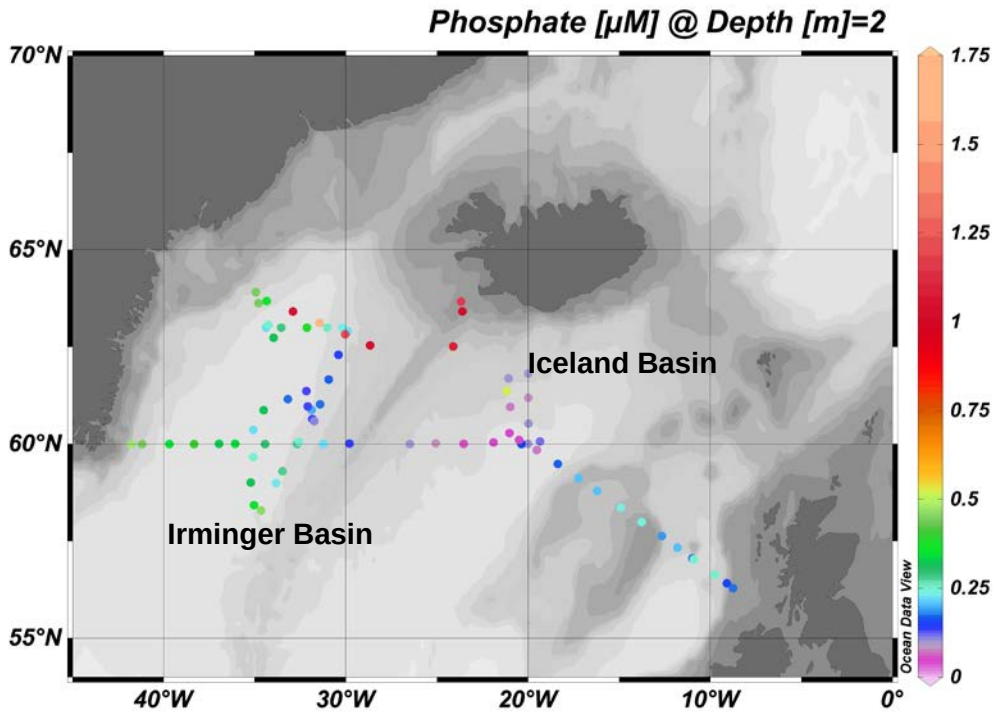

Figure 3.6 Surface phosphate PO_4^{-3} (µM) from the underway nutrient data during the D354 research cruise.

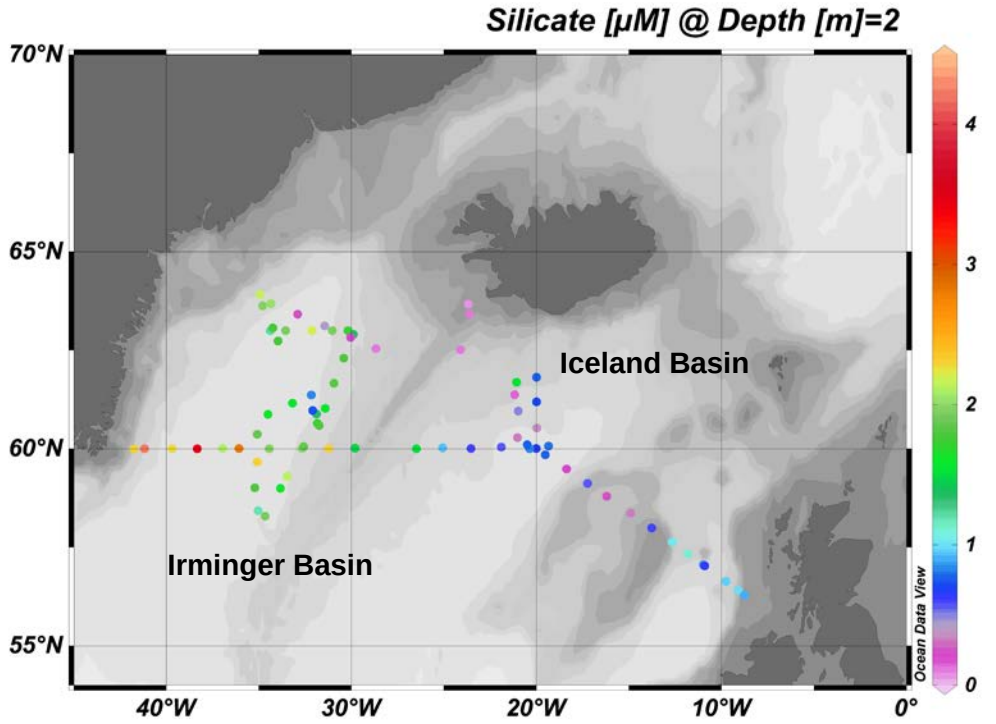

Figure 3.7 Surface silicate SiO_3^{-2} (µM) from the underway nutrient data during the D354 research cruise.

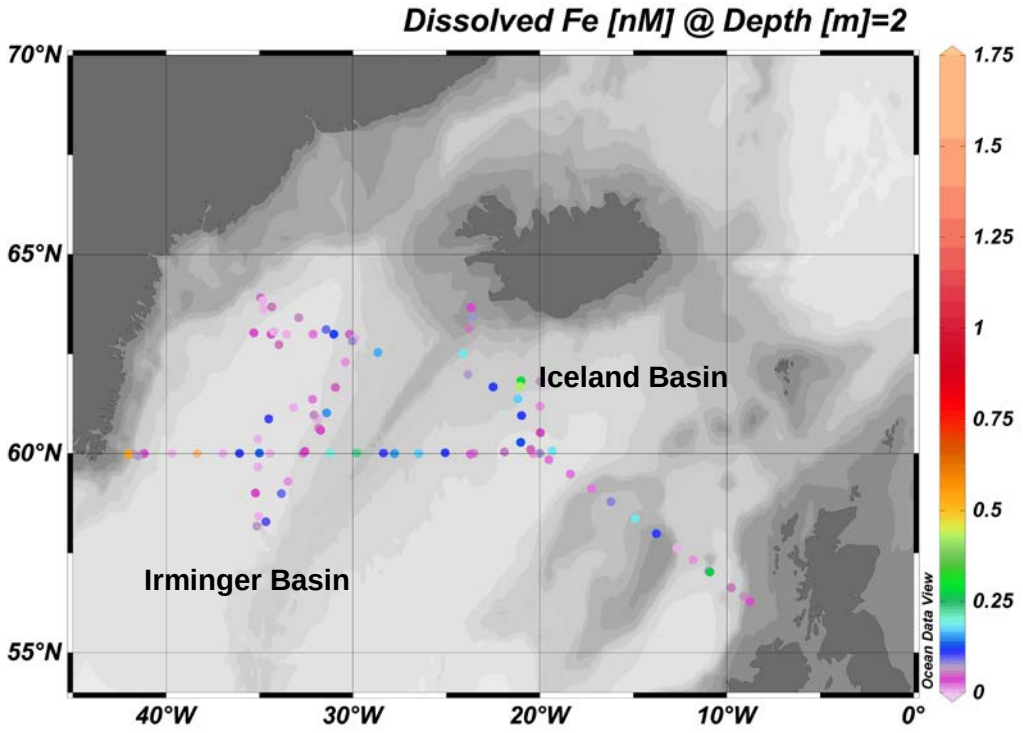

Figure 3.8 Surface dissolved iron concentrations (nM) during the D354 research cruise.

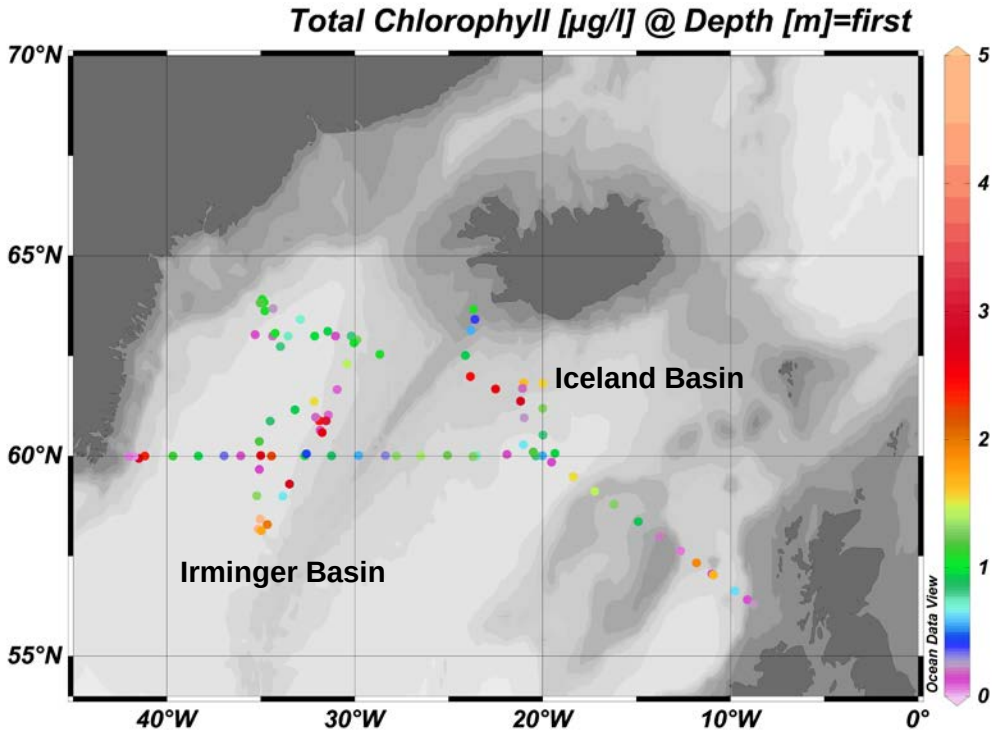

Figure 3.9 Surface total chlorophyll (µg/l) from the underway data during the D354 research cruise.

3.4.1.3 Total chlorophyll

Total chlorophyll values for all of the study area ranged between 0 and 3.2 µg/l, except for CTD 014 profile in the Greenland slope, which presented the highest chlorophyll values in the area at depths between 20-30 m (~4.55 µg/l) (Figure 3.9). The maximum profile values were observed in surface waters in all basins (≤ 10 m), decreasing to low concentrations at around 50 m depth (Figure 3.10). The lowest surface chlorophyll values were observed in the northern Irminger Basin (CTD 015 and CTD 016; ≤ 1.07 µg/l), and in general in the Iceland Basin (≤ 1.8 µg/l).

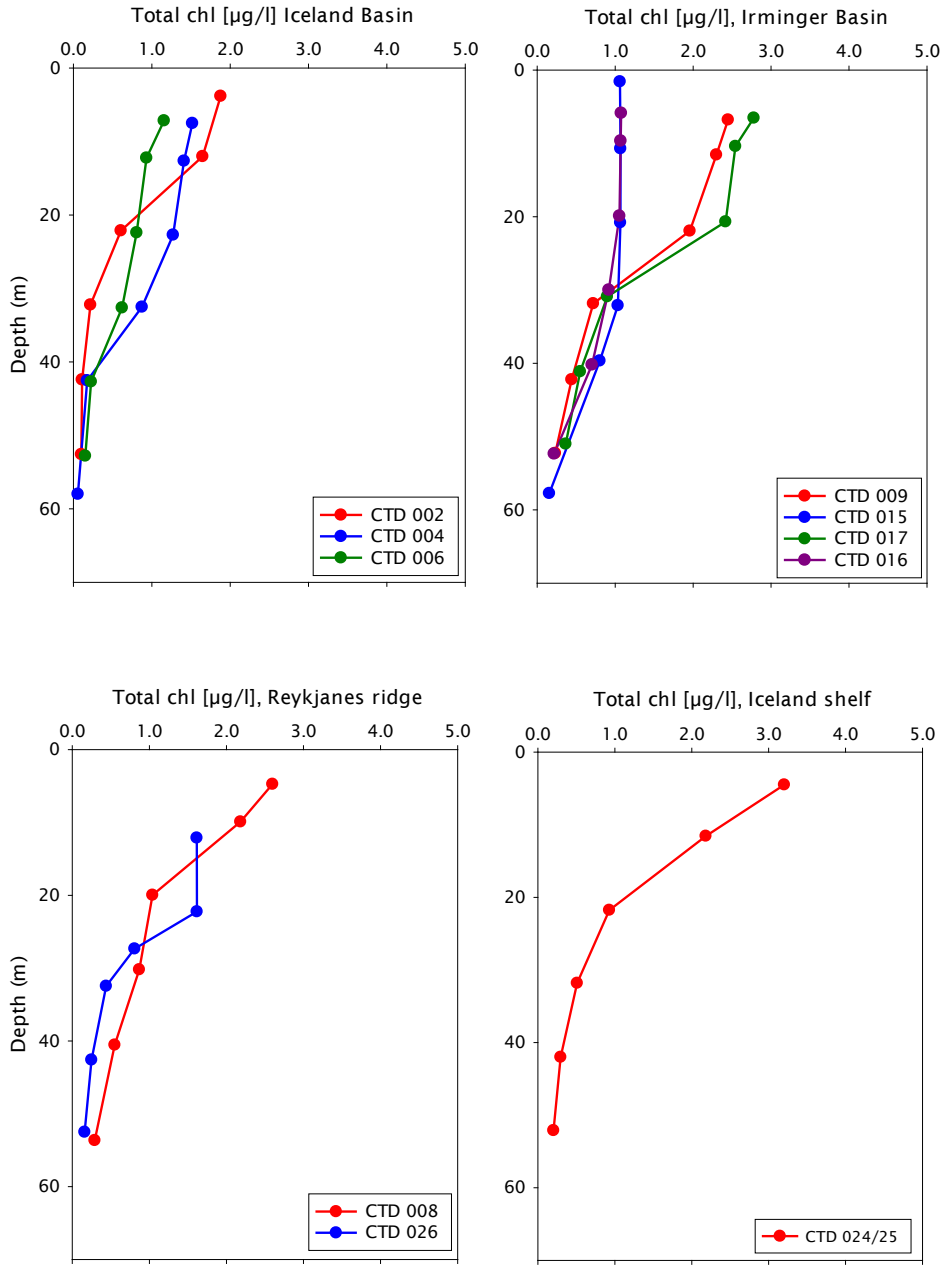

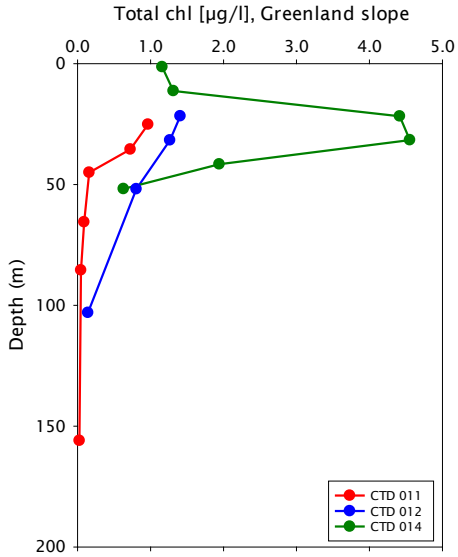

Figure 3.10 Total chlorophyll [µg/l] for the different CTD stations in the study area.

3.4.2 Dissolved iron (dFe) distribution

For most of the stations occupied during this study, dissolved iron concentrations [dFe] presented a nutrient type profile, with lower concentrations in the surface waters (down to ~30 m (Figure 3.8), between 0.03 and 0.37 nM except at CTD 014 in the Greenland slope, where values >0.5nM were observed at the surface (Figure 3.11). Along the Greenland slope, CTD 014 is a coastal station and its profile showed a rapid increase to approximately 1.2 nM in the upper 40 m. It has to be noted that all of the [dFe] values referred to during this chapter are only for data points for which a ligand concentration has been obtained. In subsurface waters at all stations down to ~150 m, [dFe] increased up to 1.37 nM (except at 100 m in CTD 015, where a high value of 3.35 nM was observed). CTD 002, in the central Iceland Basin, also showed a high [dFe] (0.85 nM at 40 m, just below the mixed layer that was persistent for at least 3 days (Steigenberger, 2010)). Below 1000 m depth, [dFe] were variable, although generally $\geq$0.6 nM (Figure 3.11).

The [dFe] in surface and subsurface waters ($\leq$150 m) of the Iceland Basin (CTD 002, 004, 005 and 006) ranged between 0.08 and 0.85 nM with an average concentration (average $\pm$ standard deviation) of 0.28 $\pm$ 0.15 nM (n=26). This average concentration is very similar to that reported on a previous study in

the same area during a summer cruise in 2009 (Mohamed *et al.*, 2011), with an average value of 0.24 ± 0.17 nM for the same depth.

Surface and subsurface [dFe] in the Irminger Basin (CTD 009, 015, 016, 017) ranged between 0.01 and 0.73 nM, with an average concentration of 0.18 ± 0.16 nM (n=21). Surface and subsurface [dFe] along the Reykjanes Ridge (CTD 008, 026) and on the Iceland Shelf (CTD 024, 025) were also depleted compared to deep waters, and ranged between 0.08 and 0.42 nM, with an average concentration of 0.27 ± 0.13 nM (n=8) along the Reykjanes Ridge, and between 0.03 and 0.44 nM, with an average concentration of 0.20 ± 0.16 nM (n=5) on the Iceland Shelf, except at 140 m in CTD 024, where a [dFe] of 1.37 nM was observed. The [dFe] in surface and subsurface waters of the Greenland slope (CTD 011, 012, 014) ranged between 0.08 and 1.21 nM, with an average concentration of 0.51 ± 0.33 nM (n=14). These relatively high values compared to the other areas during this study are a result of a coastal station in this area (CTD 014).

The low dFe concentrations found in the upper 30 m of all of the areas may be a consequence of biological uptake, indicated by the high total chlorophyll values found in surface waters during this study, in particular in surface waters of the Greenland slope (> 4 µg/l), combined with low atmospheric inputs. As mentioned before, it is known that the HLNA receives very low atmospheric inputs, comparable to those in the HNLC North Pacific (Boyd *et al.*, 2007). It has been demonstrated that dissolved aluminium (dAl) concentrations in open ocean surface waters can be used to estimate atmospheric dust fluxes to these areas, and thus it can serve as a tracer of atmospheric inputs of iron (Steigenberger, 2010). During cruise D354, surface dAl concentrations were low in both the Iceland and Irminger Basins (1.37 and 0.60 nM average for the Iceland and Irminger Basin, respectively; Klar, (2010)) from which it can be inferred that low atmospheric inputs occurred at the time of this study. However, it has been suggested that even with high dust aerosol input in surface waters, most of the supplied atmospheric Fe will form colloids and particles quickly and be removed from the surface waters (Kondo *et al.*, 2008).

Such low dFe values can limit phytoplankton primary production, as has been observed in both the Iceland and central Irminger Basins (Moore *et al.*, 2005; Nielsdottir *et al.*, 2009; Ryan-Keogh *et al.*, 2013). Although the eruption of the

Organic Fe complexation in the HLNA

Icelandic volcano (Eyjafjallajokull) in spring 2010 resulted in significant dissolved iron inputs to the surface of the Iceland Basin during spring 2010, there was no evidence of these enhanced concentrations during July-August 2010 (Achterberg *et al.*, 2013). This indicates the short residence time of dissolved Fe in the surface ocean (weeks to months) (Achterberg *et al.*, 2013).

At mid depths, [dFe] increased in the water column at all stations between >150 and 1000 m in this study. The mid-layer depth [dFe] in the Iceland Basin ranged between 0.25 and 1.03 nM, with an average of 0.71 $\pm$ 0.23 nM (n=13). In the Irminger Basin, [dFe] at mid depths ranged between 0.23 and 0.73 nM, with an average of 0.45 $\pm$ 0.17 nM (n=9). The mid-layer depth [dFe] on the Greenland slope ranged between 0.45 and 1.21 nM, with an average of 0.70 $\pm$ 0.26 nM (n=8). The mid-layer depth [dFe] along the Reykjanes Ridge ranged between 0.48 and 0.98 nM, with an average of 0.81 $\pm$ 0.21 nM (n=7), and on the Iceland Shelf ranged between 0.68 and 2.23 nM, with an average of 1.33 $\pm$ 0.81 nM (n=3).

Dissolved Fe in the deep waters (below ~1000 m) of the study area ranged between 0.39 and 1.36 nM, with an average of 0.86 $\pm$ 0.29 nM (n=14). The slightly enhanced concentrations near the seafloor in the Iceland Basin (CTD 004 and 005), are likely due to benthic iron supplies (Laes *et al.*, 2007).

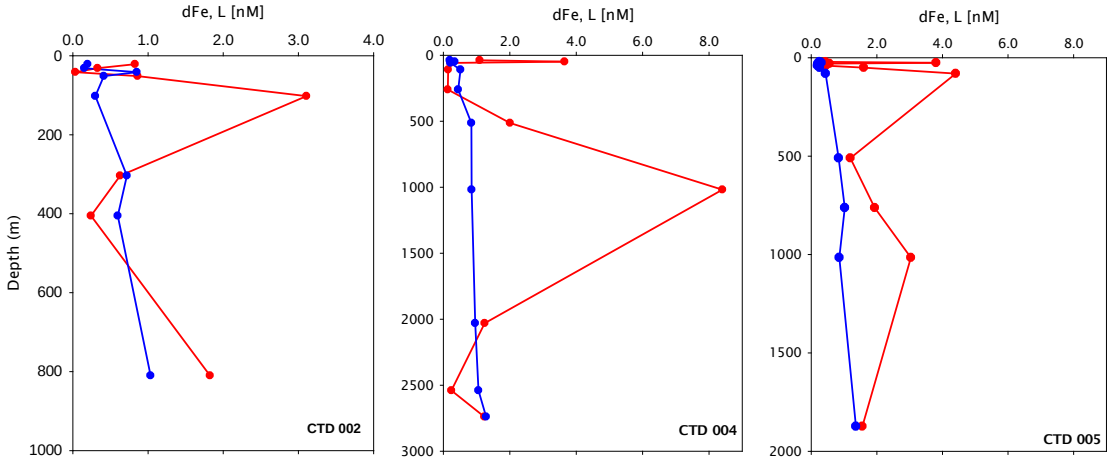

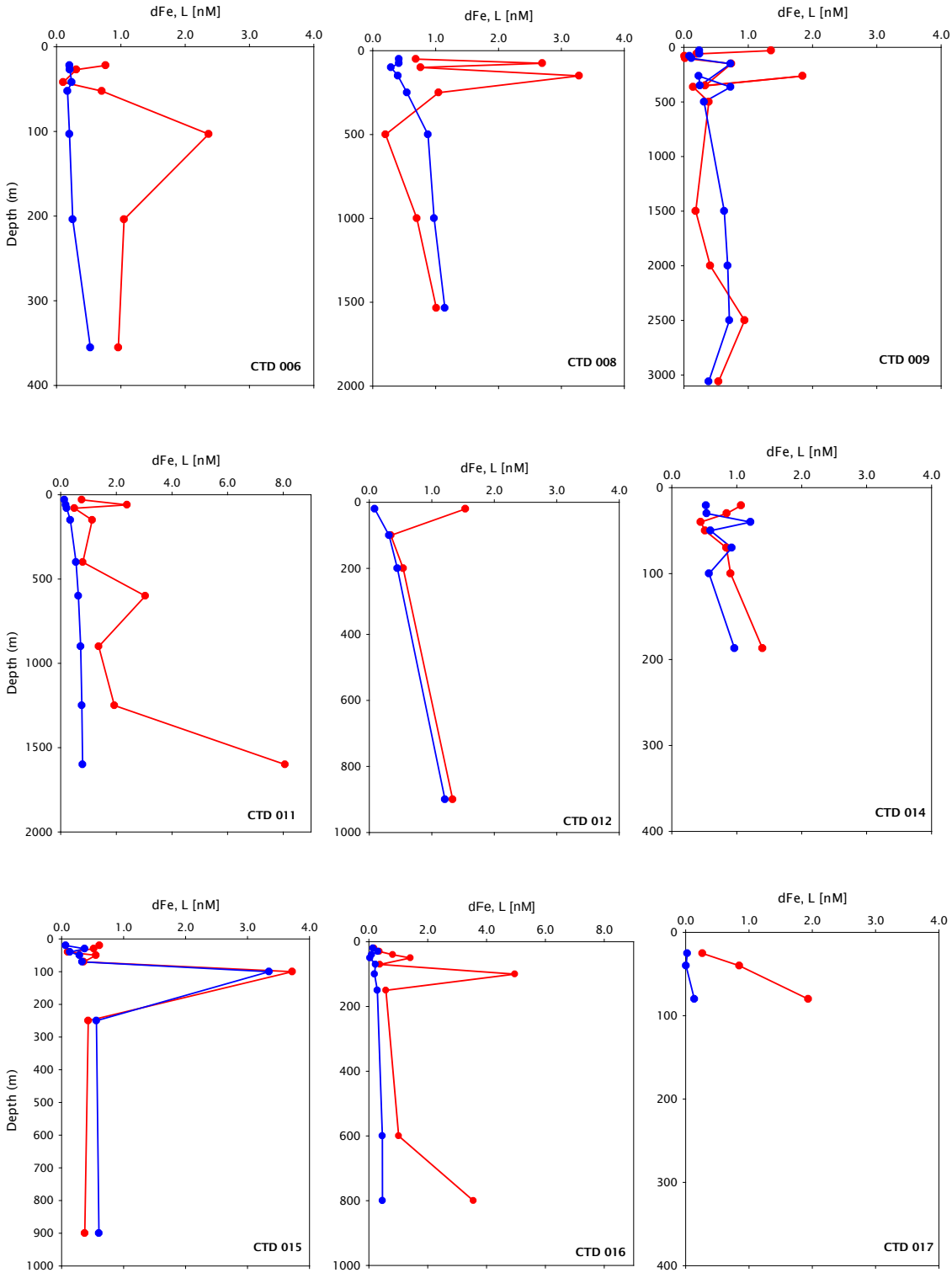
dFe, L [nM]
Depth (m)
CTD 006
CTD 008
CTD 009
CTD 011
CTD 012
CTD 014
CTD 015
CTD 016
CTD 017

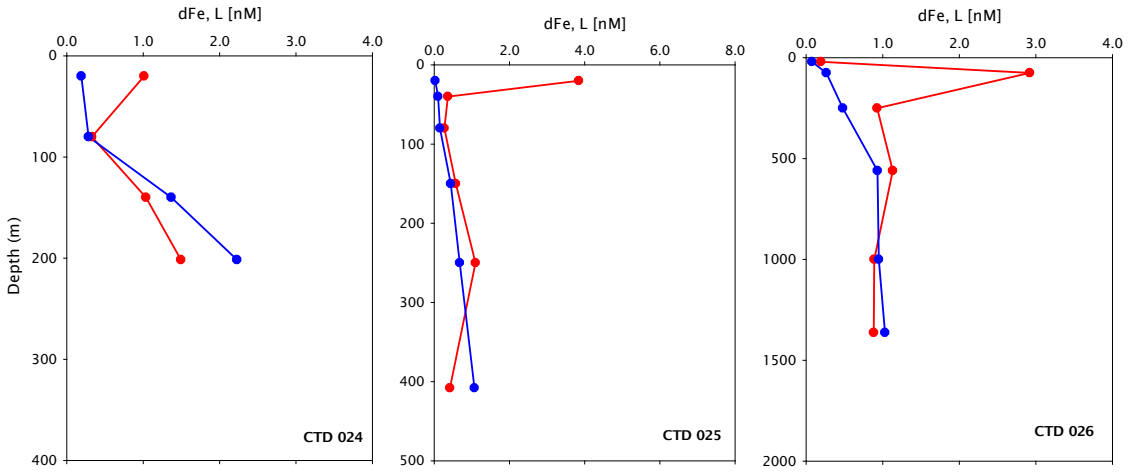

Figure 3.11 Vertical distribution of organic ligands ([L], in red) and of dissolved Fe ([dFe], in blue) for all the D354 cruise CTD stations. Concentrations are in nM.

3.4.3 Organic ligands

The organic Fe-binding ligand characteristics are presented in Table 3.2. Average total ligand concentrations [L] at different water column depths, observed during this study, can be found in Table 3.3. Water column profiles for [L] are presented in Figure 3.11.

The total ligand concentrations [L] in the surface and subsurface waters ($\leq$ 150 m) of the Iceland Basin ranged between 0.03 and 4.41 nM with an average concentration (average $\pm$ standard deviation) of 1.29 $\pm$ 1.39 nM (n=20). In the first 150 m, [L] values in the Irminger Basin ranged between 0.01 and 4.96 nM, with an average concentration of 0.95 $\pm$ 1.24 nM (n=21). In the region of the Reykjanes ridge at the same depths, [L] ranged between 0.19 and 3.28 nM, with an average of 1.76 $\pm$ 1.35 nM (n=6). In the surface and subsurface waters of the Greenland slope, the values for [L] ranged between 0.35 and 2.39 nM, with an average of 0.94 $\pm$ 0.57 nM (n=12), and finally in surface and subsurface waters on the Iceland shelf, [L] ranged between 0.27 and 3.84 nM and averaged 1.06 $\pm$ 1.27 nM (n=7).

Table 3.2 Organic iron ligand characteristics (results obtained using the R programming software) for the samples collected during cruise D354. L.SE and log K.SE are the standard errors for ligand concentration and log K, respectively. Negative eL_i were considered as 0.00 nM for the range values. NA values are reported where the R program could not resolve the linear/non-linear fit.

CTD	depth	[dFe]	L,[nM]	L.SE, [nM]	log K	log K.SE	eLi, [nM]	L/dFe
002 #12	21.11	0.20	0.83	NA	NA	NA	0.63	4.20
002 #11	31.29	0.15	0.33	0.15	22.26	0.26	0.18	2.15
002 #10	41.43	0.85	0.03	NA	NA	NA	-0.82	0.04
002 #9	51.43	0.41	0.86	0.23	22.35	0.30	0.45	2.09
002 #6	102.09	0.30	3.11	NA	NA	NA	2.81	10.40
002 #4	303.79	0.72	0.63	0.16	21.76	0.41	-0.09	0.88
002 #3	405.22	0.60	0.24	0.15	22.63	0.80	-0.36	0.40
002 #1	809.95	1.03	1.82	NA	20.75	NA	0.79	1.76
004 #11	37.70	0.19	1.09	NA	NA	NA	0.90	5.69
004 #10	48.11	0.34	3.65	NA	20.63	NA	3.31	10.68
004 #9	57.83	0.21	0.22	0.20	22.15	0.62	0.01	1.03
004 #8	108.90	0.51	0.14	NA	NA	NA	-0.37	0.28
004 #7	260.11	0.44	0.13	NA	22.08	NA	-0.31	0.30
004 #6	513.02	0.84	2.01	0.66	22.09	0.49	1.16	2.38
004 #5	1018.24	0.85	8.40	3.43	21.72	0.23	7.55	9.89
004 #3	2030.18	0.96	1.24	0.13	23.42	0.41	0.29	1.30
004 #2	2539.90	1.06	0.24	NA	NA	NA	-0.82	0.23
004 #1	2739.28	1.29	1.23	0.09	23.94	0.61	-0.05	0.96
005 #14	20.67	0.25	0.43	NA	NA	NA	0.19	1.76
005 #13	25.53	0.31	3.81	1.11	21.32	0.09	3.50	12.31
005 #12	29.56	0.21	0.55	NA	NA	NA	0.35	2.70
005 #11	34.68	0.20	0.48	0.87	22.78	1.27	0.28	2.37
005 #10	40.01	0.19	0.44	NA	NA	NA	0.25	2.33
005 #9	50.14	0.26	1.60	0.58	21.67	0.58	1.35	6.27
005 #8	80.31	0.44	4.41	1.53	21.43	0.15	3.97	10.11
005 #5	509.76	0.83	1.19	0.36	22.18	0.41	0.36	1.43
005 #4	762.55	1.02	1.93	0.16	23.30	0.28	0.91	1.89
005 #3	1015.72	0.85	3.04	NA	21.02	NA	2.18	3.55
005 #1	1873.37	1.36	1.56	0.17	22.84	0.44	0.20	1.14
006 #12	21.95	0.20	0.76	NA	NA	NA	0.56	3.77
006 #11	26.94	0.21	0.31	NA	NA	NA	0.10	1.50
006 #9	41.89	0.24	0.10	NA	NA	NA	-0.13	0.44
006 #8	52.28	0.17	0.70	NA	NA	NA	0.53	4.13
006 #6	103.10	0.20	2.37	1.89	21.12	0.52	2.16	11.74

Organic Fe complexation in the HLNA

CTD	depth	[dFe]	L,[nM]	L.SE, [nM]	log K	log K.SE	eLi, [nM]	L/dFe
006 #4	203.93	0.25	1.05	NA	NA	NA	0.80	4.18
006 #3	355.35	0.53	0.96	0.30	22.66	0.50	0.43	1.83
008 #10	50.00	0.42	0.69	0.87	22.15	0.83	0.27	1.64
008 #9	75.00	0.42	2.70	1.03	21.25	0.21	2.28	6.47
008 #7	100.00	0.29	0.76	0.69	21.35	0.34	0.47	2.62
008 #6	150.00	0.40	3.28	NA	20.94	NA	2.88	8.19
008 #5	250.00	0.54	1.05	0.30	21.62	0.35	0.50	1.92
008 #4	500.00	0.88	0.20	NA	21.33	NA	-0.67	0.23
008 #2	1000.00	0.98	0.70	0.13	22.74	0.39	-0.27	0.72
008 #1	1535.00	1.15	1.01	0.13	22.23	0.44	-0.14	0.88
009 #14	30.00	0.24	1.36	3.33	20.60	0.26	1.12	5.67
009 #13	60.00	0.24	0.20	0.04	23.03	0.33	-0.05	0.81
009 #12	80.00	0.09	0.01	NA	NA	NA	-0.08	0.10
009 #11	100.00	0.12	0.02	NA	NA	NA	-0.10	0.16
009 #10	150.00	0.73	0.74	0.03	23.22	0.66	0.01	1.01
009 #9	350.00	0.25	0.33	NA	NA	NA	0.08	1.33
009 #8	262.25	0.23	1.85	3.00	20.79	0.41	1.62	8.04
009 #7	363.28	0.73	0.14	NA	22.56	NA	-0.58	0.20
009 #6	500.00	0.31	0.39	NA	NA	NA	0.07	1.24
009 #4	1500.00	0.63	0.18	0.10	22.67	0.94	-0.44	0.29
009 #3	2000.00	0.68	0.41	0.10	23.14	0.80	-0.27	0.60
009 #2	2500.00	0.71	0.94	NA	21.08	NA	0.24	1.33
009 #1	3060.00	0.39	0.54	0.27	21.08	0.32	0.15	1.40
011 #12	30.00	0.13	0.76	0.89	21.54	0.38	0.62	5.65
011 #10	60.00	0.18	2.39	NA	21.22	NA	2.20	13.11
011 #9	80.00	0.21	0.49	1.08	22.34	1.02	0.28	2.30
011 #8	150.00	0.35	1.13	0.69	21.73	0.36	0.79	3.27
011 #6	400.00	0.55	0.79	1.38	22.00	0.85	0.24	1.44
011 #5	600.00	0.64	3.04	13.34	21.36	0.75	2.41	4.78
011 #4	900.00	0.72	1.37	NA	NA	NA	0.65	1.90
011 #3	1250.00	0.76	1.93	NA	20.77	NA	1.17	2.54
011 #2	1600.00	0.79	8.07	7.93	21.72	0.50	7.28	10.24
012 #24	20.00	0.09	1.54	NA	22.57	NA	1.45	17.98
012 #7	100.00	0.32	0.34	0.10	22.38	0.32	0.03	1.09
012 #5	200.00	0.45	0.54	0.13	22.51	0.26	0.09	1.21
012 #2	900.00	1.21	1.33	NA	21.91	NA	0.12	1.10
014 #8	20.73	0.53	1.07	0.14	21.95	0.23	0.54	2.02
014 #22	30.00	0.54	0.85	0.05	22.29	0.16	0.31	1.58
014 #6	40.00	1.21	0.45	NA	NA	NA	-0.77	0.37

CTD	depth	[dFe]	L,[nM]	L.SE, [nM]	log K	log K.SE	eLi, [nM]	L/dFe
014 #5	50.00	0.60	0.51	NA	22.60	NA	-0.08	0.86
014 #4	70.00	0.92	0.84	0.06	23.73	0.52	-0.08	0.91
014 #3	100.00	0.57	0.91	0.11	22.15	0.27	0.33	1.58
014 #1	187.00	0.97	1.40	NA	21.42	NA	0.43	1.45
015 #13	20.00	0.07	0.61	0.45	21.43	0.39	0.54	9.31
015 #12	30.00	0.37	0.52	0.09	22.90	0.28	0.15	1.40
015 #11	40.00	0.13	0.10	0.11	22.48	0.80	-0.03	0.75
015 #10	50.00	0.29	0.55	0.22	21.98	0.36	0.26	1.92
015 #9	70.00	0.33	0.36	0.11	22.34	0.32	0.02	1.07
015 #8	100.00	3.35	3.72	0.08	22.97	0.22	0.38	1.11
015 #7	250.00	0.56	0.43	0.14	22.15	0.34	-0.13	0.77
015 #5	900.00	0.60	0.37	0.22	22.30	0.54	-0.23	0.62
016 #11	20.00	0.14	0.18	0.12	21.94	0.35	0.04	1.27
016 #10	30.00	0.30	0.36	0.16	21.40	0.46	0.05	1.18
016 #9	40.00	0.10	0.81	0.15	21.63	0.19	0.71	8.45
016 #8	50.00	0.04	1.41	NA	20.87	NA	1.37	38.36
016 #7	70.00	0.22	0.38	0.05	22.43	0.70	0.15	1.67
016 #6	100.00	0.19	4.96	NA	20.16	NA	4.77	25.93
016 #5	150.00	0.29	0.58	0.12	22.14	0.48	0.29	2.02
016 #2	600.00	0.46	1.01	0.36	21.33	0.29	0.55	2.21
016 #24	800.00	0.46	3.55	NA	21.00	NA	3.09	7.69
017 #14	25.21	0.03	0.26	NA	NA	NA	0.24	10.37
017 #12	40.00	0.01	0.85	NA	21.00	NA	0.84	153.61
017 #9	80.00	0.14	1.94	5.13	20.84	0.32	1.80	14.16
024 # 5	20.00	0.19	1.01	0.20	21.47	0.17	0.82	5.32
024 # 3	80.00	0.28	0.33	0.24	22.01	0.49	0.04	1.15
024 # 2	140.00	1.37	1.04	NA	21.79	NA	-0.33	0.76
024 # 24	201.58	2.23	1.49	0.23	23.24	1.05	-0.74	0.67
025 # 9	20.00	0.03	3.84	NA	21.15	NA	3.82	141.38
025 # 7	40.00	0.10	0.36	0.15	21.19	0.40	0.26	3.57
025 # 5	80.00	0.15	0.27	NA	NA	NA	0.12	1.77
025 # 3	150.00	0.44	0.57	0.14	22.26	0.43	0.14	1.31
025 # 2	250.00	0.68	1.10	0.11	22.71	0.78	0.42	1.62
025 # 24	408.00	1.07	0.42	0.08	23.13	0.95	-0.65	0.39
026 # 12	20.00	0.08	0.19	0.13	22.61	0.72	0.12	2.54
026 # 7	75.00	0.26	2.92	NA	21.20	NA	2.66	11.08
026 # 4	250.00	0.48	0.93	0.16	22.02	0.34	0.45	1.93
026 # 3	560.00	0.93	1.13	0.17	22.41	0.66	0.20	1.21
026 # 2	1000.00	0.95	0.89	0.07	22.77	0.64	-0.06	0.94

026 # 24	1363.00	1.03	0.88	0.11	23.23	0.50	-0.15	0.86

Mid-layer depth (>150-1000 m) [L] in the Iceland Basin ranged between 0.13 and 3.04 nM, with an average concentration of 1.30 $\pm$ 0.90 nM (n=10), except at 1000 m in CTD 004, where a ligand concentration value of 8.40 nM was observed. In the Irminger Basin, mid-depth [L] ranged between 0.14 and 3.55 nM, with an average of 1.01 $\pm$ 1.17 nM (n=8). In mid-layer depth waters on the Greenland slope, [L] ranged between 0.54 and 3.04 nM, with an average of 1.41 $\pm$ 0.87 nM (n=6). In the Reykjanes ridge, mid-depth water [L] ranged between 0.20 and 1.13 nM, with an average of 0.82 $\pm$ 0.33 nM (n=6); and finally, in the Iceland Shelf, mid-depth [L] ranged between 0.42 and 1.49 nM, with an average of 1.00 $\pm$ 0.54 nM (n=3).

Deep water ligand concentrations (> 1000 m) in the Iceland Basin ranged between 0.24 and 1.56 nM, with an average of 1.07 $\pm$ 0.57 nM (n=4). Deep water [L] in the Irminger Basin ranged between 0.18 and 0.94 nM, with an average of 0.52 $\pm$ 0.32 nM (n=4). Deep water [L] on the Greenland slope ranged between 1.93 and 8.07 nM (no average was calculated, n=2); and finally over the Reykjanes ridge deep water [L] ranged between 0.88 and 1.01 nM, with an average of 0.95 $\pm$ 0.09 nM (n=2).

Mohamed *et al*. (2011) also found high and variable ligand concentrations in the surface waters of the HLNA. They reported average [L] down to $\leq$ 150 m in the Iceland Basin of 0.50 $\pm$ 0.26 (n=19), and 0.64 $\pm$ 0.28 (n=14) for their cruises in summer 2007 and 2009, respectively, which are lower than the ones observed during this work for the same regions. During their June 2009 cruise, Mohamed *et al*. (2011) observed [L] in other areas of the HLNA (Hatton Rockall and Rockall Trough regions) of 1.11 $\pm$ 0.08 nM and 0.69 $\pm$ 0.16 nM in surface and subsurface waters down to 150 m, respectively, which are similar to the ones observed during this study in the different areas of the HLNA. Mid-layer depth waters [L] in the Iceland Basin observed during this study are similar to the values observed by Mohamed *et al*. (2011) of 1.28 $\pm$ 0.77 nM (n=10) and 1.24 $\pm$ 0.6 nM (n=15) for the same cruises.

Although the total chlorophyll values observed in surface waters of the Irminger Basin (CTD 009 and CTD 017) and in CTD 014 in the Greenland slope were relatively high ($\geq$2 µg/l), a clear relationship between this variable and [L] in surface-subsurface waters of the study area was not observed. Mohamed *et*

al. (2011) observed enhanced surface and subsurface water (≤ 150 m) concentrations of nitrate, phosphate and silicate coupled to low [dFe] in the Rockall Through region and in the Iceland Basin, influencing productivity in the area. This trend was also observed during this study in the Irminger Basin.

Table 3.3 Average ligand concentrations [L] at different depths.

Area	Surface-subsurface layer (≤ 150 m) Average [L] (nM)	Mid-depth layer (>150-1000 m) Average [L] (nM)	Deep layer (>1000 m) Average [L] (nM)
Iceland Basin	1.29 ± 1.39; n=20	1.30 ± 0.90; n=10	1.07 ± 0.57; n=4
Irminger Basin	0.95 ± 1.24; n=21	1.01 ± 1.17; n=8	0.52 ± 0.32; n=4
Greenland slope	0.94 ± 0.57; n=12	1.41 ± 0.87; n=6	no average; n=2
Reykjanes Ridge	1.76 ± 1.35; n=6	0.82 ± 0.33; n=6	0.95 ± 0.09; n=2
Iceland shelf	1.06 + 1.27; n=7	1.00 ± 0.54; n=3	

3.4.3.1 Excess ligand concentrations [eL_i]

The organic ligand concentrations typically exceeded the dFe values throughout the water column ($eL_i > 0$; Figure 3.12, Table 3.4).

Excess ligand concentration [eL_i] represents the empty binding sites available for Fe (Thuroczy *et al*., 2011). [eL_i] forms an approximation for ligand undersaturation, as it does not suffer from problems related to overestimation of the Fe concentration in equilibrium with ligands (Gledhill and Buck, 2012). This study showed relatively high and variable [eL_i] in surface waters of all locations (Figure 3.12), consistent to what has been found by other authors using the [eL_i] approach (Thuroczy *et al*., 2010). These high and variable [eL_i] in surface waters can be attributed to phytoplankton uptake of iron and ligand production in most cases. However, some minimum values in [eL_i] were also observed in surface waters (e.g. CTD 014 in the Greenland slope). CTD 014 shows a clear coastal influence with higher [dFe] at the surface, which causes the near saturation of the ligands.

Excess ligand concentrations in the surface and subsurface waters (≤ 150 m) of the Iceland Basin ranged between 0.00 and 3.97 nM (n=21). In the first 150 m, [eLi] values in the Irminger Basin ranged between 0.00 and 4.77 nM (n=21). In

the region of the Reykjanes ridge at the same depths, [eL_i] ranged between 0.12 and 2.88 nM (n=6). In the surface and subsurface waters of the Greenland slope, the values for [eL_i] ranged between 0.00 and 2.20 nM (n=12), and finally in surface and subsurface waters on the Iceland shelf, [eL_i] ranged between 0.00 and 3.82 nM (n=7). The Irminger Basin showed the highest surface [eL_i] (4.77 nM, CTD 016) along with CTD 025 in the region of the Iceland Shelf (3.82 nM). Average concentrations are not presented for excess ligands due to their very variable range.

The [eL_i] at mid layer depths (>150-1000 m) was enhanced in some of the profiles in the study area (Figure 3.12). These high [eL_i] at mid-depths could suggest the release of organic ligands during remineralisation of sinking biogenic particles (Wu *et al.*, 2001). However, not all the stations within the same area displayed the same pattern. In the Iceland Basin, [eL_i] ranged between 0.00 and 7.55 nM (n=13). In the Irminger Basin, a range in [eL_i] of 0.00 and 3.09 nM (n=8) was observed. On the Greenland slope, a range in [eL_i] of 0.09 and 2.40 (n=6) was observed at mid-depths. Along the Reykjanes Ridge, a range in [eL_i] between 0.00 and 0.503 nM (n=6) was observed; whilst on the Iceland Shelf a range in [eL_i] between 0.00 and 0.42 nM (n=3) was observed.

Deep water [eL_i] (> 1000 m) in the Iceland Basin showed a range between 0.00 and 0.29 nM (n=4). In the Irminger Basin, deep water [eL_i] ranged between 0.00 and 0.71 nM (n=5). On the Greenland slope, deep water [eL_i] ranged between 1.17 and 7.28 nM (n=2); and finally over the Reykjanes Ridge, deep water [eL_i] were completely saturated (0.00 nM, n=2).

In most of the ocean, organic ligand concentrations exceed [dFe] (Gledhill and Buck, 2012). During this study the organic ligand concentrations obtained were also in excess of dFe concentrations throughout the water column, with only a few exceptions (Table 3.4, Figure 3.12). Kondo (2012) found excess [dFe] over [L] in the deep waters of the Pacific Ocean, and they attributed this excess [dFe] to the existence of organic/inorganic ligand complexes not detected by the used technique, which was the same used in this study. During the interpretation of the CLE-ACSV data, all of the [dFe] in a given sample is assumed to be in an exchangeable form with respect to the added competitive ligand. In natural oceanic samples this has a direct implication, as some of the

[dFe] exist as stable inorganic colloids or as other Fe inert components (Gledhill and Buck, 2012), which cannot be detected. These undetected complexes could, for example, be humic-like substances, due to the interaction that exist between TAC and humic substance functional groups (Laglera *et al*., 2011).

Table 3.4 Excess ligand concentrations [eL_i] range at the different depths.

Area	Surface-subsurface layer ($\leq$ 150 m) [eL_i] range (nM)	Mid-depth layer (>150-1000 m) [eL_i] range (nM)	Deep layer (>1000 m) [eL_i] range (nM)
Iceland Basin	0.00 - 3.97; n=21	0.00 - 7.55; n=11	0.00 - 0.29; n=4
Irminger Basin	0.00 - 4.77; n=21	0.00 - 3.09; n=8	0.15 - 0.71; n=5
Greenland slope	0.00 - 2.20; n=12	0.09 - 2.40; n=6	1.17 - 7.28; n=2
Reykjanes Ridge	0.12 - 2.88; n=6	0.00 - 0.50; n=6	0.00; n=2
Iceland shelf	0.00 - 3.82; n=7	0.00 - 0.42; n=3	

Ligand saturation was observed in several of the analyzed samples of D354 throughout the whole water column, especially in deep waters. However, due to the analytical difficulties associated with the current voltammetric method, it is not yet possible to determine if the ligands were saturated in these samples due to a balance between supply and removal throughout the water column or if there was a potential source of Fe not determined in the titrations. Saturation of the ligands in deep waters of the HLNA would necessarily imply that any added Fe along the water mass circulation pathways will be precipitated or removed by scavenging rather than buffered into solution.

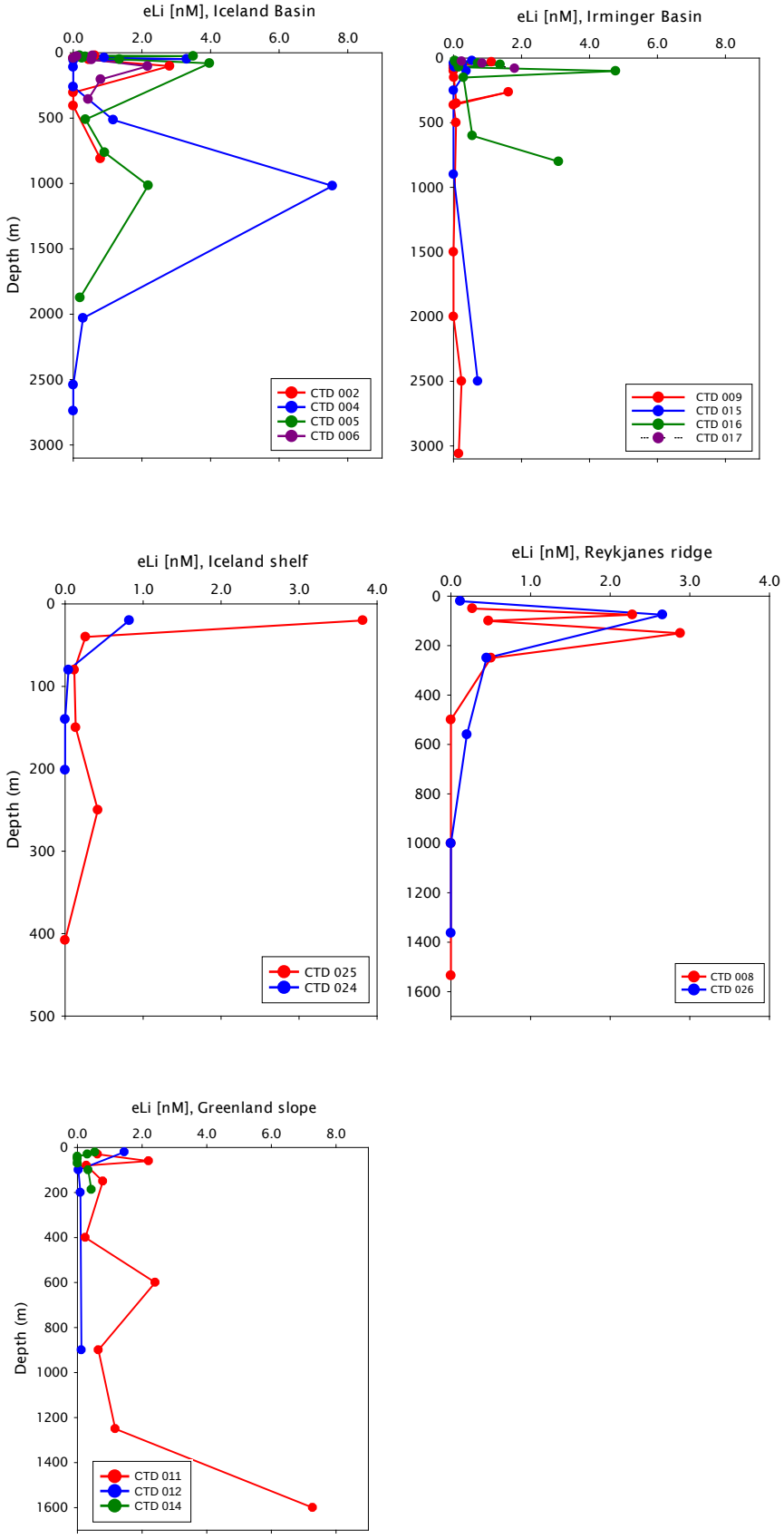

Figure 3.12 Depth profiles of excess ligand concentrations [eLi] for the different areas of D354 cruise. Concentrations are in nM.

3.4.3.2 [L]/[dFe] ratio

The [L]/[dFe] ratio shows how much more ligand there is compared to the dissolved Fe (Thuroczy *et al.*, 2011). If the [L]/[dFe] ratio equals 1, the ligand sites are fully saturated with Fe (Thuroczy *et al.*, 2011).

Iceland Basin

In surface waters of the Iceland Basin, [L]/[dFe] ratio values were relatively high and variable (1.5-12.3) in the first ~35 m (Figure 3.13). CTD 005 in the Iceland Basin showed the highest surface ratio (12.3 at 25 m, Figure 3.15) as a result of ligand production (3.8 nM). Total chlorophyll values ranged between 1 and 2 µg/l in the first 20 m of the water column for all the stations in the Iceland Basin (Figure 3.10), which indicates the presence of phytoplankton biomass and hence the possible ligand production by this community.

Surface and subsurface L/dFe ratios in the first 150 m on the Iceland Basin were also high and variable compared to deep waters, with a few exceptions that showed values <1.0 (CTD 002 and 006 at 40 m, and 004 at 100 m). A value of ~10.0 was observed at 100 m for almost all the Iceland Basin stations. Mohamed *et al*. (2011) also found high and variable [L]/[dFe] ratios in surface and subsurface waters (3.4-4.3; $\leq$ 150 m) of the Iceland Basin and a lower and more constant ratio at depth.

CTD 005 and 006 show a clear ligand production in subsurface waters at 50 m, with enhanced [L]/[dFe] ratios of 6.3 and 4.1, respectively. Thurozcy (2011) also found high [L]/[dFe] ratios in different areas of the Southern Ocean (5.6-16.2), especially in the surface 50 m of the HNLC regions, as a result of low [dFe] and variable ligand concentration (2-26).

High [L]/[dFe] ratios in the euphotic layer can be explained by the uptake of Fe and production of ligands by phytoplankton; and also by microbial activity degrading the non-resistant ligands below this layer (Rue and Bruland, 1997; Gerringa *et al.*, 2006). These high ratios thus express a potential for Fe solubilisation in surface and subsurface layers.

In mid-depth layers below 250 m, the [L]/[dFe] ratios decrease with depth down to ~800 m ($\leq$ 2.0) and thus become low and more constant. A peak in the ratio was observed at 1000 m in CTD 004 and 005 (9.9 and 3.5,

respectively). This peak was caused by a high [$L_{,Fe}$], which may be a result of the very resistant nature of the dissolved organic ligands at this depth. Below this maximum, the ratio starts to decrease again down to ~2000 m at a value near saturation in these stations (~1). The ratio decrease with depth in CTD 004 reflects an increase in [dFe], which favours scavenging and co-precipitation. CTD 004 in the Iceland Basin present a [L]/[dFe] ratio $\leq$1.0 below 2000 m.

These observed constant ratios at depth reflect either a balance between production and degradation of dissolved organic ligands or a constant highly refractory type/group of ligands, as suggested by Hunter and Boyd (2007). Mohamed *et al.* (2011) and Thuroczy et al. (2011) also found lower and more constant ratios below 450 m depth.

Irminger Basin

High and variable [L]/[dFe] ratios (>1.0-38.4; Figure 3.15) in the surface/subsurface waters of the Irminger basin were also observed down to ~150 m, and then commenced to decrease to ~2.0 or less below this depth (Figure 3.13). Values below 1.0 were observed at surface waters of CTD 009. The high and variable ratios in the surface/subsurface waters of this basin are a consequence of the low [dFe] (0.03 to 0.7 nM) down to ~150 m.

Below 150 m, CTD 009 shows [L]/[dFe] ratios near 1.0 throughout the water column down to 3000 m, reflecting a steady state between production and degradation.

The highest [L]/[dFe] ratios in the surface/subsurface waters of the Irminger Basin were observed in CTD 016 (25.9 at 100 m and 38.4 at 50 m), and were caused by a high ligand concentration (4.9 and 1.4 nM, respectively) related to a very low [dFe] (0.19 and 0.02 nM, respectively). Low [dFe] in the Irminger Basin could be a result of the low atmospheric inputs in this area along with phytoplankton uptake, which in turn could have led to ligand production, as observed by the high ratios in this area.

Greenland slope

CTD 011 and 012 on the Greenland slope present high surface/subsurface [L]/[dFe] ratios (13.2 at 60 m in CTD 011, and 18.0 at 20 m in CTD 012),

related to low [dFe] values. CTD 014 presents high surface total chlorophyll values (up to ~4.5 µg/l at ≤ 50 m). However, this station showed the lowest [L]/[dFe] ratios at the surface (0.4-2.0; Figure 3.13). Clearly, at this station Fe was not a limiting factor for phytoplankton growth. Moreover, organic ligand concentrations were low (≤ 1 nM) at depth above 100 m.

A decreasing trend is observed in CTD 011 down to 900 m (although a peak with a ratio of 4.8 was observed at 600 m), but then increased from 900 m down to 1600 m, where it reaches a high value of 10.2.

Reykjanes ridge

CTD 008 and 026 in the Reykjanes ridge region presented high [L]/[dFe] ratios (Figure 3.13) in surface and subsurface waters (≤150 m), as a consequence of enhanced ligand concentrations. Both CTD 008 and 026 showed a very clear trend in the [L]/[dFe] ratio, with high surface values (1.6-11.0) in the first 150 m, and then decreased to values near saturation with depth and steady from 250 down to 1500 m (Figure 3.13). Total chlorophyll values in CTD 008 ranged between 1 and 2.5 µg/l in the first 20 m depth. [dFe] in both stations were low at the surface (≤ 0.42 nM) ≤ 150 m, increasing with depth to ~1.1 nM down to ~1500 m (nutrient type profile). Lower ratios at depth are a result of the increasing [dFe] values, where the ligand sites for binding Fe are getting filled and even almost saturated. This near saturation reflects a consistency with the precipitation of Fe as insoluble oxyhydroxide and its removal to the deep ocean.

Iceland Shelf

CTD 025 and 024 on the Iceland Shelf showed moderately high surface [L]/[dFe] ratios, compared to surface waters of the other regions in the study area (5.3 at 20 m in CTD 024, and 3.6 at 40 m in CTD 025; Figure 3.13). However, CTD 025 at 20 m presented a very high ratio (141.4) both as a result of very low [dFe] (0.03 nM), and an enhanced ligand concentration (3.8 nM). Total chlorophyll was ~3 µg/l in surface waters of the Iceland Shelf. Below the surface maxima, relatively low [L]/[dFe] ratios were observed throughout the water column at both stations (<2.0) down to 400 m, which shows near saturation of the ligands with depth in this area.

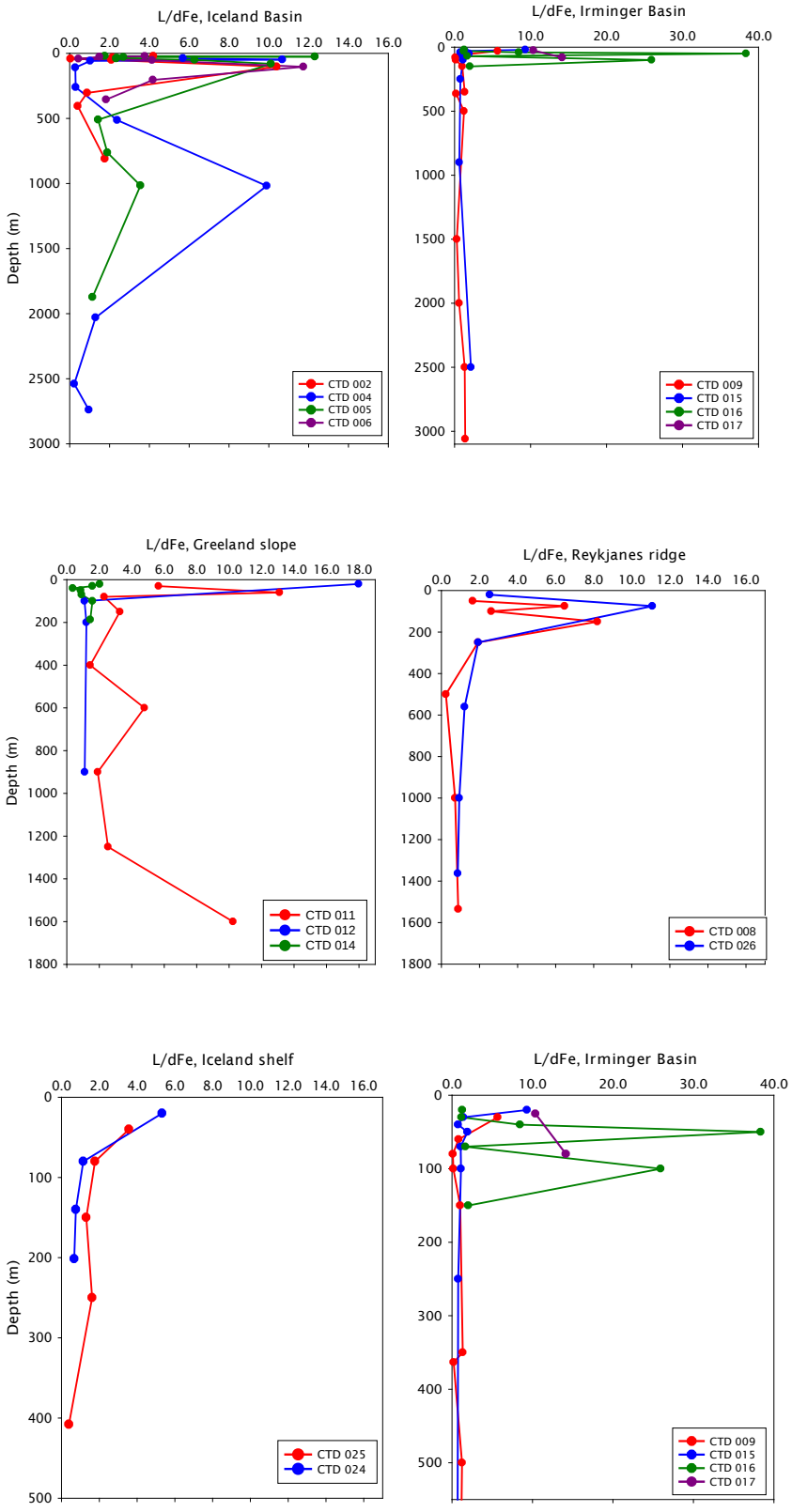

Figure 3.13 [L]/[dFe] ratios for the different CTD station in the study area (for visual purposes, the last profile corresponds to the stations on the Irminger Basin, down to the first 500 m).

3.4.3.3 Log K'_{FeL}

Stability constants (log K'_{FeL}) for the ligands found throughout the water column ranged between 20.16 and 23.94, with an average of 21.97 $\pm$ 0.80 nM (n=92, Figure 3.14). This average value was within the range reported for surface waters of the Iceland Basin and other areas of North Atlantic (21.7-23.3) (Mohamed *et al.*, 2011; Thuroczy *et al.*, 2011). In surface and subsurface waters of the Iceland Basin (<150m), log K'_{FeL} ranged between 20.63 and 22.78, with an average of 21.75 $\pm$ 0.69 (n=9). Surface and subsurface log K'_{FeL} in the Irminger Basin ranged between 20.16 and 23.23, with an average concentration of 21.85 $\pm$ 0.92 (n=18). On the Greenland slope, surface and subsurface log K'_{FeL} values ranged between 21.23 and 23.73, with an average of 22.23 $\pm$ 0.66 (n=11). On the Reykjanes ridge, surface and subsurface log K'_{FeL} values ranged between 20.94 and 22.61, with an average of 21.59 $\pm$ 0.65 (n=6), and finally over the Iceland Shelf, surface and subsurface log K'_{FeL} values ranged between 21.15 and 22.26, with an average of 21.65 $\pm$ 0.45 (n=6). These high log K'_{FeL} values reflect high stabilities of the Fe (III) complexes, and are consistent to what has been reported for most of the oceans in terms of binding strengths (log K'_{FeL} ~20-23), when referred to one ligand class only (Thuroczy *et al.*, 2010). During this study, only one class of organic Fe (III) binding ligands was detected. Previous studies in the North Atlantic Ocean have also reported only one class of organic Fe-binding ligands (Rijkenberg *et al.*, 2008; Thuroczy *et al.*, 2010; Mohamed *et al.*, 2011). This may be a consequence of the detection window used during the CLE-ACSV analysis (log $\alpha'_{Fe(TAC)2}$ =12.4). Authors who have detected two or more ligand classes have applied different detection windows (Rue and Bruland, 1995; Rue and Bruland, 1997), and also applied different data treatment approaches.

The surface log K'_{FeL} values observed in the Iceland Basin are similar to those reported for the tropical North Atlantic using the same method approach as used for my study (Rijkenberg *et al.*, 2008).

Although the value of the stability constants for the detected organic ligands was determined in this study, it was not possible to determine the type of organic ligands observed due to the lack of their chemical characterization.

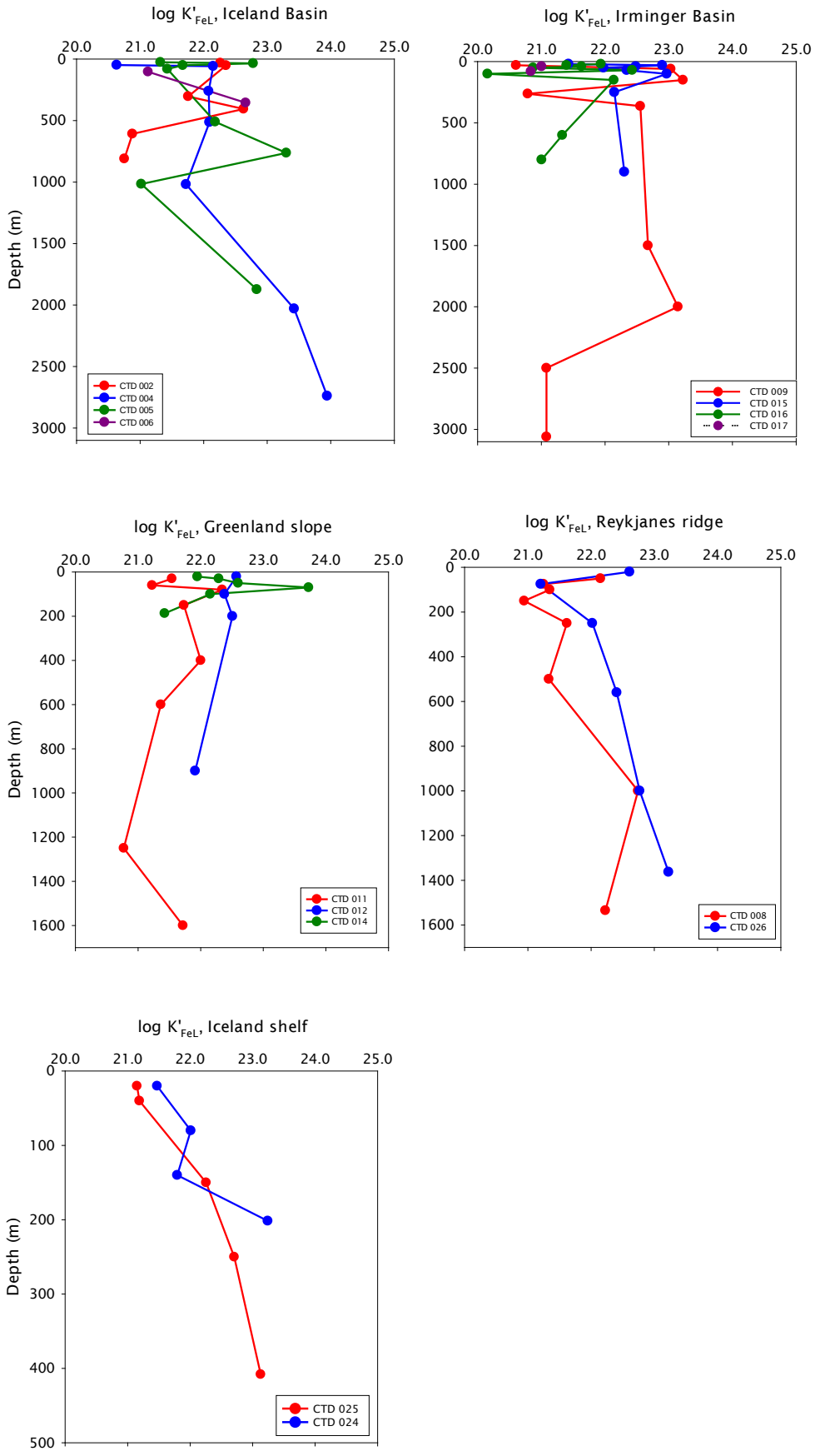

Figure 3.14 Log K'$_{FeL}$ values for the different regions of D354 cruise.

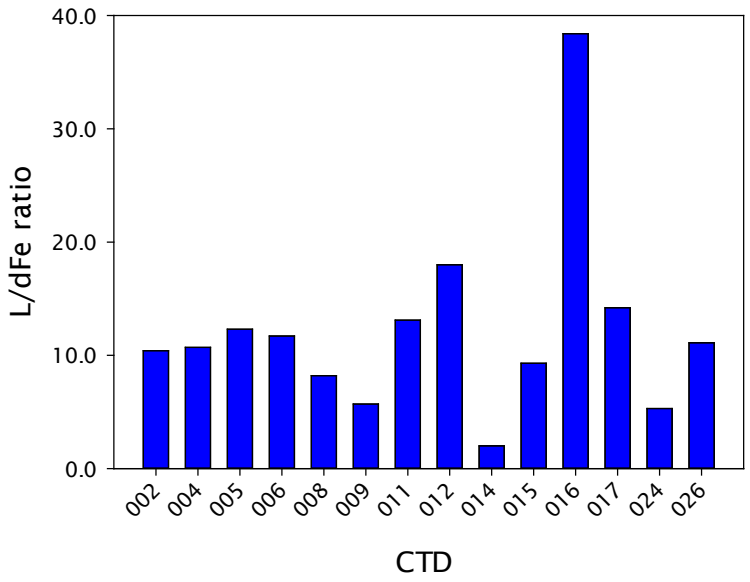

Figure 3.15 Highest surface [L]/[dFe] ratio per station in the first 150 m depth (CTD 025 was omitted due to the very high value (141.4)).

3.5 Conclusions

Iron binding ligand concentrations were typically in excess of dissolved Fe concentrations in surface/subsurface waters in the study area. This suggests a combination of biological Fe uptake along with microbial ligand production as the controlling processes.

[L]/[dFe] ratios proved to be a reliable approach to determine ligand saturation. During this study, there were clear differences in [L]/[dFe] ratios between surface/subsurface waters ($\leq$ 150 m), influenced by the presence of phytoplankton, and deeper waters (below 250 m) in dissolved organic ligand characteristics and the distribution of [dFe]. The high [L]/[dFe] values at the surface decreased to a nearly constant value and near saturation in deep waters.

Deep water mass formation in the HLNA suggests that ligand saturation at depth, as it was observed in some stations during this study, would not have the capacity to buffer any added Fe in solution; as a result, this additional Fe would tend to form precipitates and to be removed by scavenging.

A temporal scale data set is needed in order to determine processes affecting the long term variability of the ligands in the HLNA area.

Chapter 4: Influence of Ocean Acidification on the organic complexation of iron and copper in coastal waters

This chapter presents the results of a study into the effect of ocean acidification on the trace metal speciation of iron and copper, with a focus on their organic complexation. This study was conducted in the northwest European seas, as part of a NERC funded UK Ocean Acidification Consortium programme, during the RRS *Discovery* 366 oceanographic cruise.

4.1 Introduction

The rise in atmospheric CO_2 concentrations over the past two centuries has led to greater CO_2 uptake by the oceans (Feely *et al.*, 2004). The increased amount of dissolved CO_2 has lowered the surface ocean pH (Caldeira and Wickett, 2003), and it has changed the balance of the carbonate species (Doney, 2006), leading to a decrease in the carbonate ion concentration (CO_3^{-2}) and to an increase in aqueous CO_2 and bicarbonate concentrations (Zeebe and Wolf-Gladrow, 2001; Orr *et al.*, 2005a). The increase in atmospheric CO_2 concentrations from preindustrial (~280 ppm) to current levels (~400 ppm) has caused the pH of today's surface ocean to be ~ 0.1 units lower (ca. pH 8.1) than preindustrial values (Caldeira and Wickett, 2003; Feely *et al.*, 2004). If CO_2 absorption continues along current trends, a decrease in pH of about 0.3-0.5 units by the year 2100 in the surface oceans can be projected (Brewer, 1997; Zeebe and Wolf-Gladrow, 2001; Feely *et al.*, 2004; Orr *et al.*, 2005a; Orr *et al.*, 2005b; Doney, 2006). Carbonate ion concentrations are expected to drop by half over this century, making it more difficult for marine calcifying organisms to form biogenic calcium carbonate ($CaCO_3$), and to maintain their external skeletons (Orr *et al.*, 2005a). These changes in ocean chemistry could cause strong impacts on marine ecosystems, even under future scenarios in which most of the remaining fossil fuel CO_2 is never released (Kleypas *et al.*, 1999; Riebesell *et al.*, 2000; Caldeira and Wickett, 2003; Langdon *et al.*, 2003). Several studies have also suggested that continued release of CO_2 to the atmosphere may result in undersaturation of the surface ocean with respect to the calcium carbonate minerals (calcite and aragonite) in the coming decades

(Caldeira and Wickett, 2003; Feely *et al.*, 2004; Caldeira and Wickett, 2005; Orr *et al.*, 2005a). In addition to changes in carbonate saturation state, other changes to ocean chemistry are also possible. For example, ocean acidification is likely to affect the chemical speciation of essential trace elements in seawater, although the extent of this affect is so far unknown.

In the surface ocean, the trace metals that have a significant biological role for oceanic phytoplankton include manganese, iron, cobalt, copper, zinc and cadmium (Morel and Price, 2003). These metals are necessary for the growth and survival of photosynthetic organisms (Morel and Price, 2003). Iron is an essential micronutrient involved in fundamental cellular processes, including respiration, photosynthesis, nitrogen uptake and nitrogen fixation (Geider *et al.*, 1993; Raven *et al.*, 1999), and therefore controlling the productivity, species composition and trophic structure of microbial communities in large regions of the ocean (Sunda and Huntsman, 1995b; Johnson *et al.*, 1997; Hunter and Boyd, 2007). Iron concentrations in oceanic waters are very low due to its effective removal from the water column by phytoplankton, and to its very low solubility (Rue and Bruland, 1995; Morel and Price, 2003). Organic complexation is thought to maintain dissolved iron concentrations above its inorganic solubility (Liu and Millero, 2002). These organic ligands buffer dissolved iron in seawater against hydrolysis, and prevent scavenging (Hunter and Boyd, 2007; Boyd and Ellwood, 2010). Marine phytoplankton is responsible for about half of the photosynthetic carbon fixation (primary production) on earth (Morel and Price, 2003). It has been demonstrated that iron deficiency limits phytoplankton growth in High Nitrate Low Chlorophyll (HNLC) waters such as the equatorial and subarctic Pacific, the Southern Ocean, and coastal upwelling regions (Martin and Fitzwater, 1988; Boye *et al.*, 2005; Boyd *et al.*, 2007). HNLC waters make up around 25% of the world ocean's (de Baar *et al.*, 2005). Furthermore, in nutrient-poor-low latitude waters iron helps to regulate nitrogen fixation (Moore *et al.*, 2009). As a consequence, iron controls primary productivity in up to 40% of the world's oceans (Boyd and Ellwood, 2010), and consequently strongly influencing oceanic CO_2 drawdown in these regions.

A decrease in seawater pH from 8.1 to 7.4 will increase the solubility of Fe (III) by about 40%, which could have a large impact on biogeochemical cycles (Morel and Price, 2003; Millero *et al.*, 2009). A decrease in pH has also been suggested to result in higher iron availability to phytoplankton, as a result of

enhanced proton competition for the available iron-binding ligand places (Royal Society, 2005; Millero *et al.*, 2009). However, it has also been pointed out that the bioavailability of dissolved Fe to marine phytoplankton may decline with the reduction in pH to an extent dictated by the acid-base chemistry of the chelating ligands (Shi *et al.*, 2010). This could in turn reduce the ability of the ocean to take up atmospheric CO_2 (Sunda, 2010).

Copper is both an essential micronutrient and a toxic element (Moffett and Dupont, 2007). A role of copper in iron uptake by phytoplankton and in nitrogen cycling has been proposed (Peers *et al.*, 2005; Jacquot *et al.*, 2013), although no limitation in primary productivity has been observed as a result of low copper iron concentrations in the open ocean. Cu (II) has been shown to be toxic at concentrations as low as 10^{-12} M to marine phytoplankton (Brand *et al.*, 1986). Complexation of a metal cation by organic ligands can decrease its toxicity by decreasing the metal's free ion concentration (Donat *et al.*, 1994). However, a pH decrease may also reduce copper binding by organic ligands, therefore making copper more bioavailable and consequently toxic to marine organisms (Campbell *et al.*, 2014). It has been predicted that the increase for the free form of copper under a 7.5 pH scenario will be as high as 30% (Millero *et al.*, 2009), which could result in negative effects for the marine ecosystems.

The majority of the dissolved concentrations of the bioactive trace metals Fe, Cu, Co, Ni and Zn are in the form of metal organic complexes (up to 99% in the case of Fe and Cu) in seawater (Sunda and Hanson, 1987; Coale and Bruland, 1988; Donat and van den Berg, 1992; Gledhill and van den Berg, 1994; Rue and Bruland, 1995), which control their solubility and bioavailability. Measuring the organic complexation of trace metals is, thus, extremely important for the understanding of their biogeochemistry (Buck *et al.*, 2012). Considering that the organic complexation of trace metals is pH dependent (Millero *et al.*, 2009; Breitbarth *et al.*, 2010), it is also highly important to determine the effect of a more acidic surface ocean on their complexation.

There are only a few studies that have considered the effect of ocean acidification on the speciation and/or bioavailability of trace metals to marine organisms (Turner *et al.*, 1981; Byrne *et al.*, 1988; Byrne, 2002; Millero *et al.*, 2009; Shi *et al.*, 2010; Gledhill *et al.*, submitted). The chemical form of an element in seawater (its speciation) is affected by the presence of other ions

with which it may interact. Among these is the hydrogen ion concentration. Consequently, a decrease in surface ocean pH can potentially alter the speciation of these elements.

Dissolved metals exist in two forms in seawater, organically complexed and inorganic dissolved. The toxicity and availability of trace metals are thought to be controlled by their inorganic metal ion concentration. A decrease in pH generally increases the fraction of free inorganic dissolved forms; especially of those metals that form strong complexes with OH^- and CO_3^{-2} ions (e.g., Cu (II) and Fe (III)). These anions are expected to decrease in surface waters by 82% and 77% by the year 2100, respectively (Millero *et al.*, 2009).

The organic complexation of trace metals in seawater is often determined using competitive ligand exchange–adsorptive cathodic stripping voltammetry (CLE-ACSV). To date, CLE-ACSV is the only widely accepted technique employed for measuring organic ligand concentrations in seawater and their associated conditional stability constants with the metal of interest (Buck *et al.*, 2012; Gledhill and Buck, 2012). However, given the indirect approach and the complexity of the method, there can be multiple methodological distinctions between CLE-ACSV techniques applied by different laboratories to measure the complexation of a particular metal. These variations include the use of a different added ligand (AL) and/or concentration of AL, the buffer and pH of titrations, the choice of HMDE and mercury drop size, and the application of different linear and/or nonlinear data interpretations (Buck *et al.*, 2012).

As no reference standards currently exist for dissolved metal speciation, intercomparison exercises of the techniques commonly used have been undertaken (Bruland *et al.*, 2000; Buck *et al.*, 2012), in order to detect potential artefacts in the analyses. The results of these exercises demonstrated that there are variabilities in result interpretation amongst laboratories, due to both experimental conditions and data processing methods. The concentration and choice of the AL results in distinct analytical windows ($\alpha_{Me(AL)x}$) applied to the titration, which in turn gives distinct variations in speciation results (as it was shown in the case of copper) (Bruland *et al.*, 2000). The use of different methods for calculating the sensitivity of the analysis also causes variability in data interpretation (Hudson *et al.*, 2003; Wu and Jin, 2009; Buck *et al.*, 2012).

The aim of this study is to determine the effects of a decrease in surface ocean pH on the trace metal speciation of iron and copper, with focus on their organic complexation.

4.2 Materials and methods

4.2.1 Sample collection

Seawater samples were collected in northwest European shelf sea waters (Figure 4.1) during the RRS Discovery 366 cruise in June and July 2011. Surface seawater (ca. 2-4 m deep) was collected daily from a towed fish and was filtered in-line through a 0.2 µm pore size filter capsule (Sartobran P-300, Sartorious) in a trace metal clean container.

Seawater from the filter capsule was collected in 250 ml acid cleaned low density polyethylene bottles (LDPE; Nalgene) for the determination of trace metal (iron, copper) speciation. Sample bottles were rinsed thoroughly with deionised water (MilliQ, Millipore; 18.2 mΩ cm^{-1}) and then with seawater before collection. Samples for the determination of Fe speciation were immediately frozen after collection (-20˚C, not acidified) for their analysis on land. Samples for the determination of total dissolved trace metals were collected using 60 ml low density polyethylene bottles (LDPE; Nalgene). These bottles were immediately acidified to pH 2 (80 µl; 0.011 M final concentration) using ultraclean HCl (Romil UpA grade) and stored at room temperature for their analysis on land.

All LDPE bottles (Nalgene) were cleaned according to the standard protocol described by Achterberg *et al*. (2001). Samples for Cu-binding ligand analysis were stored at 4˚C for subsequent analysis (within 1day).

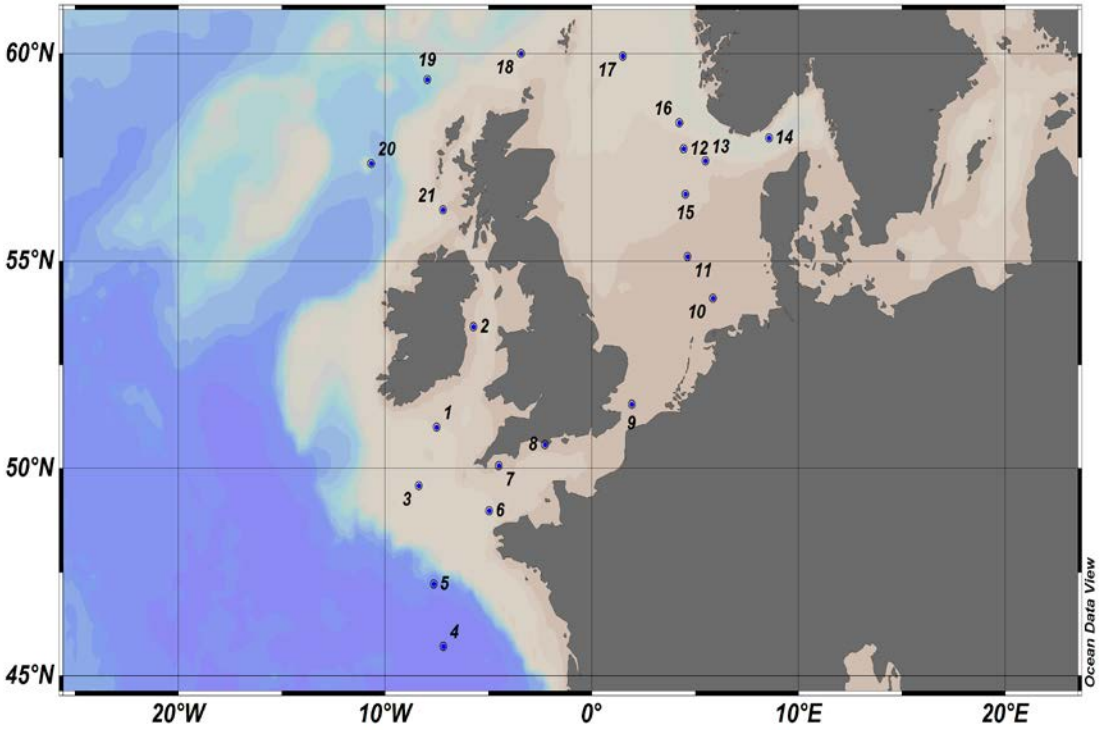

Figure 4.1 Sampling stations along the northwest European shelf seas for the determination of the effect of ocean acidification on iron and copper speciation.

4.2.2 Instrumental and chemicals

The voltammetry system consisted of a potentiostat (μAutolab Echochemie, Netherlands) with a static mercury drop electrode (Metrohm, 663 VA stand), a KCl reference electrode (Ag/AgCl in 3M KCl saturated with AgCl) and a counter electrode of glassy carbon.

All chemicals were prepared in a clean electrochemistry laboratory under a Class 100 laminar flow bench at room temperature (20˚C). A stock solution of 0.01 M 1-nitroso-2-naphthol (HNN; Sigma) was prepared in methanol (Fisher, HPLC grade). A stock solution of 0.01 M salicylaldoxime (H_2SA; Sigma) was prepared in 0.1 M HCl (Romil, SpA grade). As the aim of this study was to compare changes in metal speciation at three different pH values, HNN was used as the complexing ligand due to the high stability of the $Fe(HNN)_3$ complex at lower pH values (optimal analytical pH = 6.9), compared to the current seawater pH (Gledhill and van den Berg, 1994); whereas the $Fe(TAC)_2$ complex is very stable at pH 8.0 and above (used as the complexing ligand in the previous chapter; Croot and Johansson (2000)). Consequently, sensitivity of the $Fe(HNN)_3$ technique is improved at lower pH values. No interferences were

apparent in the voltammetric analyses in this work's seawater samples using low concentrations of HNN.

The detection windows (centred by $\alpha_{Me(AL)x}$ and within one order of magnitude on either side of it, and calculated from $K'_{Me(AL)x}$ $[AL]^x$) at the concentration of HNN and H_2SA used in this work's experiments are shown in Tables 4.1 and 4.2, respectively. The detection window for the complexation of Fe with TAC in Chapter 3 of this study (centred at log $\alpha_{Fe(TAC)2}$ =12.4) is higher than the detection windows obtained with HNN for Fe complexation at the three different pH levels in this section (Table 4.1).

Standard iron (III) and copper (II) solutions of 10^{-6} M for additions were prepared using a 1000 mg/L ICP-MS stock solutions (Fisher Scientific), and were acidified to pH 2 using HCl (Romil, SpA grade).

pH buffer values were determined on the IUPAC (NBS) scale (pH_{NBS}) using a Metrohm pH meter. Buffered seawater was also measured with a spectrophotometric technique (Rerolle *et al.*, 2012), and a relationship of $pH_{total} = 1.05 \times (pH_{NBS}) - 0.58$ (n =3, $r^2 = 0.999$) was obtained for this work's conditions. Stock solutions of 1 M N-2-hydroxyethylpiperazine-N'-ethanesulphonic acid (HEPES; Fisher Aristar grade) pH buffer were prepared in 0.35, 0.6, and 0.9 M ammonia (Romil, SpA grade) in order to provide a pH_{NBS} of 7.2, 7.6, and 8.05 upon 100-fold dilution with sea water. HEPES was cleaned prior to use by the addition of HNN with subsequent removal of HNN and $Fe(HNN)_3$ using a previously activated C_{18} SepPak column (Whatman). De-ionised water was used to prepare aqueous solutions.

Table 4.1 Detection windows for the complexation of Fe with HNN at the pH values analysed during this study.

pH	NN [μM]	Detection window (centered at log $\alpha(FeNN)_3$)	Log α_{FeL}
7.2	1	10.5-12.5	12.16-13.98
7.6	1	10.5-12.5	10.69-12.25
8.05	2	8.9-10.9	9.91-10.60

Table 4.2 Detection windows for the complexation of Cu with H_2SA at the pH values analysed during this study.

pH	SA [μM]	Detection window (centered at log $\alpha(CuSA)_2$)	Log α_{CuL}
7.2	10	2.04-4.04	2.40-4.00
7.6	10	2.14-4.14	2.77-4.10
8.05	10	3.12-5.12	3.54-4.38

4.2.3 Determination of the iron and copper binding capacity

Determination of the Fe and Cu binding capacity in seawater was performed using the CLE-ACSV method, with HNN for Fe (Gledhill and van den Berg, 1994) and H_2SA for Cu (Campos and Van Den Berg, 1994) as the competing ligands.

For the determination of the Cu binding capacity, the pH was adjusted in three individual 250 ml LDPE bottles to 8.05, 7.6 and 7.2 through addition of pH adjusted 1M HEPES buffers (0.01 M final concentration) immediately after collection, and with a 0.01 M solution of H_2SA (10 μM final concentration). The samples were subsequently equilibrated for a minimum period of 1h at room temperature (~21ºC). An aliquot of 15 ml of the sample solution was then pipetted into 30 ml polyestyrene cups. A Cu (II) standard solution was spiked to give an added concentration range between 0 and 30 nM in 14 steps. The Cu and ligands in the sample aliquots were allowed to equilibrate overnight (>12 h) at room temperature (~21ºC).

The concentration of $Cu(HSA)_2$ in the samples was determined using the following procedure: i) removal of oxygen from the samples for 5 min with nitrogen gas (oxygen free grade), after which 5 fresh Hg drops were formed, ii) a deposition potential of -0.1 V was applied for 60 s whilst the solution was stirred to facilitate the adsorption of the $Cu(HSA)_2$ to the Hg drop, and iii) at the end of the adsorption period, the stirrer was stopped and the potential was scanned from -0.1 to -0.4 V using the square wave method at a frequency of 100 Hz. The stripping current (peak height) from the reduction of the adsorbed $Cu(HSA)_2$ complex was recorded. pH on each of the titration steps was recorded with a pH meter after each measurement.

All of the Fe samples were analyzed in a clean electrochemistry laboratory under a Class 100 laminar flow bench, at the National Oceanographic Centre (NOC). Each of the frozen samples for the Fe binding capacity analysis were thawed prior to analysis to reach room temperature, and then buffered with the same procedure as for the Cu samples. In the case of the Fe titrations, a concentration of 1 μM HNN was used, with the exception of the pH 8.05 experiment (2 μM NN). Added Fe concentrations ranged between 0 and 8 nM in 14 steps, pipetted into 30 ml polytetrafluoroethene (PTFE) vessels.

A deposition potential at -0.4 V was used with a deposition time of 3 min; the scanning mode was sample-DC from -0.15V to -0.65 V at a scan rate of 50 mV/s, the reduction peak of Fe appearing at -0.45 V (Gledhill and van den Berg, 1994). A voltammogram for the reduction of the adsorbed $Fe(HNN)_3$ complex is shown in Figure 4.2. Sample titrations are shown in Figure 4.3.

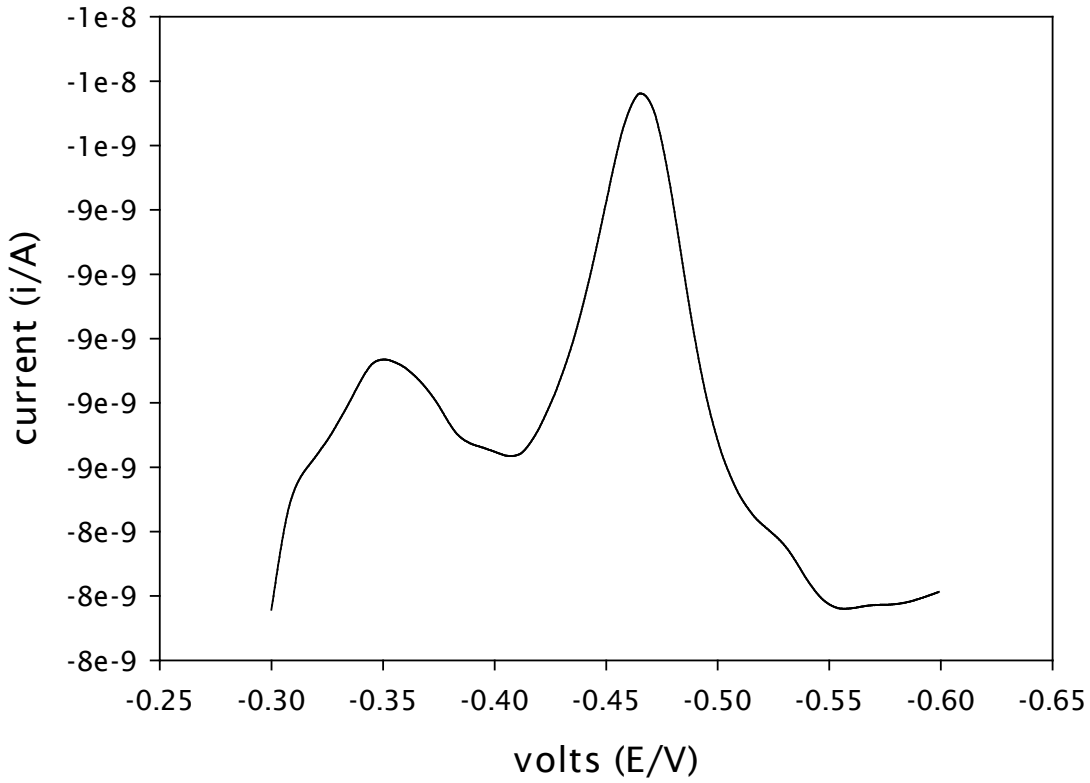

Figure 4.2 Example of a voltammogram obtained for the reduction of the adsorbed $Fe(HNN)_3$ complex to the Hg drop. The concentration of added Fe is 1 nM.

4.2.4 Theoretical considerations

The theoretical considerations for the determination of natural ligand binding characteristics of Fe using HNN as the competing ligand have been described in detail by Gledhill and van den Berg (1994), and in the case of Cu with H_2SA by Campos and van den Berg (1994). A sufficiently high concentration of a known added ligand (AL), in this case HNN or H_2SA, is added to a sample, and competes with the natural Fe or Cu binding ligands for reversibly bound Fe or Cu.

A script code developed in the R programming language (by Dr M. Rijkenberg, Royal NIOZ) was used to calculate the metal-ligand characteristics. Details about this code and the script file can be found in Gerringa *et al*. (2014). Both the linear (van den Berg/Ruzic; Scatchard) and non-linear regression (Gerringa-Maas) methods are used to compare the results in ligand parameters. This script in R was utilized as the main approach for obtaining the Fe and Cu ligand parameters during this study.

4.2.4.1 Linear regression method (van den Berg/Ruzic)

The equilibrium equation for the association between Cu^{2+} or Fe^{3+} (Me) and one class of natural organic ligands L is:

$$[Me^{x+}] + [L'] \leftrightarrow [MeL] \quad (4.1)$$

where $[Me^{x+}]$ is the free metal ion concentration, and [L'] is the concentration of L not complexed by Me (free [L'] and complexes of L with the major cations, protons and maybe other trace metals).

The equilibrium expression for this equation is:

$$K'_{MeL} = [MeL]/[Me^{x+}][L'] \quad (4.2)$$

where K'_{MeL} is the conditional stability constant for the formation of the MeL complex, and is conditional upon the seawater composition (salinity, pH and competing trace metals).

The total ligand concentration (free and complexed species) in a given sample is represented by C_L:

$$C_L = [L'] + [MeL] \quad (4.3)$$

Equations (2) and (3) form the basis of the linear relationship between [Me^{x+}] and [MeL].

By substituting [L'] from equation (3) into equation (2), the following relationship is obtained:

$$\frac{[Me^{x+}]}{[MeL]} = \frac{[Me^{x+}]}{C_L} + \frac{1}{K'_{MeL}\,[C_L]} \tag{4.4}$$

A plot of [Me^{x+}]/[MeL] as a function of [Me^{x+}] produces a straight line, assuming a simple model of 1:1 complex formation (Me^{x+} complexation by only one type or class of organic ligand (Ruzic, 1982; van den Berg, 1982b)).

The CSV peak height (i_p) is related to the labile Me concentration via the sensitivity:

$$i_p = S[Me_{labile}] \tag{4.5}$$

Where S is obtained from the slope of the titration curve at high concentration of total (and labile) metal where all organic ligands (L) are saturated (high end of the titration).

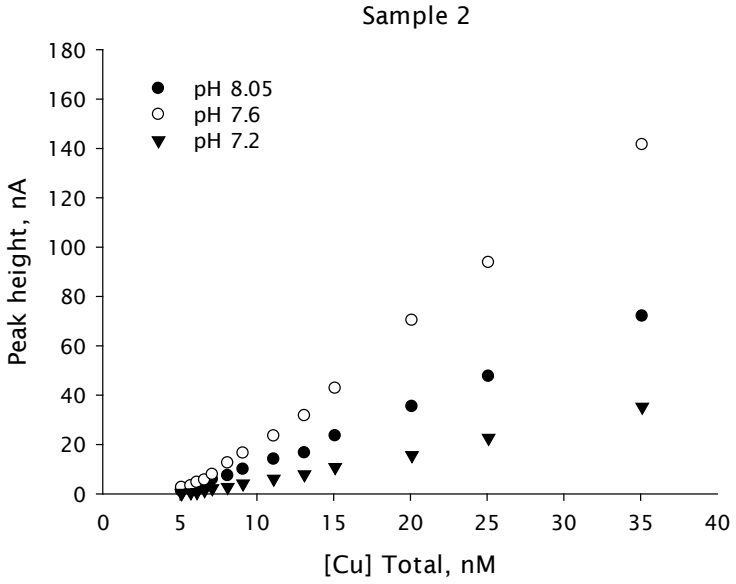

a)

Influence of OA on the organic complexation of Fe and Cu

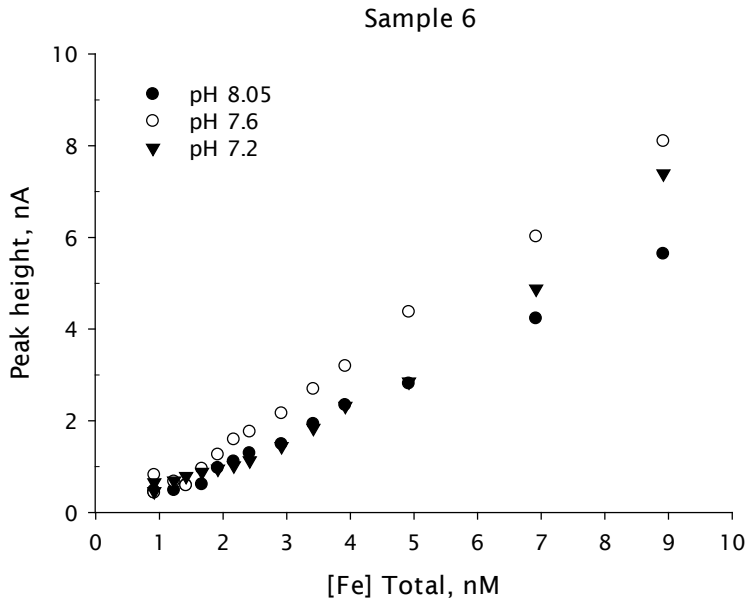

b)

Figure 4.3 Titration plots for a Cu (a) and Fe (b) sample at the different pH treatments.

4.2.4.2 Non-linear regression method

The non-linear regression method considers the solution to be at equilibrium and can be applied using the equation:

$$\frac{K'_{MeAL}[AL]^X}{K'_{MeL}[L]} = \frac{[Me(AL)_X]}{[MeL]} \qquad (4.6)$$

where K' is the conditional stability constant of Me (metal, i.e. Fe or Cu) with the added ligand (AL) or the natural ligand (L), and [AL] and [L] are the concentrations of free Me-binding ligands. The [Me(AL)x] and [MeL] represent the concentrations of Me complexes with AL and L. Peak heights as a function of the added metal (Fe or Cu) concentration, and representing Me(AL)x were obtained from the complexing ligand titrations. Since the concentration of AL (HNN or H_2SA) and its binding strength with the metals (Fe or Cu) are known, it is possible to determine L and K'_{MeL} of the natural Fe or Cu binding ligands from the curved response (van den Berg, 1982a) using non-linear regression of the Langmuir isotherm (Gerringa *et al.*, 1995).

Data for the calculation of the complexing ligand concentration is obtained from a titration of each seawater sample with the metal. The concentration of MeL at each point of the titration is calculated from the total dissolved metal concentration C_{Me}:

$$[MeL] = C_{Me} - [Me_{labile}] \quad (4.7)$$

where C_{Me} equals to the total dissolved metal initially present in the sample augmented by that added during titration. $[Me_{labile}]$ is the labile metal concentration:

$$[Me_{labile}] = [Me'] + [Me(AL)_X] \quad (4.8)$$

where $[Me(AL)_x]$ is the concentration of metal bound by the added ligand AL. The labile metal concentration is that which reacts and equilibrates with the added ligand (AL), and includes all inorganic Me and the Me released from complexes with L upon addition of AL. [Me'] is the concentration of inorganic Me (not complexed by AL or L), and is included because of the way the labile metal concentration is quantified by metal additions, which always include a fraction as Me'. $[Me^{x+}]$ is directly related to the labile Me concentration by α', which is the overall α-coefficient (Ringbom and Still, 1972) for labile metal:

$$\alpha' = \alpha'_{Me} + \alpha'_{Me(AL)x} \quad (4.9)$$

where α'_{Me} is the α-coefficient for inorganic complexation of free metal ion. Values for α'_{Fe} and α'_{Cu} in sea water at the pH_{NBS} range (8.05-7.2) and salinity 35.0 were determined by Gledhill *et al.* (submitted) (

Table **4.3**) using the chemical speciation modelling software visual MINTEQ v 3.0. $\alpha_{Me(AL)x}$ is the α-coefficient for the complexation of free metal ion by the added ligand, α_{FeHNN} and $\alpha_{\Sigma CuHSA}$ for Fe and Cu, respectively:

$$\alpha_{FeHNN} = K'_{Fe(HNN)3}\,[NN^{-\prime}]^3 \quad (4.10)$$

$$\alpha_{\sum CuSA} = (K'_{Cu(HSA)^-}[HSA^{-\prime}]) + (\beta'_{Cu(HSA)2}[HSA^{-\prime}]^2) \quad (4.11)$$

where $[NN^{-\prime}]$ and $[HSA^{-\prime}]$ are the concentrations of the added ligand, not complexed by the metal. $K'_{Fe(HNN)3}$ is the conditional stability constant for the formation of $Fe(HNN)_3$, whilst $K'_{Cu(HSA)^-}$ and $\beta'_{Cu(HSA)2}$ are the conditional stability constants for $Cu(HSA)^-$, and $Cu(HSA)_2$ respectively.

As the binding between the AL and Me is pH dependent, side reaction coefficients ($\alpha_{Me(AL)x}$) for each AL and pH_{NBS} in this work's experiments were used. These values were obtained from the calculations made by Gledhill *et al.* (submitted) after ligand competition with EDTA and by reverse titration against

inorganic complexes (for Cu). Log $\alpha_{Cu(HSA)2}$ values used for pH_{NBS} 8.05, 7.6 and 7.2 were 4.12, 3.15 and 3.04, respectively, whereas the $\alpha_{Fe(HNN)3}$ values used for the same pH range were 9.9, 11.5 and 11.5, respectively.

There was no evidence for the presence of two classes of ligands during this study, so all data in the present work have been calculated assuming that only one class of Fe or Cu-binding ligand was present. All uncertainties are reported as standard deviation unless noted otherwise. Total dissolved Fe and Cu were measured, along with other trace metals, with the high resolution magnetic sector inductively coupled mass spectrometry (HR-ICP-MS) method (Milne *et al.*, 2010). Details on the dissolved metal determination analysis are provided in Chapter 5 of this work.

Table 4.3 Values for the inorganic side reaction coefficient for Fe (α'_{Fe}) and Cu (α'_{Cu}), for a salinity of 35 at 20 ˚C. These values were calculated using visual MINTEQ v. 3.0 by Gledhill *et al.* (submitted).

pH	$\log \alpha'_{Fe}$	$\log \alpha'_{Cu}$
7.2	8.65	0.40
7.6	9.68	0.54
8.0	10.00	1.11

4.3 Results

4.3.1 Salinity, Sea Surface Temperature (SST ˚C) and surface pH

Salinity ranged between 31.3 and 35.8 at the 21 occupied sampling stations, except in the Skagerrak area where salinity had a value of 27.4 (Figure 4.4). The lowest salinities were observed in the Norwegian coast and in the Skagerrak area (stations 13, 14 and 16).

Sea surface temperature (SST) ranged between 11.2 and 17.1 ˚C at the 21 sampling stations (Figure 4.4), with the lowest temperatures observed at the start of the cruise around Ireland in the Celtic sea (station 1) and the Irish Sea (station 2), as well as in the northern North Sea (station 17) and in the Atlantic sector (station 19). Highest temperatures were observed in the southernmost

part of the cruise in the Bay of Biscay (station 4), the southern North Sea (station 10) and the Skagerrak area (station 14).

In order to facilitate the presentation of the results and discussion, a modified definition of the regions proposed by Rérolle et al. (2014) for the D366 cruise track sampling (Figure 4.1,Table 4.4) is utilized. A smaller number of regions is proposed as a result of this work's low sampling resolution for organic ligand characteristics.

Table 4.4 Localization of the sampling stations within 5 regions of the D366 cruise defined by Rérolle *et al.* (2014) (modified version), according to geographical and water mass (*T-S*) characteristics.

Stations	Regions
1,2,3,4,5	Irish Sea, Celtic Sea and Bay of Biscay
6,7,8,9	English Channel
10,11,12,15	Southern North Sea
13,14,16	Norwegian coast and Skagerrak
17,18,19,20,21	Northern North Sea to Atlantic

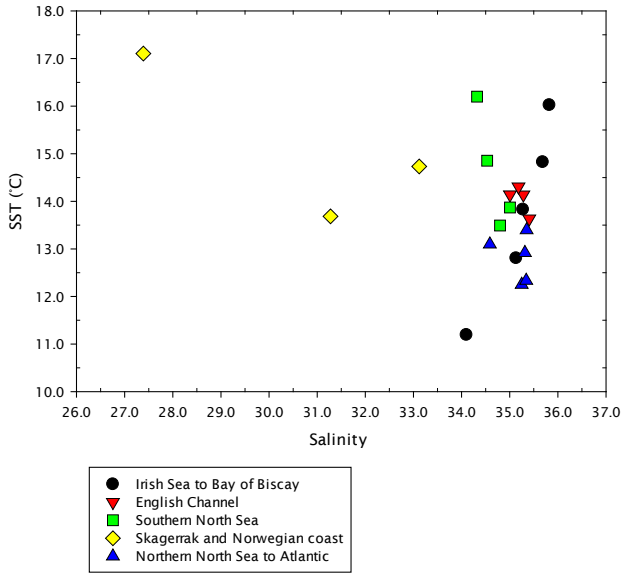

Figure 4.4 T-S diagram along the northwest European shelf seas for the 21 occupied sampling stations during cruise D366.

Surface seawater pH_{total} at the 21 sampling stations ranged between 8.04 and 8.23 (Figure 4.5), with the highest values observed in the northern North Sea (station 18) and in the Atlantic sector of the cruise (station 19), which had

some of the lowest temperature values observed during the cruise (Figure 4.4), and featured enhanced chlorophyll concentrations (up to 1.6 μgL^{-1}; Rérolle *et al.* (2014)). Lowest pH values were observed in the English Channel (station 8) and in the southern North Sea (stations 10, 11, 15). Part of this area (near station 15) presented a well-mixed water column with enhanced dissolved organic carbon (DOC) concentrations, which was presumed to result in enhanced organic matter respiration, with a consequent decrease in pH (Rérolle *et al.*, 2014). During the whole cruise track, surface pH was found to be strongly correlated with dissolved oxygen suggesting both parameters were affected by biological activity and remineralisation (Rérolle *et al.*, 2014).

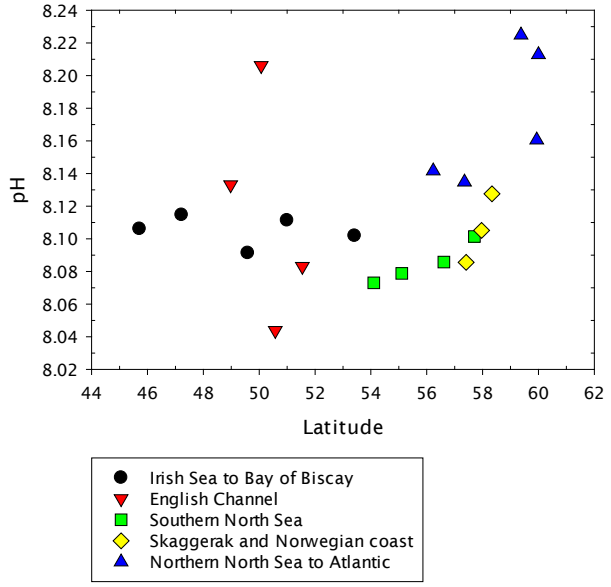

Figure 4.5 pH_{Total} values along the northwest European shelf seas for the 21 occupied sampling stations during cruise D366.

4.3.2 Surface water dissolved iron (dFe) and dissolved copper (dCu) concentrations

Surface dFe concentrations ranged between 0.5 and 5.4 nM (Figure 4.6), except in the southern North Sea (station 10) and in the Skagerrak area (station 14), where dFe showed enhanced values of 21.0 and 10.6 nM, respectively. Surface dFe concentrations had an average value of 2.2 $\pm$ 1.5 nM along the sampling stations (excluding stations 10 and 14). Surface dCu concentrations ranged between 0.4 and 5.1 nM (Figure 4.6), with an average of 2.3 $\pm$ 1.3 nM. Reported surface concentrations of dFe and dCu from this region are scarce

(Kremling and Hydes, 1988; Statham *et al.*, 1993; Tappin *et al.*, 1993; Achterberg and van den Berg, 1996; Achterberg *et al.*, 1999). A one way Anova showed that both dFe and dCu did not change significantly between the 5 region groups (Kruskal-Wallis one way Anova on ranks, P = 0.315 (dFe); one way Anova, P = 0.807 (dCu)). A more detailed analysis of dissolved iron and copper concentrations will be presented on chapter 5 of this work.

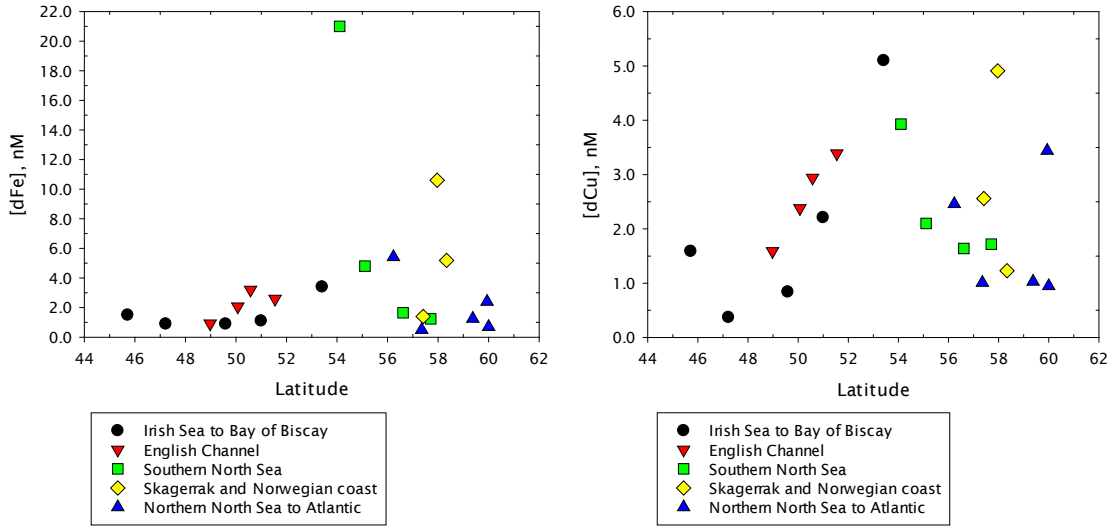

Figure 4.6 Surface dissolved iron (dFe) and copper (dCu) concentrations along the northwest European shelf seas for the 21 sampling stations during cruise D366.

4.3.3 Organic and copper binding ligand characteristics in the northwest European shelf seas – the effect of acidification

4.3.3.1 Iron and copper binding ligands [$L,_{Fe}$], [$L,_{Cu}$]

The total Fe-binding ligand concentrations [$L,_{Fe}$] in northwest European surface waters in the experimental range of pH_{NBS} 8.05 - 7.2 are shown in Figure 4.7. The highest [$L,_{Fe}$] were observed at station 10 (southern North Sea), and the lowest concentrations were observed at stations 3 to 5 (Celtic sea and Bay of Biscay, Figure 4.7). [$L,_{Fe}$] at pH_{NBS} 8.05 ranged between below detection up to 15.0 nM, except in the southern North Sea (station 10), where a high value of 20.8 nM was observed. The result defined as "below detection" is derived from the station 18 sample, where it could be inferred from the titration plot that the ligands were saturated at low added iron concentrations, and thus the fit could not be resolved in this case. At pH_{NBS} 7.6, [$L,_{Fe}$] ranged between 0.4 and

10.6 nM, except at station 10, where a high value of 20.6 nM was observed. At pH_{NBS} 7.2, $[L,_{Fe}]$ ranged between 0.6 and 9.8 nM, except at station 10, where a value of 22.5 nM was observed.

The statistical analysis conducted in order to find significant differences between iron and copper organic ligand characteristics is presented in Table 4.5.

A one way Anova on ranks showed that ligand concentrations did not change significantly with the decline of pH_{NBS} from 8.05 to 7.2 (Kruskal-Wallis one way Anova on ranks, P = 0.425, Figure 4.7, Table 4.5). A one way Anova was also conducted to compare differences between the pH treatments within the 5 region groups, for each of the variables presented in this work (ligand concentration, stability constant and free and inorganically complexed concentrations). With the decline of pH_{NBS} from 8.05 to 7.2, no significant differences were observed in $[L,_{Fe}]$ within each of the 5 different region groups (one way Anova). Differences between the pH treatments within the 5 region groups for the other variables will be discussed in the sections below.

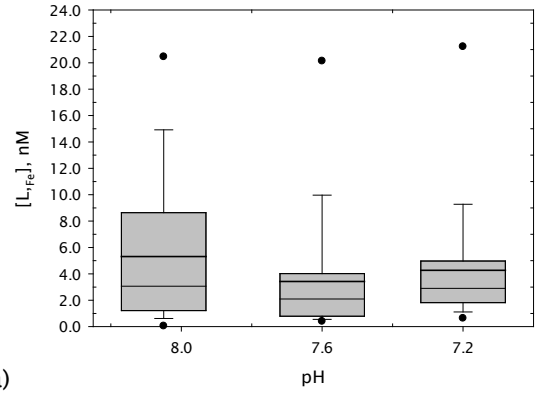

a)

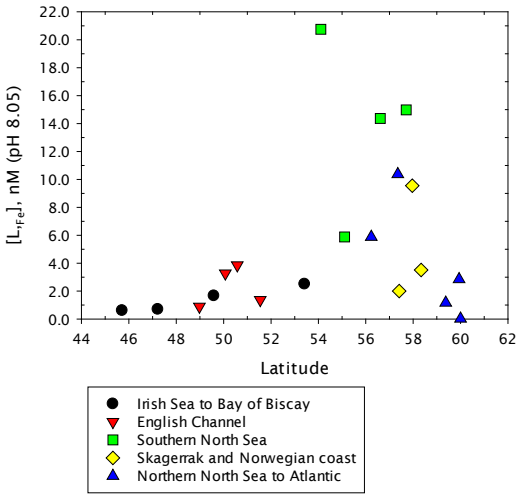

b)

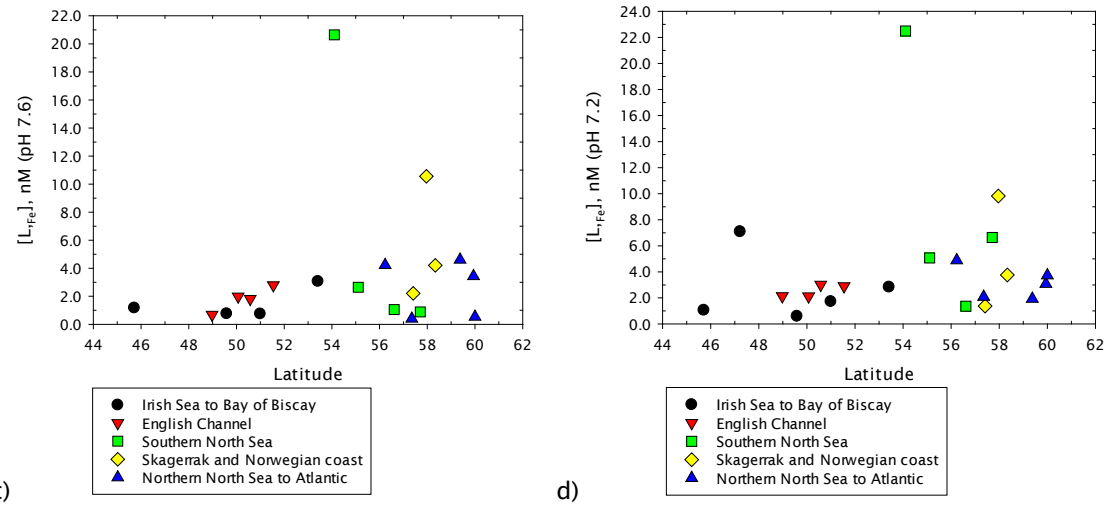

c) d)

Figure 4.7 Iron binding ligand concentrations [$L,_{Fe}$] along the northwest European shelf seas for the three different experimental pH_{NBS} values. (a) box plot, showing differences in the median and data distribution for each experimental pH in boxes with error bars. Each box shows the median (bold horizontal line) within each pH group. Variability outside the upper and lower quartiles are shown as the 5th and 95th percentiles, and the outliers as individual points; (b) [$L,_{Fe}$] (pH_{NBS} 8.05) vs latitude; (c) [$L,_{Fe}$] (pH_{NBS} 7.6) vs latitude, and (d) [$L,_{Fe}$] (pH_{NBS} 7.2) vs latitude.

The total Cu-binding ligand concentrations [$L,_{Cu}$] in northwest European shelf surface waters for the experimental pH_{NBS} range 8.05 - 7.2 are shown in Figure 4.8. The highest [$L,_{Cu}$] were observed at pH_{NBS} 7.6, at stations 7 (English Channel), and 14 (Skagerrak). The lowest concentrations were observed for all the pH_{NBS} values at stations 13 and 16 (Norwegian coast, Figure 4.8). Cu-binding ligands at pH_{NBS} 8.05 ranged between 0.3 and 5.5 nM, with an average of 2.9 $\pm$ 1.3 nM (n=18). At pH_{NBS} 7.6, [$L,_{Cu}$] ranged between 0.6 and 11.1 nM, with an average of 3.8 $\pm$ 2.8 nM (n=20). At pH_{NBS} 7.2, [$L,_{Cu}$] ranged between 0.9 and 9.8 nM, with an average of 3.8 $\pm$ 1.9 nM (n=21). A one way Anova on ranks showed that [$L,_{Cu}$] did not change significantly with the decline of pH_{NBS} from 8.05 to 7.2 (Kruskal-Wallis one way Anova on ranks, P = 0.470, Figure 4.8, Table 4.5). With the decline of pH_{NBS} from 8.05 to 7.2, no significant differences were observed in [$L,_{Cu}$] within each of the 5 different region groups (one way Anova).

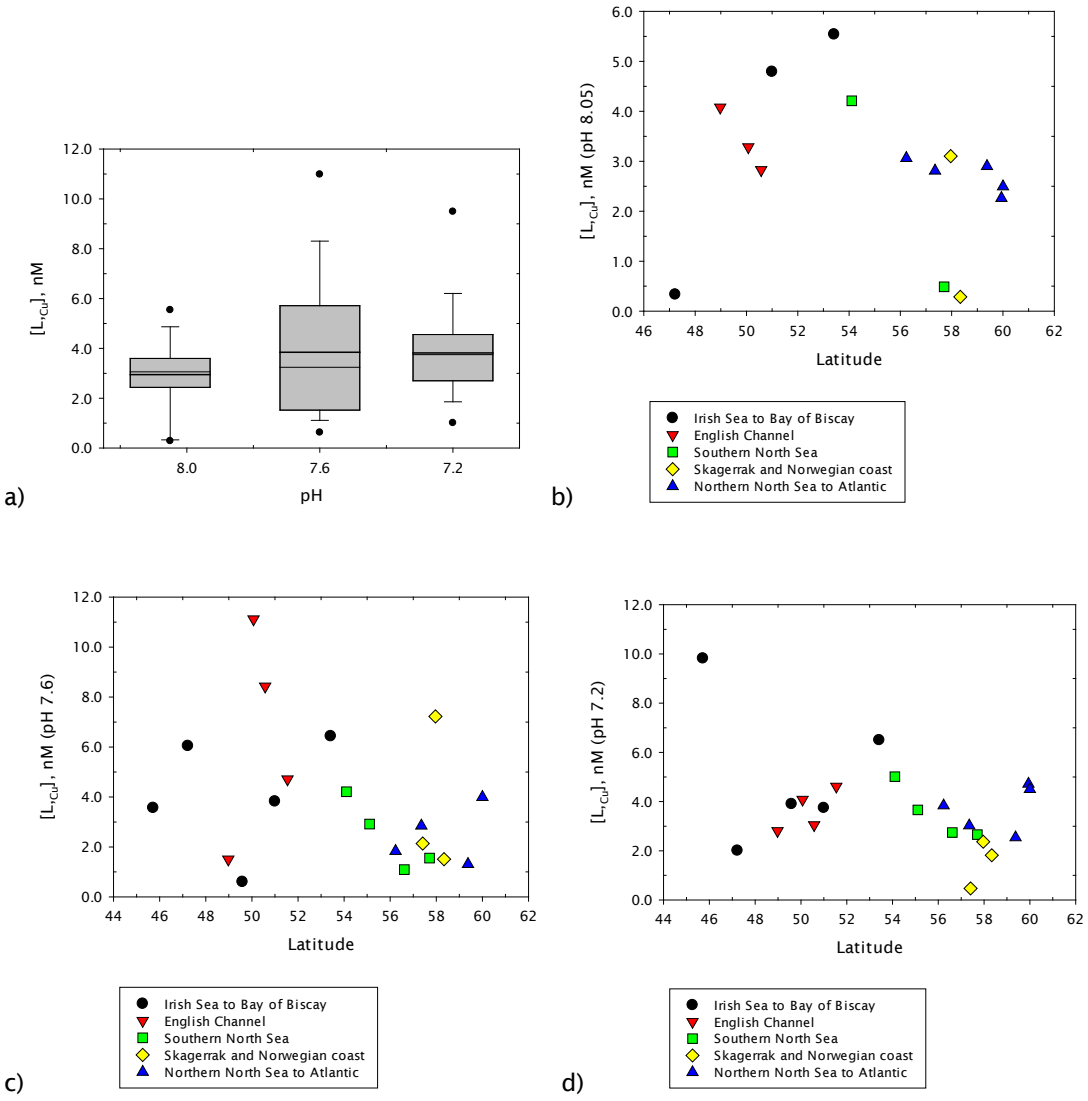

Figure 4.8 Copper binding ligand concentrations [L,$_{Cu}$] along the northwest European shelf seas for the three different experimental pH$_{NBS}$ values. (a) box plot, showing differences in the median and data distribution for each experimental pH in boxes with error bars. Each box shows the median (bold horizontal line) within each pH group. Variability outside the upper and lower quartiles are shown as the 5th and 95th percentiles, and the outliers as individual points; (b) [L,$_{Cu}$] (pH$_{NBS}$ 8.05) vs latitude; (c) [L,$_{Cu}$] (pH$_{NBS}$ 7.6) vs latitude, and (d) [L,$_{Cu}$] (pH$_{NBS}$ 7.2) vs latitude.

4.3.3.2 Stability constants for the organic complexation of iron and copper (log $K_{FeL,(Fe')}$, log $K_{CuL,(Cu')}$)

The results of the stability constants for iron with respect to Fe' (log $K_{FeL,(Fe')}$) in the range of pH$_{NBS}$ 8.05 - 7.2 are shown in Figure 4.9a. The highest log $K_{FeL,(Fe')}$ values were observed at pH$_{NBS}$ 7.2 in stations 2 (Irish Sea), 3 (Celtic sea), and 11 (southern North Sea). The lowest log $K_{FeL,(Fe')}$ values are found in station 12, 15 (southern North Sea) and 20 (Atlantic Sector). Log $K_{FeL,(Fe')}$ at pH$_{NBS}$ 8.05 ranged

between 10.5 and 13.3, with an average of 11.7 ± 0.8 (n=18). At pH_{NBS} 7.6, log $K_{FeL,(Fe')}$ ranged between 11.5 and 13.7, with an average of 12.3 ± 0.7 (n=17). At pH_{NBS} 7.2, log $K_{FeL,(Fe')}$ ranged between 11.2 and 14.3, with an average of 13.1 ± 0.9 (n=19). A one way Anova showed that stability constant values increased significantly with the decline of pH_{NBS} from 8.05 to 7.2 (One way Anova, P=< 0.001, Figure 4.9a, Table 4.5). Log $K_{FeL,(Fe')}$ mean value at logarithmic scale increased by about 1.4 from pH_{NBS} 8.05 to pH_{NBS} 7.2, suggesting that the ability of the ligands to bind iron depends strongly on the pH of seawater, and that with this decrease in pH the conditional stability of the iron complexes appears to increase. A one way Anova showed that log $K_{FeL,(Fe')}$ values were significantly different within one of the 5 region groups (English Channel) with the decline of pH_{NBS} from 8.05 to 7.2 (Kruskal-Wallis one way Anova on ranks, P = 0.014). The values at pH_{NBS} 7.2 were significantly higher than the values at pH_{NBS} 8.05.

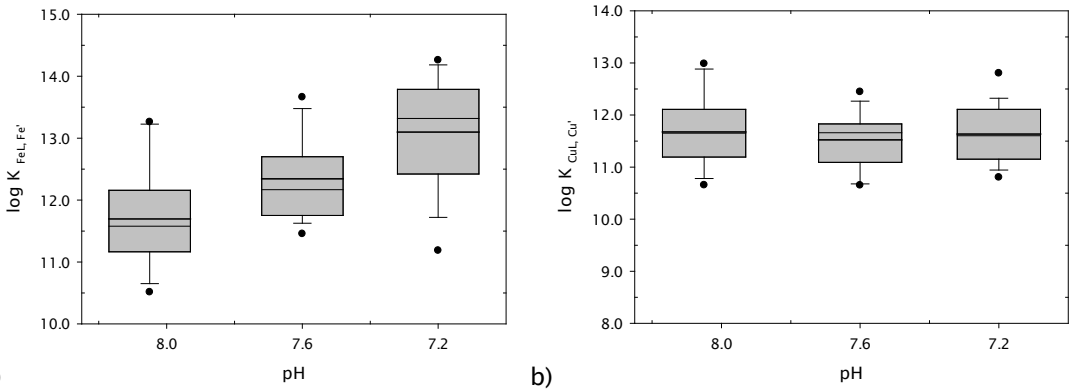

Figure 4.9 (a) Stability constant (log $K_{FeL,(Fe')}$) for iron complexes with respect to Fe', and (b) stability constant (log $K_{CuL,(Cu')}$) for copper complexes with respect to Cu' in the northwest European shelf seas for the three different experimental pH_{NBS} values (8.05, 7.6 and 7.2). Box plots show differences in the median and data distribution for each experimental pH in boxes with error bars. Each box shows the median (bold horizontal line) within each pH group. Variability outside the upper and lower quartiles are shown as the 5th and 95th percentiles, and the outliers as individual points.

The results of the stability constants for copper with respect to Cu' (log $K_{CuL,(Cu')}$) in the range of pH_{NBS} 8.05 - 7.2 are shown in Figure 4.9b. The highest log $K_{CuL,(Cu')}$ values were observed in stations 2 (Irish Sea), 8 (English Channel), and 14 (Skagerrak). The lowest log $K_{CuL,(Cu')}$ values are observed in station 13 and 16 (Norwegian coast). As in the case of iron, the trends were very similar for all of the three pH values (Figure 4.9b). Log $K_{CuL,(Cu')}$ at pH_{NBS} 8.05 ranged between 10.7 and 13.0, with an average of 11.7 ± 0.7 (n=15). At pH_{NBS} 7.6, log $K_{CuL,(Cu')}$ ranged

between 10.7 and 12.5, with an average of 11.5 ± 0.5 (n=20). At pH_{NBS} 7.2, log $K_{CuL,(Cu')}$ ranged between 10.8 and 12.8, with an average of 11.6 ± 0.6 (n=21). A one way Anova showed that stability constant values did not change significantly with the decline of pH_{NBS} from 8.05 to 7.2 (One way Anova, P= 0.710, Figure 4.9b, Table 4.5). A one way Anova showed that the log $K_{CuL,(Cu')}$ values were not significantly different within the 5 region groups with the decline of pH_{NBS} from 8.05 to 7.2 (one way Anova).

4.3.3.3 Free and inorganically complexed iron and copper concentrations [Fe'], [Cu']

A one way Anova on ranks showed that the free and inorganically bound iron concentration [Fe'] decreased significantly with the decline of pH_{NBS} from 8.05 to 7.2 (Kruskal-Wallis one way Anova on ranks, P = 0.048, Figure 4.10a, Table 4.5). The values at pH_{NBS} 7.6 and 7.2 were significantly lower than at pH 8.05. With the decline of pH_{NBS} from 8.05 to 7.2, no significant differences were found in [Fe'] within each of the 5 different region groups (one way Anova).

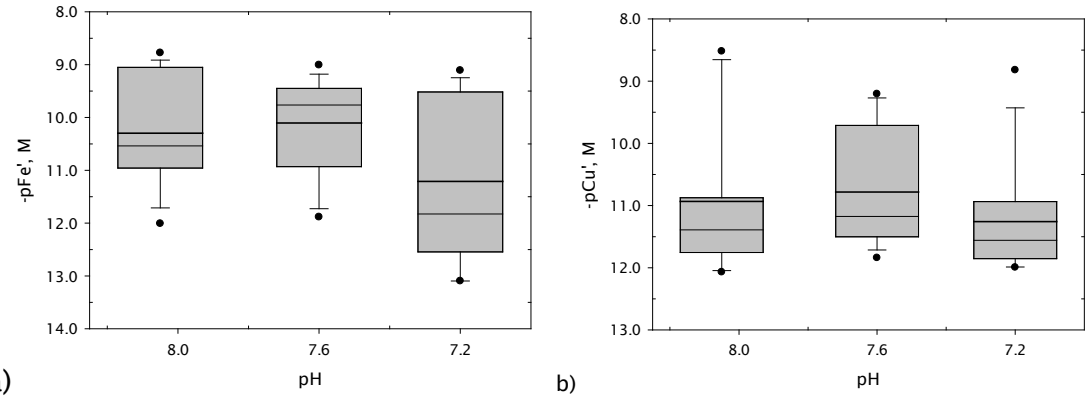

Figure 4.10 (a) Free and inorganically bound iron (III) concentration [Fe'], and (b) free and inorganically bound copper (II) concentration [Cu'], in the northwest European shelf seas for the three different experimental pH_{NBS} values (8.05, 7.6 and 7.2). Box plots show differences in the median and data distribution for each experimental pH in boxes with error bars. Each box shows the median (bold horizontal line) within each pH group; the outliers are shown as the 5th and 95th percentiles.

A one way Anova on ranks showed that the free and inorganically bound copper concentration did not change significantly with the decline of pH_{NBS} from 8.05 to 7.2 (Kruskal-Wallis one way Anova on ranks, P = 0.185, Figure

4.10b, Table 4.5). Gledhill *et al.* (submitted) found an increase in this fraction with a pH decrease from 8.18 to 7.41. With the decline of pH_{NBS} from 8.05 to 7.2, no significant differences were found in [Cu'] within each of the 5 different region groups (one way Anova).

4.3.3.4 Organically complexed metal fraction [FeL]/[Fe], [CuL]/[Cu]

Changes in organic metal complexation may be directly influenced by a shift in ocean pH. However, these alterations may also be a consequence of biological ligand production processes, which in turn are affected by pH and/or temperature changes (Breitbarth *et al.*, 2010).

With the decline of pH_{NBS} from 8.05 to 7.6, the organic iron complex fraction decreased approximately 5.32%. With the decline of pH_{NBS} from 7.6 to 7.2, this trend reverses and iron complexation increased about 7.8% (Figure 4.11). These results agree with the model results obtained by Gledhill *et al.* (submitted), who found that iron complexation first decreases and then increases, associated with the changes of $Fe(OH)_3$ and $Fe(OH)^{2+}$.

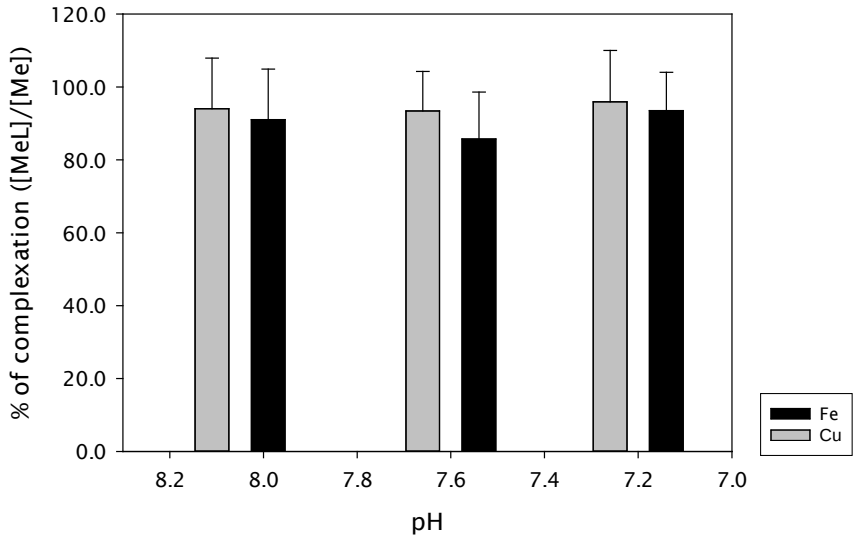

Figure 4.11 Percentage of metal complexation ([MeL]/[Me]) for iron and copper in the northwest European shelf seas for the three different pH_{NBS} values (8.05, 7.6 and 7.2).

A one way Anova showed that the organic copper complexed fraction did not change significantly with the decline of pH_{NBS} from 8.05 to 7.2, (Kruskal-Wallis one way Anova, P = 0.290, Figure 4.11). Gledhill *et al.* (submitted) model

results showed a decrease in the percentage of organically complexed copper with a decrease in pH_{NBS} from 8.18 to 7.41, which could be associated with an overall decrease in the α'_{Cu} with pH, driven by decreases in carbonate complexation.

Table 4.5 Statistical analysis across the decline of pH_{NBS} from 8.05 to 7.2 for the iron and copper organic ligand characteristics.

Variables	Significant differences with the decline of pH (from 8.05 to 7.2)	Statistical analysis
$L_{,Fe}$	No	P=0.425, Kruskal-Wallis one way Anova on ranks
$L_{,Cu}$	No	P=0.470, Kruskal-Wallis one way Anova on ranks
$\log K'_{FeL,Fe,}$	Increased	P=<0.001, one way Anova
$\log K'_{CuL,Cu,}$	No	P=0.710, one way Anova
Fe'	Decreased	P=0.048, Kruskal-Wallis one way Anova on ranks
Cu'	No	P=0.185, Kruskal-Wallis one way Anova on ranks
$[FeL]/[Fe]$	Decreased/increased	
$[CuL]/[Cu]$	No	P=0.209, Kruskal-Wallis one way Anova on ranks

4.3.3.5 Iron solubility

Liu and Millero (1999) measured the solubility of iron (III) in NaCl solutions as a function of pH, at different temperatures (5–50˚C) and ionic strengths (0–5 M). Their results at 25 ˚C and 0.7M NaCl at pH 8.04, 7.69 and 7.25 were compared with the results calculated for [Fe'] in this study for the three different pH_{NBS} levels (Figure 4.12). Their results between pH 7.5 and 9 are constant (close to 10^{-11} M), and are usually lower (Figure 4.12, (a) and (b)) than those found in this study for the pH_{NBS} 7.6 and 8.05 results, and to those usually found in seawater (>10^-10) for this pH range. However, at pH_{NBS} 7.2, the solubility of Fe

(III) found by these authors is, in most samples, higher than the values found during this study.

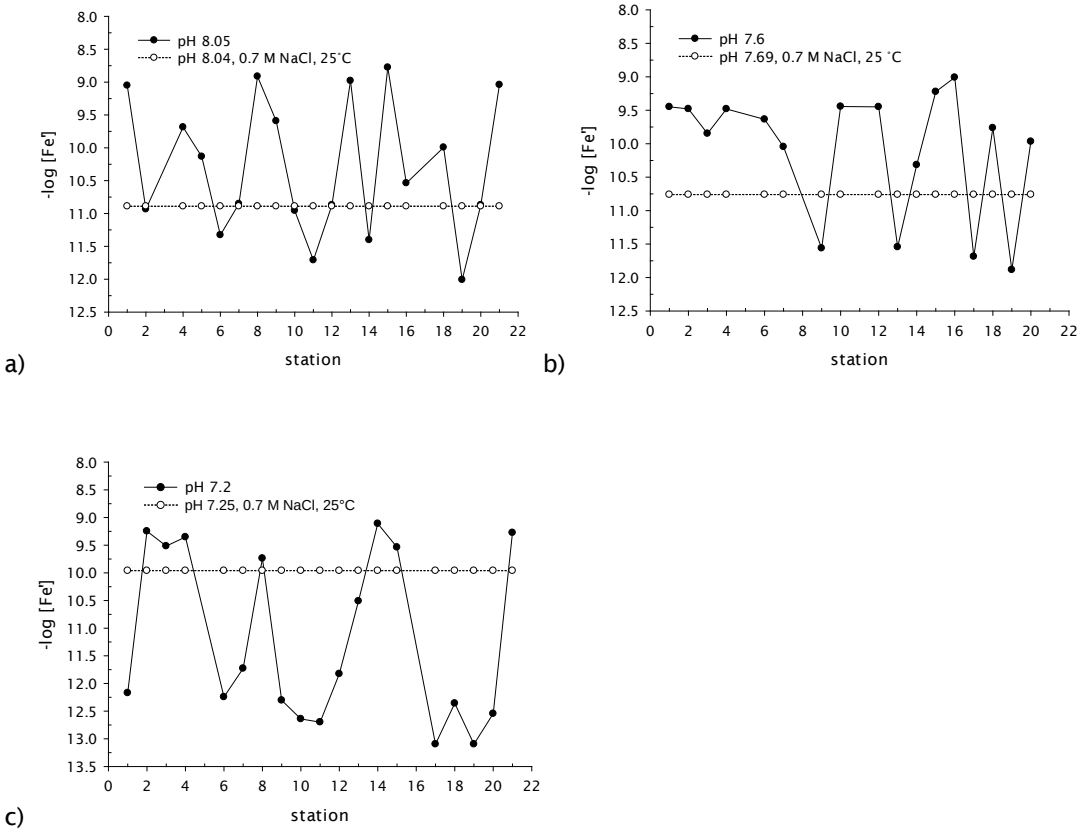

Figure 4.12 Solubility of iron (III) in NaCl solutions at 25 ˚C and 0.7 M NaCl (Liu and Millero, 1999) at pH 8.04 (a), 7.69 (b) and 7.25 (c), compared to the results obtained during this study.

4.4 Discussion

4.4.1 Iron and copper binding ligands $[L,_{Fe}]$, $[L,_{Cu}]$

In the marine environment, the hydroxide ion and organic ligands compete for binding Fe (III). A decrease in ocean pH should then affect the extent of organic Fe complexation (Shi *et al.*, 2010). This effect is not only due to changes in OH^- and H^+ ion composition, but also because the dissolved organic fraction that can complex metals is a function of pH. This is due to the presence of phenolic and carboxylic functional groups on organic material that are typical chelators for iron in the ocean (Millero *et al.*, 2009; Breitbarth *et al.*, 2010). It has been predicted that these surface sites may become less available to adsorb metals with a decrease in pH (Millero *et al.*, 2009), and it has been suggested that the

potential effect of a decrease in pH on iron ligand complexes will depend on the nature of the Fe-binding functional groups (Shi *et al*., 2010). The H^+ stoichiometry of the Fe (III) binding sites defines the magnitude of the stability constants for the iron ligand complexes (Breitbarth *et al*., 2010).

However, predicting the effect of pH on the speciation of metal organic complexes is a challenging task, due to the non-homogenous composition and unknown structures of the organic ligands (Millero *et al*., 2009). Despite the difficulties, a few attempts have been made to assess the potential effect of ocean acidification on the speciation and/or bioavailability of trace metals. Millero *et al*. (2009), for instance, assessed this effect using the ionic Pitzer (1991) interaction model. In the case of iron organic complexes, the authors infer that Fe(III) complexes may be affected by ocean acidification, as it is demonstrated that lower pH values increase the solubility of Fe in seawater (Liu and Millero, 2002). Also, as enhanced Fe solubility between pH 7 and 9 is attributed to the presence of organic ligands, then any change in solubility due to ocean acidification would probably be strongly related to changes in organic iron complexation (Liu and Millero, 2002). In the case of copper organic complexes, they believe that these will decrease with a decrease in pH, and that the Cu (II) speciation will shift towards an increase of the free Cu^{2+} ion.

A study conducted by Shi *et al*. (2010) assessed the potential effect of ocean acidification on the bioavailability of iron to marine microorganisms. They examined the effect of pH on iron uptake by four phytoplankton species, under conditions in which Fe was bound to a variety of organic ligands representing a range in functional groups. These authors observed a significant decrease in the steady state uptake rate of all phytoplankton species with decreasing pH in the range of 8.6 to 7.7. As the iron uptake rate is proportional to Fe', they showed that the effect of pH is due to a change in the chemical speciation of Fe. As Fe uptake by marine phytoplankton also depends on the extent of Fe (III) complexation; they believe that this process will also be affected by the nature of the chelating ligand (Shi *et al*., 2010). The authors conclude therefore that ocean acidification could cause a decrease in Fe availability to an extent dictated by the acid-base chemistry of the chelating ligands.

Furthermore, the extent of decrease in Fe' (which determines iron solubility) with decreasing pH will depend on the number of the protons released upon

dissociation of Fe (Shi *et al.*, 2010). Therefore, no effect of pH on Fe' should be seen when Fe is bound to chelators that are protonated in seawater and whose dissociation from Fe does not release H^+. This is the case of catechols, which are known to serve as strong ligands for Fe (III) binding and have been identified as components of organic matter (Macrellis *et al.*, 2001).

Gledhill *et al.* (submitted) reported the influence of a decrease in ocean pH on trace metal speciation. With a surface seawater sample collected from a UK estuary, and using the same analytical method as in this study (CLE-ACSV), along with a speciation model, they simulated the fate of iron and copper at different pH and DOC levels. According to their model results, the % of organically complexed copper decreased approximately 6-7% when pH decreased from 8.18 to 7.41. This decrease in copper complexation was believed to be a consequence of changes in the relative strengths of inorganic and organic complexes.

In the case of iron, Gledhill *et al.* (submitted) also found a small decrease in organic iron complexation with a decrease in pH. However, they acknowledge in their paper that the experimental results on which the model was based were not particularly reliable below pH 8 as the concentration of added ligand in the lower pH experiments was too strong relative to the inorganic complexation of iron and thus the ligands appeared to be saturated. Results obtained in this study, where the detection window for iron complexation was decreased at lower pH, are thus more reliable. The increase in iron complexation observed in this study (approximately 7.8%, with a decrease in pH_{NBS} from 7.6 to 7.2) was likely associated with reduced competition for iron by hydroxides ($Fe(OH)_3$ and $Fe(OH)^{2+}$) relative to the functional groups of the organic ligands.

de Baar *et al.* (2008) modelled organic iron complexation in an oceanic sample (2500 m depth) at three different pH values (7.75, 8.05 and 8.25). With the decrease in pH, they did not find a significant difference in the ligand concentration, or in their respective stability constants. They did not find any changes in copper organic complexation either (>99.99%) with a decrease in pH from 8.07 to 7.5, when an equilibrium thermodynamics speciation model ($Mineql^+$ 4.6) was used. These findings agree with the experimental results observed during this study (Kruskal-Wallis one way Anova, P=0.425 ($L,_{Fe}$), and

P=0.470 ($L_{,Cu}$); Figures 4.6 and 4.7). The results observed during this study along with the ones obtained by de Baar *et al.* (2008), suggest that any changes in complexation due to a decrease in pH are possibly too small to be detected by the current precision of the CLE-ACSV technique.

4.4.2 Stability constants (log $K_{FeL,(Fe')}$, log $K_{CuL,(Cu')}$)

It has been suggested that a pH decrease may affect iron stability constants (Breitbarth *et al.*, 2010). Log $K_{MeL,(Me')}$ is the constant that most readily provides an insight into the effective influence of the metal binding organic ligands on speciation, since the ratio of organically complexed metal to the inorganic forms of the metal is given by [MeL]/[Me'] = log $K_{MeL,(Me')}$ [L'] (Rue and Bruland, 1995).

As mentioned before, the potential effect of pH acting directly on FeL complexes will depend on the nature of the Fe-binding functional groups (Shi *et al.*, 2010). Natural iron chelators in the marine environment, such as siderophores (Mawji *et al.*, 2008) have functional groups with different acid dissociation constants (pK_a). The H^+ stoichiometry of the Fe (III) binding sites defines the magnitude of the pK_a values, and consequently the value of the conditional stability constant of the resultant FeL complex (log K_{FeL}).

During a study conducted by Averyt *et al.* (2004) in two lakes, a decrease in log K_{CuL} value was found with a decrease in pH. Similar effects were found for cadmium ligands.

Sunda and Huntsman (2003) demonstrated that the conditional equilibrium constant for the dissociation of the Fe-EDTA chelates in the dark increased with pH. These values were similar at different temperatures (10 and 20 ˚C), but increased by 600-fold as the pH was increased from 7.7 to 9.0. They believe that these pH effects are not specific to Fe-EDTA and should also occur in other hydrolyzable ferric-chelates. However, during this work, an increase in log $K_{FeL,(Fe')}$ was observed with a decrease in pH (One way Anova, P=<0.001), as a result of a decrease in α'_{Fe} when pH decreases.

The increase in log $K_{FeL,(Fe')}$ could suggest that in a more acidic ocean the predominant iron complexes could be of a stronger binding nature, relative to the inorganic iron complexation. An increase in log $K_{FeL,(Fe')}$ could also suggest

that iron complexation is likely to increase with a decline in pH, as it was observed in the amount of the complexed fraction [MeL]/[Me], when pH declined from 7.6 to 7.2 (Figure 4.11). Gledhill *et al.* (submitted) found in their experimental results that log $K_{FeL,(Fe3+)}$ decreased from 22.43 $\pm$ 0.03 to 20.76 $\pm$ 0.09 with the decline of pH from 8.3 to 6.8, suggesting that natural ligands were acidic and thus deprotonated at natural seawater pH, as it happens in the case of EDTA. However, when normalized to Fe' during the same study, log $K_{FeL,(Fe')}$ increased by approximately 1 log unit with a decrease in pH from 8.3 to 6.8, in agreement with this work's observations of an increase of approximately 1.4 log units. They found the same trend in the case of log $K_{CuL,(Cu2+)}$, which decreased from 12.1 $\pm$ 0.01 to 10.2 $\pm$ 0.01 with the decline of pH from 8.2 to 6.8. However, this trend was not as strong as for iron, so when normalised to Cu' log $K_{CuL\ (Cu')}$ does not change more than 0.7 units, although their results are still in contrast compared to the ones found during this study, as no significant changes were observed in log $K_{CuL\ (Cu')}$ with a decrease in pH (One way Anova, P=0.710).

4.4.3 Free and inorganically complexed iron and copper concentrations [Fe'], [Cu']

The speciation of many metals, including iron and copper, is influenced by pH. A decrease in ocean pH will consequently alter their bioavailable forms, which are usually related to their inorganic complexed forms (Millero *et al.*, 2009).

Millero *et al.* (2009) suggested, from the results of their speciation model, that metals that form strong inorganic complexes with hydroxide and carbonate ions (such as Fe (III) and Cu (II)) will have a higher fraction in their free forms at lower pH. The copper free ionic form (Cu^{2+}) is expected to increase approximately 30% with a decrease in pH from 8.1 to 7.7. During this study, Cu' did not show any significant changes with a decrease in pH (Kruskal-Wallis one way Anova on ranks, P=0.185). However, the free metal form is expected to increase at lower pH due to changes in inorganic equilibria, even if the Cu' overall magnitude does not show apparent changes.

Cu (II) speciation is predicted to experiment major changes in its inorganic speciation. $CuCO_3$ (aq) is the most abundant of the inorganic copper species. Using a speciation model, de Baar *et al.* (2008) predicted for the % of $CuCO_3$

(aq) species to decrease from 81% at pH 8.07, to 72% at pH 7.5. With a decrease in pH from 8.07 to 7.5, the same authors projected that the free Cu^{2+} would increase from 6 to 17% of the total inorganic species (de Baar *et al.*, 2008).

de Baar *et al.* (2008) projected, from the results of the same speciation model, that Fe' increases from 8 to 24 pM, when the pH decreases from 8.07 to 7.5. They also found that FeL increases from 514 to 698 pM with the same decrease in pH. As total dFe = Fe' + FeL, they would expect an increase in the dissolved Fe fraction with ocean acidification. If Fe' increases with a decrease in pH as predicted in these models (de Baar *et al.*, 2008; Millero *et al.*, 2009), then Fe' will be presumably more available to phytoplankton and consequently large portions of the oceans currently limited by Fe' may experience higher productivity.

The opposite trend has been found in other experimental results. An experiment conducted on the effect of pH on iron speciation in seawater showed that, in a sample of surface water from the north sea, Fe' decreased with decreasing pH (Gledhill *et al.*, 1998), which is consistent with the present work's observations (Kruskal-Wallis one way Anova on ranks, P=0.048). These results could also imply that the effectiveness of natural ligands in maintaining Fe in solution might be increased at low pH and may result in a slower Fe loss via the formation of Fe oxyhydroxide precipitates (Shi *et al.*, 2010).

Gledhill *et al.* (submitted) model results suggest that the overall impact of pH on the concentrations of Fe' is dependent on both iron and DOC concentration, with changes in pH becoming more pronounced as the difference between the total Fe and DOC concentrations increased. In the case of copper, Gledhill *et al.* (submitted) found that the increased competition between copper and hydrogen ions for the functional groups result in an increase in the cupric ion concentrations with a decrease in pH, from ca. 30 to 90 pM, in agreement with de Baar *et al.* (2008) and Millero *et al.* (2009) results.

4.4.4 Iron solubility

Metal solubility in seawater is a strong function of pH (Millero *et al.*, 2009). Fe availability to phytoplankton is a function of its solubility and oxidation state. As mentioned before, Fe (III) solubility is strongly influenced by organic

complexation at the current pH of seawater. The fraction that is not chelated is present as hydrolysed species, $Fe(OH)_x^{(3-x)}$, with the metal tri-hydroxy species, $Fe(OH)_3$, being very insoluble (Liu and Millero, 1999; Liu and Millero, 2002). When seawater pH falls below 8, changes in the inorganic speciation result in an increase of the thermodynamic Fe (III) hydroxide solubility. Millero *et al.* (2009) suggest that this increased solubility along with changes in kinetics will consequently make iron more available to phytoplankton.

Due to the extremely complex chemical behaviour of iron in seawater, the solubility of inorganic iron species is uncertain (Kuma *et al.*, 1996; Liu and Millero, 1999) as is the exact composition of its various soluble ferric hydrolysis species ($Fe(OH)_2^+$, $Fe(OH)_3$, and $Fe(OH)_4^-$) (Waite, 2001). However, knowing the composition of ferric hydrolysis species is important since the extent of hydrolysis has a major impact on the kinetics and equilibria of iron chelation reactions (Morel *et al.*, 1991; Albrecht-Gary and Crumbliss, 1998), and thus controls both iron complexation dynamics and biological uptake rates (Hudson and Morel, 1990; Sunda and Huntsman, 2003).

Gledhill *et al.* (submitted) assessed the solubility of iron over the pH range used in their study. They found that as pH decreased, concentrations of dissolved iron increased. Millero *et al.* (2009) also projected an increase in the dissolved Fe fraction with a speciation model.

4.5 Conclusions

Previous studies provide a first insight of the fate of iron and copper speciation in a more acidic future ocean. It seems that changes in iron solubility and bioavailability as a result of ocean acidification will be dictated by the nature of the organic chelating material present in the marine environment. In the case of copper, these studies propose a decrease in the amount of organic complexation, and that this decrease is going to be more likely associated to the relative strengths of the inorganic and organic complexes, as copper is known to form strong complexes with CO_3^{-2} ions, and which are expected to decrease approximately 77% by the year 2100 (Millero *et al.*, 2009).

This work's results suggested that ocean acidification will potentially result in a reduction of the inorganic metal fraction (Fe'). An increase in the organic iron

complexed fraction was observed during this study, when pH decreased from 7.6 to 7.2.

Several studies have suggested that the proportion of inorganic copper that is present as the free cupric form (Cu^{2+}) will increase with ocean acidification, due to changes in its inorganic equilibria (speciation). However, the overall Cu' magnitude may not be affected with a decrease in pH relative to organic complexation, as it was observed during this study.

In summary, ocean acidification could have potential harmful effects on primary productivity by increasing the concentration of free ionic copper. However, ocean acidification could also stimulate primary productivity as a result of an increase in the iron's dissolved fraction, as previous studies have suggested.

It is necessary to take into account the limitations that the analysts have when using the currently available CLE-ACSV technique, in order to assess metal speciation. The limitations inherent to CLE-ACSV data interpretation could raise questions about the accuracy of the technique. Discerning on how big a change in ligand parameters should be due to a reduction in pH in order to be detected by the technique is one of the main concerns. The accuracy of the technique is subject then, due to its indirect nature and multiple subjective variations during the experimental and analytical processes, to potential systematic errors that could underestimate the results when trying to find significant differences in ligand concentrations due to ocean acidification.

Chapter 5: Total dissolved metals (Fe, Cu, Zn, Cd, Ni, Pb) in surface waters of the northwest European shelf

5.1 Introduction

Coastal and estuarine environments are highly dynamic and complex systems with often significant spatial and temporal variabilities. Around the world, these environments are often densely populated and as a consequence they receive significant amounts of anthropogenic inputs, which are transported via rivers to the ocean.

Anthropogenic pollutants, such as metals, have put coastal ecosystems under strong environmental pressure over the past decades due to enhanced human activities (Pan and Wang, 2012). The waters of the northwest European shelf seas are also subjected to coastal environmental pressure. The catchment areas of the rivers draining to the North Sea are highly populated; highly industrialized and intensively farmed (Achterberg *et al.*, 1999), and therefore comprises an important source of trace metals to the shelf seas.

Continental shelf regions represent effective traps for dissolved and land-derived sediments associated trace elements. They are highly productive and the sedimentation of that productivity provides an additional mechanism to trap elements inputs to the coastal zone from land (Chester and Jickells, 2012). Between 80-90% of the total trace metal input to the oceans accumulates in ocean margins, including shelf regions and estuaries (Martin and Windom, 1991; Chester and Jickells, 2012).

The surface distribution of dissolved trace metals is influenced by several physical and chemical processes such as biogenic uptake, remineralisation, atmospheric deposition to surface waters, vertical mixing by upwelling or convection, inputs from hydrothermal vents and continental input from rivers or shelf sediments (Kremling, 1985; Klunder *et al.*, 2011). Another important physical hydrodynamic process influencing trace metal distributions is the advection of water masses enriched in trace metals, following contact with continental margins (Bown *et al.*, 2011). Metals such as Al, Pb, Co and Mn

show higher concentrations in surface waters, suggesting a strong influence by external sources (Kremling, 1985).

A number of trace metals (e.g. Cd, Zn and Ni) are strongly biologically mediated, with a nutrient type distribution (phosphate, nitrate or silicate) (Boyle, 1988; Ellwood, 2008; Croot *et al.*, 2011; Boye *et al.*, 2012). Other metals (Al, Pb) present a scavenged type distribution (Flegal and Patterson, 1983), while others such as Mn, Fe and Cu are considered as hybrid-type metals, as their distribution is controlled by both recycling and relatively intense scavenging processes (Bruland and Lohan, 2004). Other metals, such as Mo, have a conservative type distribution, as they only interact weakly with particles, and consequently have oceanic residence times greater than 10,000 years (much greater than the mixing time of the oceans), and have concentrations that maintain a relatively constant ratio to salinity (Bruland and Lohan, 2004).

Biologically mediated metals, or trace metal micronutrients, can play a key role in the productivity of the oceans (Wyatt *et al.*, 2014). Laboratory studies and shipboard incubation experiments have demonstrated the relationships between certain trace nutrients for phytoplankton uptake (Boye *et al.*, 2012). Cd and Zn for example, can interact with Co in cellular metabolism (Price and Morel, 1990; Sunda and Huntsman, 1995a).

The coupling between trace metals and major nutrient cycles, such as the correlations between Cd and PO_4^{-3} or Zn and SiO_4^{-4} in the Southern Ocean (Bruland *et al.*, 1978a; Boyle, 1988; de Baar *et al.*, 1994; Ellwood, 2008), indicate the removal of these metals in the surface due to phytoplankton uptake and their later sinking and remineralisation in deep waters (Boye *et al.*, 2012).

Zn is an essential cofactor in many phytoplankton enzymatic processes (Morel and Price, 2003). The coupling between zinc and the major nutrients such as silicate and phosphate represents an important control on the efficiency and size of the biological carbon pump (Wyatt *et al.*, 2014). In oceanic surface waters, Zn is present at concentrations of <0.1 nM, with 98% of this pool chelated by strong organic ligands (Bruland, 1989; Lohan *et al.*, 2005) and hence reducing the bioavailable reduced free Zn^{2+} to concentrations < 2pM (Wyatt *et al.*, 2014). These concentrations have been shown to limit

phytoplankton growth in culture experiments (Brand *et al.*, 1983; Sunda and Huntsman, 1992; Sunda and Huntsman, 1995a; De La Rocha *et al.*, 2000). In diatoms, the uptake of silicate has also been shown to be limited by low Zn concentrations (De La Rocha *et al.*, 2000).

Cd is predominantly supplied to open ocean surface waters via vertical mixing, and removed by physical adsorption and biological uptake by microorganisms (Bruland, 1980; Baars *et al.*, 2014). Cd is toxic to microalgae at elevated concentrations (Brand *et al.*, 1986) but can also have beneficial effects at levels found in the open ocean by alleviating Zn limitation stress in phytoplankton (Price and Morel, 1990). The vertical distribution of dissolved Cd strongly correlates with phosphate in oceanic waters (de Baar *et al.*, 1994). The same linear relationship has been observed for Ni and phosphate in the subantarctic zone (Ellwood, 2008). Dissolved Cu has shown a strong relationship with silicate in the water column in the Southern Ocean (Boye *et al.*, 2012).

Knowledge of dissolved trace metal distributions in the oceans has increased with the development of new sensitive analytical techniques such as isotope dilution inductively coupled mass spectrometry (ID-ICPMS), which now allows for multi-element analyses with low limits of detection (Milne *et al.*, 2010).

Information about the spatial distribution of trace metals in the northwest European shelf seas is still limited. Kremling (1983) highlighted that the remobilization of trace metals from partly reduced sediments and subsequent mixing into the surface waters is of high importance around the British Isles. Furthermore, these processes can be variable due to seasonal changes in the currents, hydrography and possibly on temporal variations in the chemistry and biology of the shelf sediments (Kremling, 1983).

It is well known that the tidal currents west of Britain and in the North Sea enhance mixing to a degree that some regions are vertically homogeneous throughout the year whereas others are seasonally stratified, thus preventing continuous transfer of properties from near bottom waters into the upper layers during the summer, when this cruise took part. Therefore, local and seasonal variations in the surface values over the shelf area should be taken into account (Kremling, 1983).

Dissolved metals in the NW European shelf

The horizontal distribution of the dissolved trace metals Cd, Cu, Fe, Ni, Pb and Zn in the northwest European shelf seas, where a high resolution pH database was created for the first time during the same cruise, is presented in this chapter in order to determine their sources, spatial variabilities, their coupling with major nutrients and their connection with the hydrography of the area and biogeochemical processes.

5.1.1 Hydrography of the northwest European shelf seas

5.1.1.1 North Sea

The North Sea is located on the northwest European continental shelf with an open north boundary to the North Atlantic Ocean (Thomas *et al.*, 2005). The shallow North Sea is divided into the southern North Sea, the central North Sea, the Norwegian Trench and the Skagerrak Strait (OSPAR Commission, 2000). The hydrography of this area presents two major inflows into the North Sea: the first consists of Atlantic water entering from the north between the Shetlands and Norway (Holt *et al.*, 2009), and from the south via the strait of Dover; the other major inflow consists of Baltic Sea waters entering via the Skagerrak between Denmark and Norway (Kremling, 1985; Thomas *et al.*, 2005).

The mean depth of the North Sea is 74 m with increasing depth from south to north. Topographical exceptions are the Doggerbank (south-west of Central North Sea) with a depth of 15 m, and the Norwegian Trench with depths larger than 300 m and up to 700 m in the Skagerrak area (OSPAR Commission, 2000; Lenhart *et al.*, 2004).

The North Sea is significantly influenced by riverine freshwater inputs, from the Somme and Seine in the English Channel, the Humber in northern England, and from the Elbe, Weser, Rhine, Meuse, Scheldt, and Thames in the southern North Sea. The annual input of freshwater into the North Sea is in the order of 300 km^3, with about one third of the total run-off coming from the melted water from Norway and Sweden, and the rest from the river system discharges. However, the principal source of fresh water to the North Sea is the rivers that discharge into the Baltic Sea, with an annual water supply of around 470 km^3 (OSPAR Commission, 2000).

The mean currents of the North Sea form a cyclonic circulation (Figure 5.1). The bulk of the transport in this circulation is concentrated to the northern part of the North Sea due to major water exchange with the Norwegian Sea. The major transport pathway out of the North Sea is the Norwegian Coastal Current (NCC, Figure 5.1) (Holt *et al.*, 2009). The circulation in the North Sea can occasionally reverse into an anti-cyclonic direction. Before it leaves the North Sea, most of the water passes through the Skagerrak area, with an average cyclonic "counter clockwise" circulation before leaving along the Norwegian coast (OSPAR Commission, 2000).

There are three major forces acting within the North Sea: the tides, the wind-driven circulation and surface heat fluxes as well as the horizontal and vertical density gradient. The tidal induced transport processes of advection and mixing are more vigorous in the southern, shallow parts than in the northern, deep parts. The most important agent for vertical exchange is heat exchange at the sea surface (Lenhart *et al.*, 2004).

Driven by strong winds, most areas of the North Sea outside the Norwegian Trench and the Skagerrak area are vertically well mixed in winter. As the Norwegian Trench and Skagerrak Strait are strongly influenced by fresh water input, they have a stable stratification all year round.

Fronts are a common feature in the North Sea. They may restrict horizontal dispersion and can be of particular importance due to the enhanced biological activity in these regions (OSPAR Commission, 2000).

5.1.1.2 Irish and Celtic Seas

The Irish Sea is a relatively shallow, semi enclosed water body, with overall residual water flow from south to north.

Oceanic water from the North Atlantic enters from the south and west of the Irish Sea and moves northwards through the area to exit into arctic waters to the north (Figure 5.1) or, after flowing around the north of Scotland, to enter the North Sea (OSPAR Commission, 2000).

In the Irish Sea, there is substantial freshwater input to the inlet of the Bristol Channel from the river Severn, accounting for 60% of the total freshwater input

at the extreme east of the inlet. The welsh rivers to the north account for a further 30% (OSPAR Commission, 2000).

There is a north-westerly shelf edge current that follows the slope edge from the Bay of Biscay to the southwest of Ireland. During summer the Celtic Sea is strongly stratified (OSPAR Commission, 2000).

The incoming oceanic water to the southern Irish Sea, and the water to the west of Ireland and the Western Isles of Scotland and within the Celtic Sea, is almost unaffected by human activities. Only the freshwater influenced component which flows into the Irish Sea from the south receives much in terms of land-based inputs of contaminants (OSPAR Commission, 2000).

In the Irish Sea, frontal systems tend to develop in late spring at the confluence of mixed and stratified areas, for example, the Celtic sea front to the south of the Irish Sea and the Irish Sea front to the west of Ireland. Stratification also occurs in the Irish Sea, especially to the west of the Isle of Man where the water is deeper (OSPAR Commission, 2000).

5.2 Materials and methods

5.2.1 Sample collection

Seawater samples were collected during the RRS Discovery 366 research cruise from the 6th June – 7th July 2011, in the northwest European shelf seas (Figure 5.2). Sampling stations are the same as described in the previous chapter, and the division of regions is also the same. Samples were collected daily with the use of a towed fish (ca. 0.2 m deep) and a Teflon bellows pump (Almatec A15) which pumped water through an acid cleaned PVC hose into a clean container where the samples were filtered into acid-cleaned 60 ml low density polyethylene bottles (LDPE; Nalgene) using online filtration with a 0.2 µm Sartobran P-300 filter capsule (Sartorious). Each sample was immediately acidified to pH ~2 (80 µl; 0.011 M) on board in a laminar flow hood (class 100) with ultrapure HCl (Romil UpA) and stored in double bags in the dark at ambient temperature until their analyses in the shore-based laboratory about 22 months after their collection.

Surface macronutrients (nitrite+ nitrate, silicate and phosphate) were collected every two hours from the underway supply during the cruise.

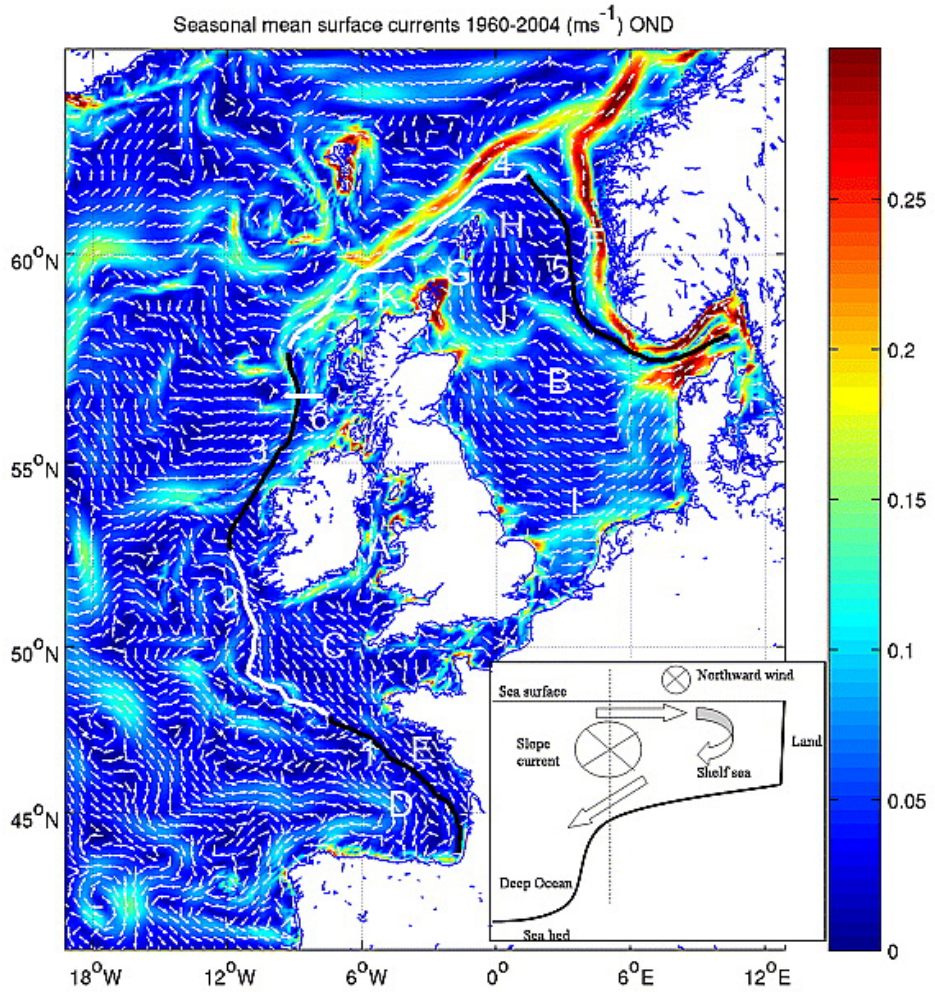

Figure 5.1 Mean surface currents for autumn and the numbered sections following the 200 m isobath used for flux calculations (black and white heavy lines). Insert shows a schematic of the slope current and the Ekman circulation. Geographical areas are: A, Irish Sea; B, North Sea; C, Celtic Sea; D, Biscay; E, Armorican Shelf; F, Norwegian Trench/Coastal Current; G, Fair Isle Channel/current; H, Shetland to Norway; I, Dogger Bank; J, Dooley Current; K, Malin-Hebrides shelf. Source: Holt *et al.* (2009).

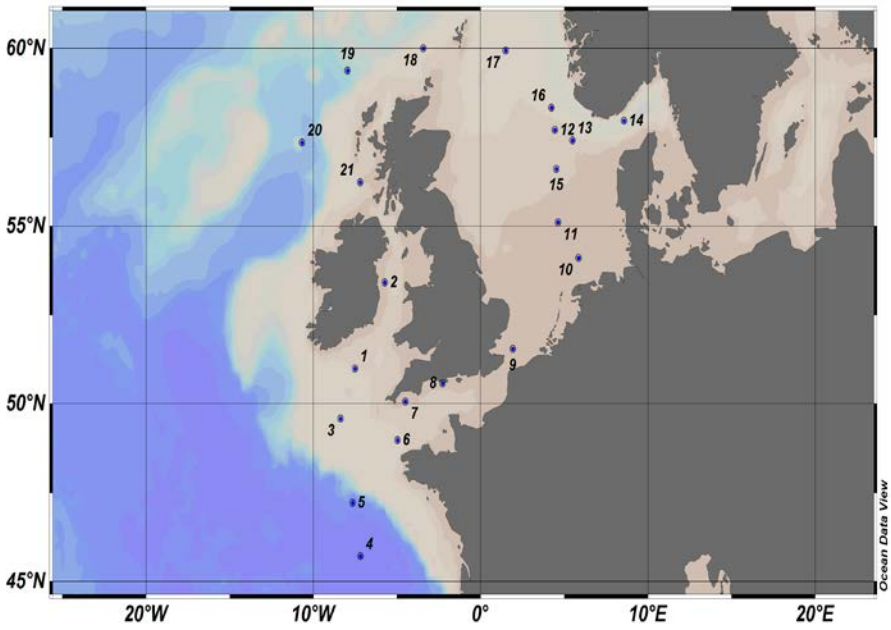

Figure 5.2 Sampling stations along the northwest European shelf seas for the determination of total dissolved trace metals (Fe, Cu, Zn, Cd, Ni, Pb).

5.2.2 Total dissolved trace metal determination

Concentrations of dissolved trace metals (Fe, Cu, Zn, Cd, Ni, Pb) were determined using the isotope dilution approach followed by high resolution magnetic sector inductively coupled mass spectrometry (HR-ICPMS) detection, following the methods described in Milne *et al.* (2010). The whole determination procedure was performed with the help and supervision of Dr Christian Schlosser, NOC. Certified Reference Materials, detection limits and blank values used for the dissolved trace metal determination for the samples collected during the D366 research cruise are provided in Appendix D.

The analysis was conducted following an offline preconcentration/matrix removal step on a Toyopearl AF-650M chelating column (Milne *et al.*, 2010). Briefly, 15 ml of the acidified sample in an acid cleaned 30 ml FEP bottle (Nalgene) was spiked with 100 µl of a multi-element standard of isotopes (containing the stable isotopes ^{65}Cu, ^{111}Cd, ^{62}Ni, ^{57}Fe, ^{68}Zn and ^{207}Pb) with known enrichments over their natural abundance. A working solution of ^{65}Cu, ^{111}Cd , ^{62}Ni, ^{57}Fe, ^{68}Zn and ^{207}Pb was prepared in 0.024 M ultrapure HNO_3 (Romil UpA), and the exact concentrations of the enriched isotope spikes in the mixed solutions were determined by ICP optical emission spectroscopy calibration against known natural standards (10 mg l^{-1}, ICP High Purity Standards) (Milne

et al., 2010). The spiked samples were left for overnight equilibration. Subsequently, the samples were buffered to pH 6.4 ± 0.2 using 2M ammonium acetate, prepared with ultrapure acetic acid and ammonia (Romil UpA).

The buffered sample was then pumped over the preconcentration column, at 2 ml min^{-1}. The column was rinsed with 1 ml de-ionised water to remove salts, and subsequently the metals were eluted for 30 s using 1 ml of 1M HNO_3 (Romil UpA). The eluent was collected into acid cleaned autosampler polypropylene vials (OmniVials; 4 ml) and capped.

Prior to loading of the next sample, the column was washed with an acid solution (1.5M HCl) to remove residual trace elements. The extracted samples were analysed using a HR-ICP-MS (Element XR, Thermofisher, NOC laboratory). The sample was introduced via a 100 µl Teflon nebuliser connected to a quartz spray chamber. Measurements for Fe, Ni, Cu and Zn were performed in medium resolution mode (R=4000), whilst the isotopes for Cd and Pb were analysed in low resolution mode (R=300).

5.2.3 Surface macronutrients and total chlorophyll *a*

Surface macronutrients (nitrite+ nitrate, silicate and phosphate) concentrations were analyzed onboard by Mark Stinchcombe, NOCS, using a segmented flow autoanalyser following standard colourimetric methods (Grasshoff *et al.*, 1999).

Total chlorophyll *a* concentrations were measured onboard by David Suggett, following Poulton *et al.* (2010), with water samples (0.25 L) filtered onto Whatman GF/F filters, extracted in 8mL 90% acetone, and stored at 4 ˚C for 18–20 h. Fluorescence was measured on a Turner Designs Trilogy Fluorometer, calibrated with purified chlorophyll *a* (Sigma, UK).

5.3 Results and discussion

5.3.1 Surface macronutrients

Phosphate concentrations ranged between 0.01 (below the detection limit) and 0.54 µM, along the whole cruise track. Average concentration was 0.11 ± 0.09 µM. Highest phosphate concentrations were observed in the Irish Sea, Malin

Sea and northern North Sea (Figure 5.3). At the dissolved metals sampling stations, phosphate concentration had a high value of 0.53 µM at station 12 in the southern North Sea, and phosphate concentrations were below the detection limit at stations 13, 14 and 16 (Norwegian coast and Skagerrak area).

Silicate concentrations ranged between 0.01 and 5.15 µM, with an average of 0.97$\pm$ 0.80 µM, along the whole cruise track. Highest silicate concentrations were observed at the English Channel the southern North Sea, and in the Irish and Malin Seas (Figure 5.4). Highest silicate concentrations at the dissolved metals sampling stations were observed at stations 3, 6, 8 and 10 (Celtic sea, English channel and southern North Sea, respectively), whereas lowest silicate concentrations were observed at the northern part of the transect (Skagerrak, Norwegian coast and northern North Sea).

Nitrite + nitrate concentrations ranged between 0.01 and 6.17 µM, along the whole cruise track. Average concentration had a value of 1.00 $\pm$ 1.37 µM. Highest nitrite + nitrate concentrations were observed at the English Channel, southern North Sea, and in the Irish and Malin Seas (Figure 5.5). Highest nitrite + nitrate concentrations at the dissolved metals sampling stations were observed at stations 5, 6 and 20, with high values of 1.29, 3.05 and 1.42, respectively.

Nitrite and nitrate vs. phosphate presented a low linear relationship (r^2 = 0.58), in the study area (Figure 5.6). This is likely due to the different regional sources for these two nutrients, as nitrates are more influenced by fresh water sources, with anthropogenic nitrogen in rivers originating mostly from the leaching of fertilised agricultural soils (highest concentrations in the English Channel) whilst phosphates are mostly related to domestic wastewater (highest concentrations in the Irish and Malin Seas).

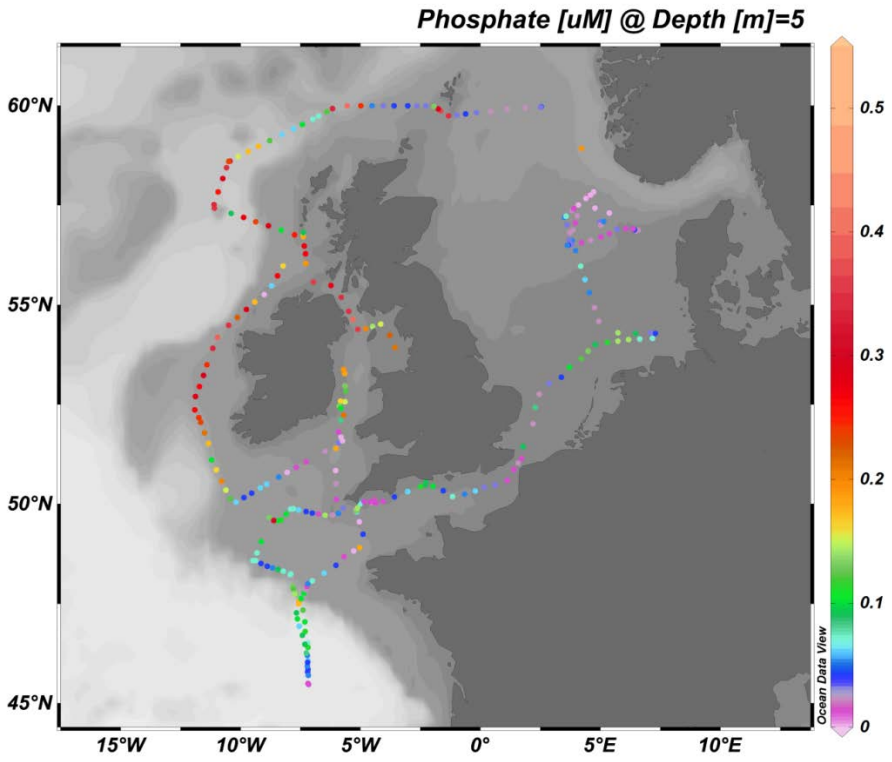

Figure 5.3 PO_4^{-3} concentrations (µM) as a function of latitude in the study area (cruise D366 underway data).

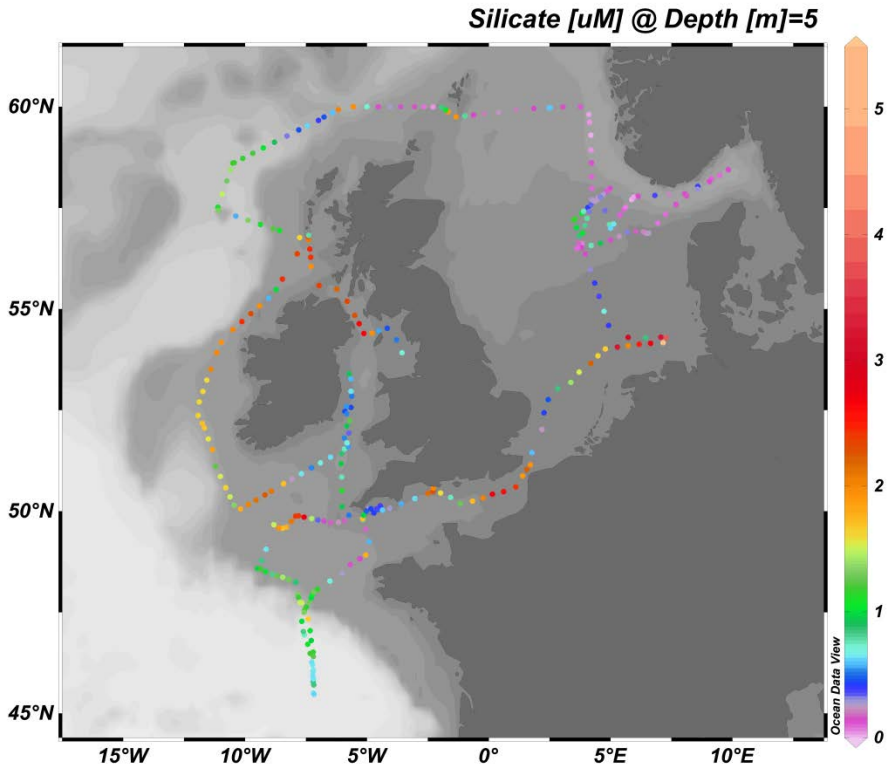

Figure 5.4 SiO_4^{-4} concentrations (µM) as a function of latitude in the study area (cruise D366 underway data).

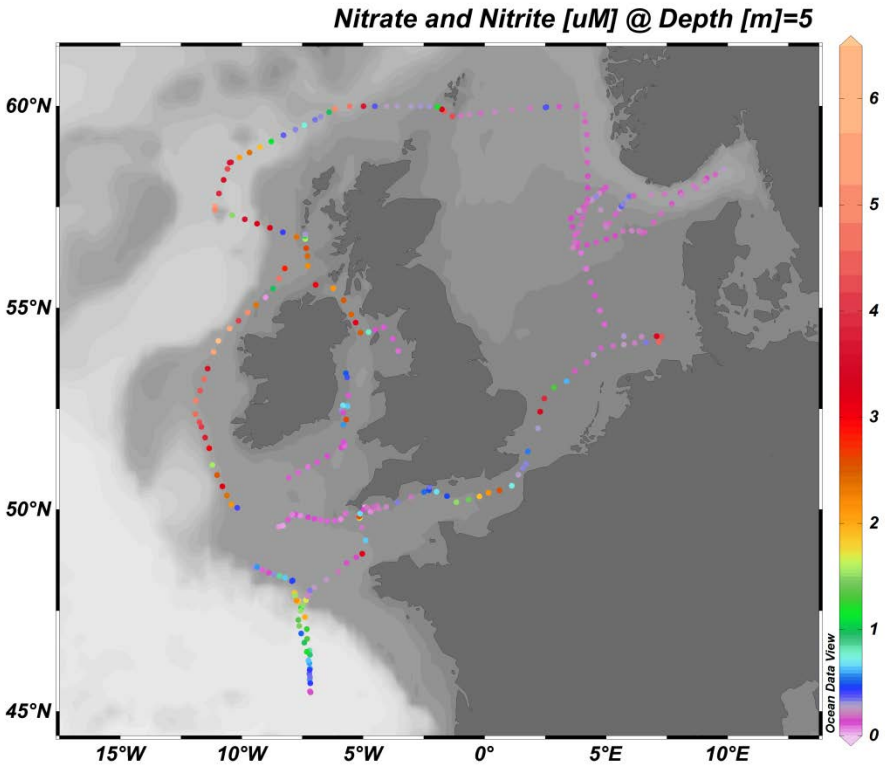

Figure 5.5 $NO_2^-+NO_3^-$ concentrations (µM) as a function of latitude in the study area (cruise D366 underway data).

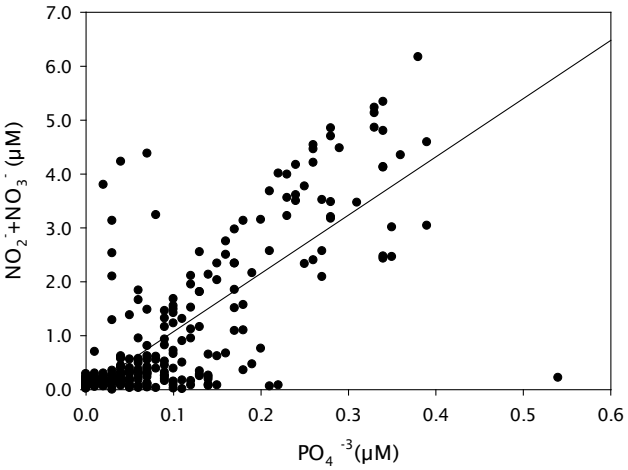

Figure 5.6 $NO_2^-+NO_3^-$ (µM) vs. PO_4^{-3} (µM) concentrations (cruise D366 underway data).

5.3.2 Total chlorophyll *a*

Surface (≤ 10 m) total chlorophyll *a* levels ranged between 0.26 and 3.6 µg/L along the whole cruise track. Highest chlorophyll levels were observed in the northwest part of the cruise (northern North Sea and Malin Sea), whereas the lowest levels were observed in the central North Sea and the Skagerrak region (Figure 5.7).

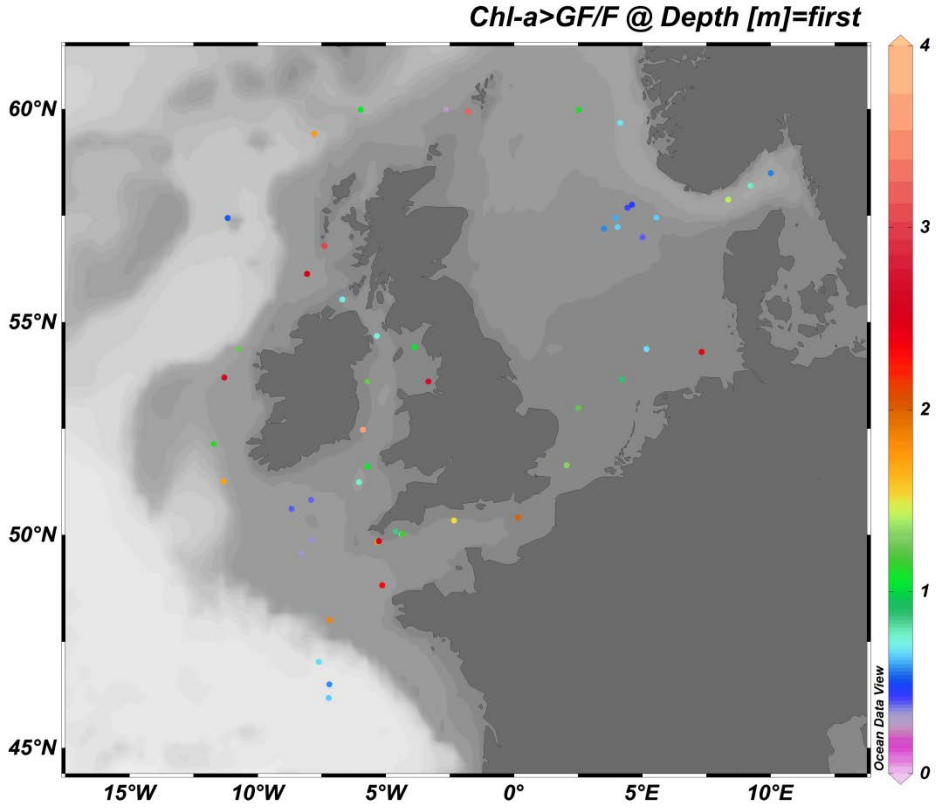

Figure 5.7 Surface chlorophyll a concentrations (µg/L) as a function of latitude in the study area (≤ 10 m; cruise D366 bottle data).

5.3.3 Total dissolved metal distribution in surface waters of the northwest European Shelf

5.3.3.1 Dissolved cadmium

Surface dissolved Cd concentrations [dCd] ranged between 0.01 nM (station 18, northern North Sea) and 0.15 nM (station 2, Irish Sea), with an average of 0.08 ± 0.04 nM (Figure 5.8a).

Dissolved metals in the NW European shelf

In regions with large river inputs such as the North Sea, the surface water distributions of dCd may be described by simple covariance with salinity, which simply describes the interaction between coastal waters of high Cd concentrations and the low-level oceanic surface waters (Kremling and Streu, 2001). The degree of linearity or data scattering can be considerably modified by different freshwater inputs (from different sources and with different concentrations), sediment interactions, phytoplankton growth, and atmospheric or anthropogenic inputs.

In the northern North Sea, [dCd] was strongly depleted (again coinciding with the highest chlorophyll values observed during the cruise), which occurred at PO_4^{-3} concentrations of less than 0.2 µM. Except at one station (12, southern North Sea), PO_4^{-3} values were very low (<0.2 µM) in all the study area. This depletion of both Cd and PO_4^{-3} in the northern North Sea, along with the [dZn] minimum (see below) and the highest chlorophyll values, could indicate phytoplankton uptake in this area.

The large variability of the Cd/PO_4^{-3} relationship (Figure 5.9) could be partly attributed to the different hydrographic regimes and the source strengths of the various Cd and PO_4^{-3} sources encountered in the northwest European shelf.

Waeles *et al.* (2004) reported dCd concentrations between 0.11 and 0.26 nM, whereas dCu ranged between 1.7 and 8.0 nM in the surface waters of the North Biscay continental shelf. They concluded that river inputs from the Loire affected Cd and Cu distribution in this area, judging from the higher values observed compared to previously reported values for the area. During our study, dissolved Cd was lower (0.01-0.15 nM) in general than the values reported by Waeles *et al.* (2004).

During this study, the appearance of fronts between the Atlantic and shelf waters did not cause any maxima in nutrient or metal concentrations, as it has been previously observed by Kremling (1983). However, the highest Cd and Cu (see below) concentrations were found at station 2 in the Irish Sea, where there are also important frontal systems (and in particular the one developed from the Irish Sea to the west of Ireland).

5.3.3.2 Dissolved copper

The distribution of dissolved Cu concentrations [dCu] along the coastal waters of the North West European shelf seas was variable. Dissolved Cu ranged between 0.37 nM (station 5, Bay of Biscay) and 5.10 nM (station 2, Irish Sea), with an average of 2.26 $\pm$ 1.31 nM (Figure 5.8b). The lowest surface values were observed at stations 5 and 3 (Bay of Biscay and Celtic Sea, respectively), whereas the maximum values were observed at stations 2 and 14 (Irish Sea and Skagerrak area, respectively). The high concentration value in the Skagerrak area coincides with the salinity minimum, suggesting the influence of Baltic waters.

5.3.3.3 Dissolved iron

Surface dissolved Fe concentrations [dFe] ranged between 0.50 nM (station 20, Atlantic Ocean) and 21.21 nM (station 10, southern North Sea), with an average of 2.55 $\pm$ 2.44 nM (excluding stations 10 and 14; Figure 5.8c).

5.3.3.4 Dissolved lead

Surface dissolved Pb concentrations [dPb] ranged between 0.02 nM (station 14, Skagerrak area) and 0.19 nM (station 10, southern North Sea), with an average of 0.06 $\pm$ 0.04 nM (Figure 5.8d).

It is well established that Pb concentrations in seawater depend predominantly on anthropogenic inputs (Patterson and Settle, 1987).

However, the variabilities in Pb concentrations may be attributed to the variability in atmospheric transport from continental sources, and to the short residence time of Pb in surface waters, which acts to preserve the patchiness, rather than to mix it out (Kremling and Streu, 2001).

Kremling and Streu (2001) did not find concentration gradients for Pb from the northeast Atlantic towards the northwest European shelf area. However, earlier data showed a clear Pb increase of ca. 25% in waters of the northern North Sea and the English Channel above open Atlantic values.

5.3.3.5 Dissolved nickel

Surface dissolved Ni concentrations [dNi] ranged between 2.73 nM (station 4, Bay of Biscay) and 6.27 nM (station 14, Skagerrak), with an average of 3.88 $\pm$ 1.05 nM (Figure 5.8e).

5.3.3.6 Dissolved zinc

Surface dissolved Zn concentrations [dZn] ranged between 0.21 nM (station 4, Bay of Biscay) and 15.04 nM (station 16, Norwegian coast), with an average of 2.21 $\pm$ 1.62 (without considering station 16; Figure 5.8f). Surface [dZn] minimum values were observed in the north-western part of the cruise (stations 18, 19 and 20; northern North Sea and Atlantic Sector), which coincided with the maximum chlorophyll levels observed (~3.6 µg/L). This could indicate that uptake from phytoplankton and export from surface waters are important mechanisms for the removal of Zn from the mixed layer. This hypothesis has been proposed by Kremling and Streu (2001). They found a dominance of undetectable surface water concentrations in the northeast Atlantic, which lead them to support the "zinc hypothesis", which suggest that Zn may limit phytoplankton productivity (Price and Morel, 1990; Morel *et al.*, 1991; Sunda and Huntsman, 1992; Morel *et al.*, 1994). However, the limitations of the analytical detection mechanisms for dZn about 15 year ago (detection limit of 0.07 nM for Zn), may have contributed to this observation, which is unlikely to be relevant anymore.

Furthermore, studies have shown that uptake of nutrient type metals take place in coastal waters as well as in the open ocean (Turner *et al.*, 1992). If it is considered that Zn is ~96-98% complexed by organic ligands in north Atlantic surface waters (Bruland, 1989; Ellwood and van den Berg, 2000), then the free ionic activity (Zn^{2+}) could be reduced to about 5-10 pM In large regions of the North Atlantic Ocean (Kremling and Streu, 2001).

Laboratory work has also shown that there is a strong link between Zn limitation and Cd uptake by algae (Price and Morel, 1990; Morel *et al.*, 1994). However, posterior studies did not find a correlation between surface water Cd and Zn (Ellwood, 2008).

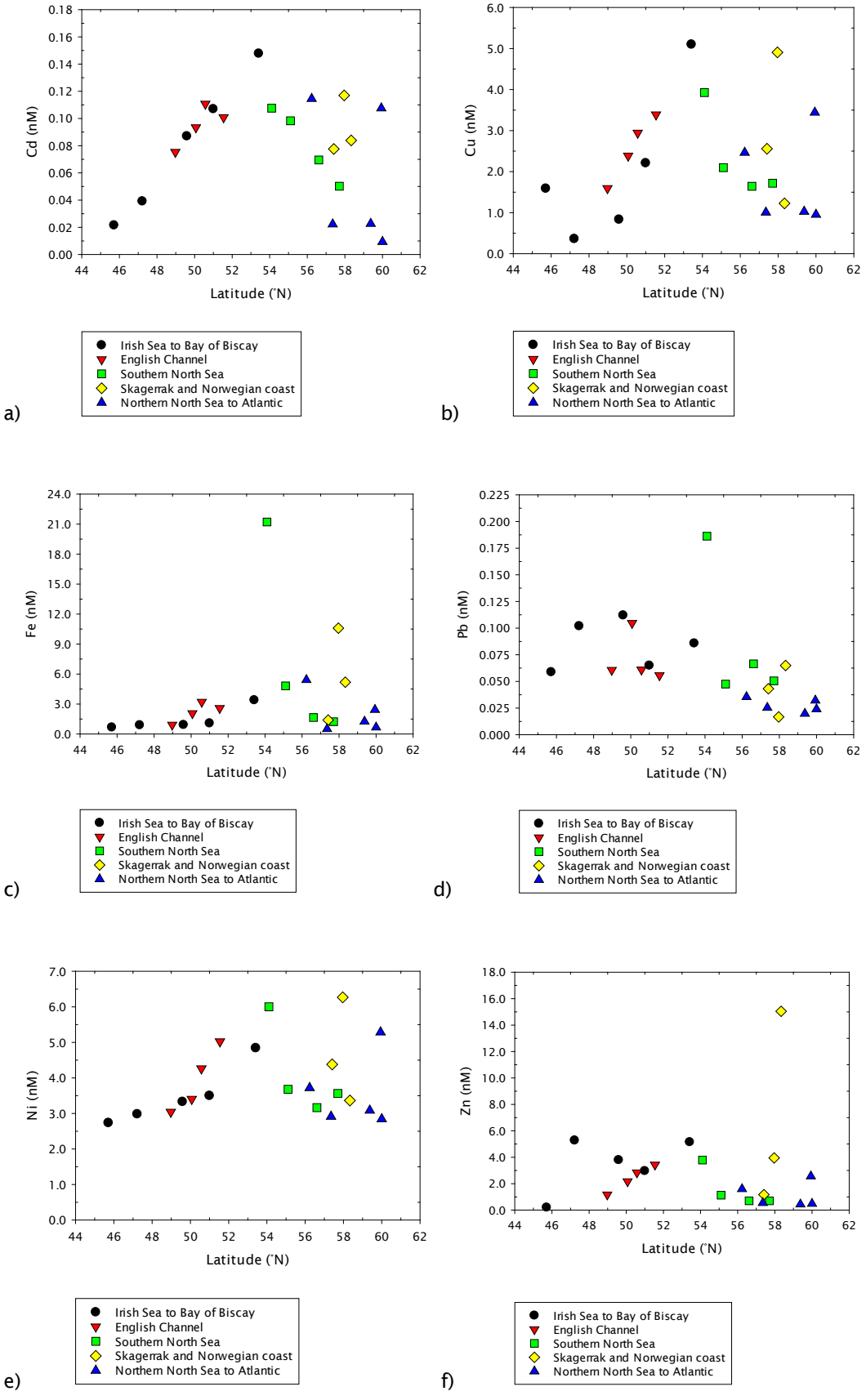

Figure 5.8 Dissolved metal concentrations (nM) as a function of latitude in the northwest European shelf seas a) Cd, b) Cu, c) Fe, d) Pb, e) Ni, f) Zn.

5.3.3.7 Dissolved metals correlations

Correlation between trace metals are indicative of an influence by the same biogeochemical controlling processes, and hence exhibit similar behaviour. A positive correlation ($P < 0.05$, Pearson correlation) would indicate that the trace metals increase or decrease at the same time.

Table 5.1 presents the relationship obtained between the different pairs of dissolved trace metals in the study area. Positive correlations were obtained for different pairs of metals. Dissolved Fe, Cu, Cd and Ni appear to have a positive correlation amongst each other, while no correlation was found between Pb or Zn with the rest of the metals ($P > 0.05$, Pearson correlation). In the case of Fe, no correlation was obtained with Cd, and a positive correlation was obtained with Pb.

Fe, Cu, Cd and Ni are known to be biologically mediated metals. Zn has a biological role in the ocean as well. However, relationships between Zn and the other metals may have not been observed due to a different source.

Table 5.1 Pearson correlation coefficients for the different pairs of the trace metals analysed during this study. No correlation ($P > 0.05$) is shown by the "N" values.

	Cu	Cd	Fe	Ni	Pb	Zn
Cu		+	+	+	N	N
Cd	+		N	+	N	N
Fe	+	N		+	+	N
Ni	+	+	+		N	N
Pb	N	N	+	N		N
Zn	N	N	N	N	N	

5.3.3.8 Dissolved metals relations to nutrients

In the open ocean, dissolved trace metals are often well correlated with major nutrients. Strong linear relationships between Cd and Ni with PO_4^{-3}, and Zn and Cu with SiO_4^{-4} have been observed in vertical profiles of the major ocean basins, such as the south Atlantic and the northeast Pacific waters (Bruland *et al.*, 1978b; Bruland, 1980; Martin *et al.*, 1993; Ellwood, 2008; Boye *et al.*,

2012; Wyatt *et al.*, 2014). These trace metals have similar spatial distribution pattern in open ocean deep and surface waters (Boyle, 1988). However, during this study, these relationships were not significant (r^2<0.1,Figure 5.9). In coastal waters, nutrient-trace metal relationships are difficult to observe with a small database as a consequence of the very dynamic coastal system in which a range of different input and removal processes change the concentration of dissolved trace metals on relatively short time and space scales (Achterberg *et al.*, 1999).

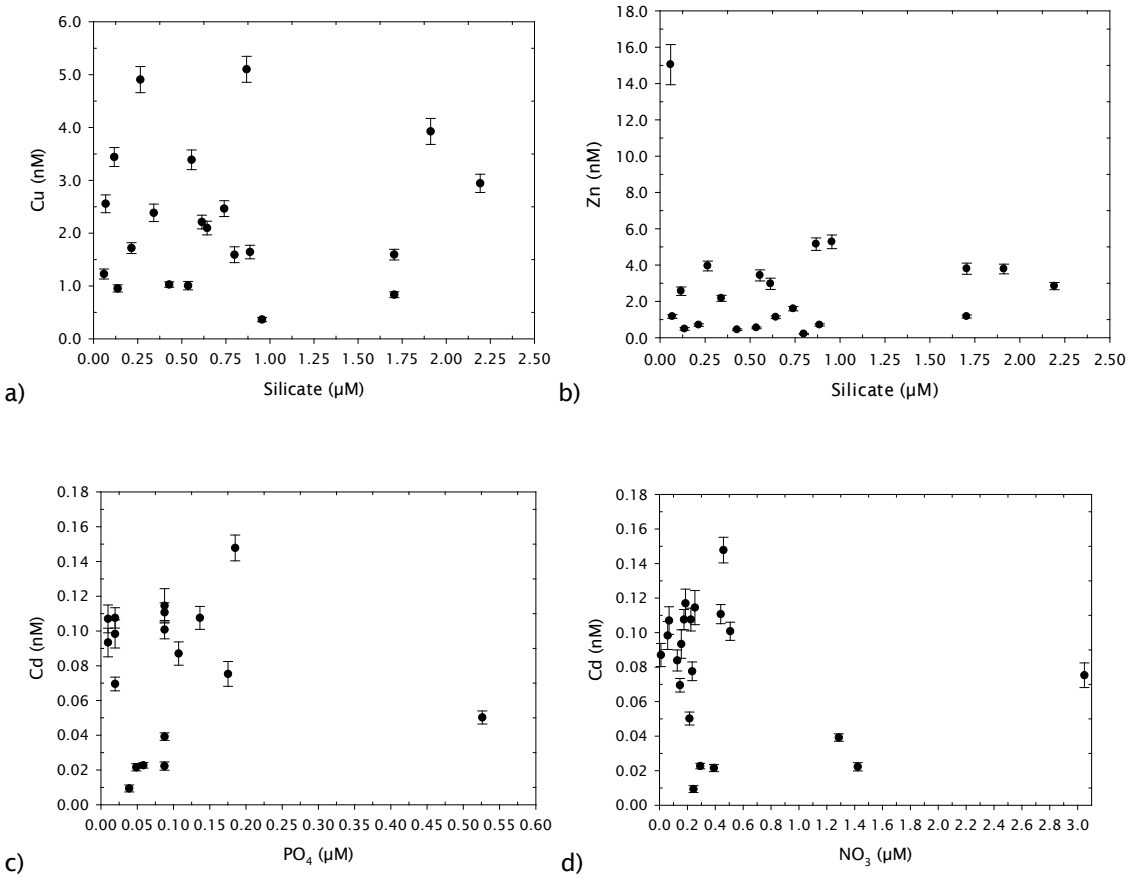

Figure 5.9 Dissolved metals vs nutrients. a) dCu (nM) vs SiO_4^{-4} (µM), b) dZn (nM) vs SiO_4^{-4} (µM), c) dCd (nM) vs PO_4^{-3} (µM), and d) dCd (nM) vs NO_3^{-} (µM).

5.3.3.9 Dissolved metals and salinity

The sample locations include areas of intense tidal mixing (the northern Scotland-Shetland area and the English Channel), and also regions with the typical summer stratification (northern and central North Sea; Try and Price (1995)).

Dissolved metals in the NW European shelf

The total dissolved trace metal data has been plotted against salinity, therefore visually showing the changes (if any) in concentrations from Atlantic surface waters to the river influenced coastal waters. Low salinity values associated with river water inputs to the coastal waters are apparent in Figure 5.10.

Dissolved Cd, Cu, Fe and Ni data in Figure 5.10 appear to fall along a salinity mixing line, with a scatter at low salinities corresponding to the Norwegian coast and Skagerrak stations.

Salinity ranged between 27.4 and 35.8 at the 21 sampling stations. The lowest salinities were observed at the Norwegian coast (stations 13 and 16), and at the Skagerrak area (station 14). One of the main freshwater sources into the North Sea is the inflow coming from the Baltic Sea, having a big influence in the hydrography and water movements in the eastern parts of the North Sea (OSPAR Commission, 2000), passing through the Skagerrak and following the Norwegian coast. This freshwater influence from the Baltic Sea strongly determined the low salinity values observed at the Norwegian coast and Skagerrak stations.

The majority of the metal data presented was observed at salinities typical of oceanic water masses (>34). However, the observed scattering of the data in some cases might be caused by the freshwater inputs which mix with the shelf waters, and by several processes that can affect the lower estuary end member concentration, hence leading towards lower salinity values. These can include precipitation during estuarine mixing, desorption from riverborne suspended particulate matter, redox reactions, or anthropogenic inputs within the mixing zone (Duinker and Nolting, 1982; Try and Price, 1995).

The zero salinity end member is often utilized to estimate the chemical composition of river water that has passed through the estuarine filter and reached coastal waters, yielding estimates of the net flux of components from individual river-estuarine systems (Chester and Jickells, 2012). Multiplication of this value (EZSEM) by the river flow yields the flux of the metal, in this case, out of the estuary after estuarine modification (Fitter and Raffaelli, 1999).

Table 5.2 Results from regressions of dissolved trace metals with salinity. Correlations with Cd, Cu, Fe, Ni and Zn were significant (Pearson product moment correlation; $P < 0.05$), while correlation with Pb was not ($P > 0.05$). Linear regression was calculated for each metal (except for Zn) without the low salinity stations at the Norwegian coast and Skagerrak area.

Metal	Intercept S= 0; nM	Slope	r^2
Cd	2.19	- 0.06	0.46
Cu	69.77	- 1.93	0.51
Fe	90.84	- 2.53	0.53
Ni	50.12	- 1.32	0.40
Pb	0.945	- 0.03	0.08
Zn	29.28	- 0.77	0.21

Effective concentrations in freshwater discharged into the coastal shelf during this cruise (estimated by extrapolation to zero salinity) were: 2.19 nM for Cd, 69.77 nM for Cu, 90.84 nM for Fe, 50.12 for Ni, 0.945 for Pb, and 37.80 nM for Zn (Table 5.2). These EZSEM concentrations are an average of the end members of the fresh water sources discharging into the waters of this work's study area. Achterberg *et al.* (1999) have estimated higher average EZSEM concentrations than the ones in this study for dissolved Cu, Ni and Zn for the Humber estuary and the river Severn. However, it is not possible with our data to compare end member concentrations with the ones that are river specific.

A linear relationship between a metal and salinity would indicate conservative behaviour (Officer, 1979). Dissolved Cd, Cu, Fe and Ni had the highest linear relationship with salinity, when the low salinity stations localized in the Norwegian coast and Skagerrak area are removed from the regression line, although this relationship was not very strong ($r^2<0.6$,Table 5.2). A scatter in the linear regression line on the whole data set is caused mainly by the presence of several rivers and saline end-members, and by processes including atmospheric and benthic inputs, and water column removal (Achterberg *et al.*, 1999). Correlation analysis showed that there were statistically significant ($P<0.05$, Pearson correlation) inverse relationships with salinity for Cd, Cu, Fe, Ni and Zn, but not for Pb ($P> 0.05$). This significant correlation between the former metals with salinity could imply that they are predominantly associated with riverine inputs. In the case of Pb, the lack of linearity with salinity could indicate that processes other than mixing between riverine and saline end-

member waters were more important for the distribution of this metal, and hence exhibiting a non-conservative behaviour (Achterberg *et al.*, 1999). These processes may include atmospheric and benthic inputs (as it has been observed in the case of Pb), removal by particulate matter and phytoplankton uptake.

Studies have shown a biologically mediated removal of dCu, dNi and dZn in the surface with subsequent down column transport in association with biogenic particles (Bruland and Franks, 1983). However, several authors (Burton *et al.*, 1993; Tappin *et al.*, 1995; Achterberg *et al.*, 1999) observed no clear coupling of dNi, dCu and dZn to the utilisation and regeneration of nutrients in the North Sea.

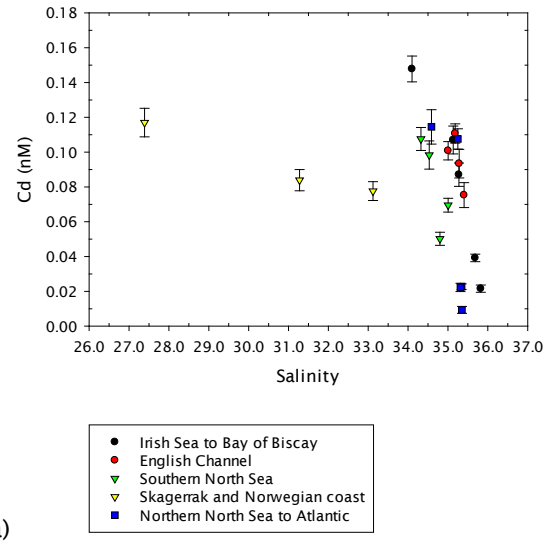

a)

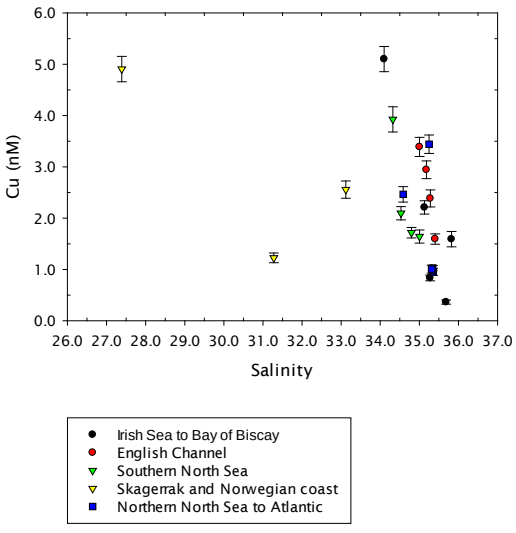

b)

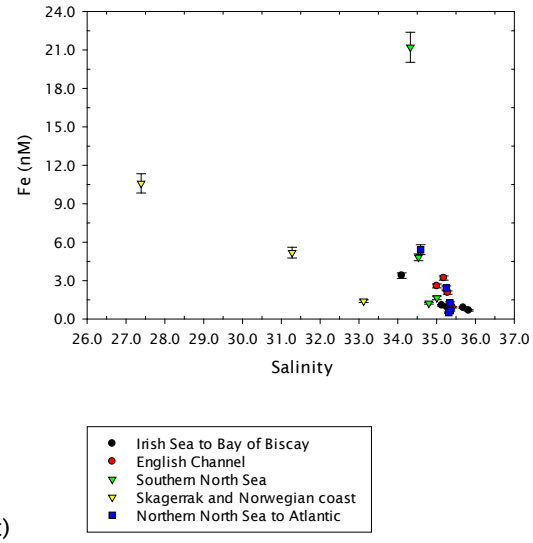

c)

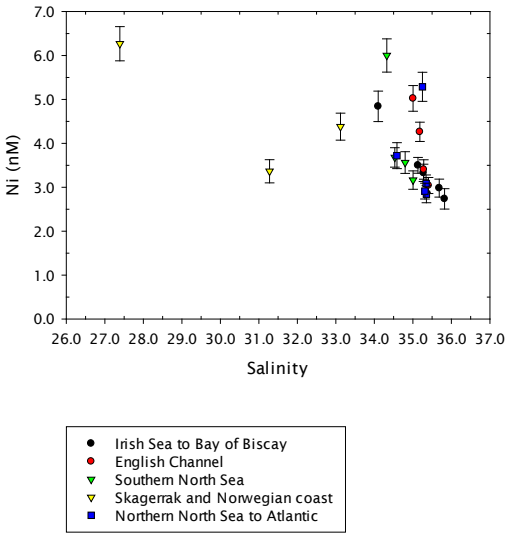

d)

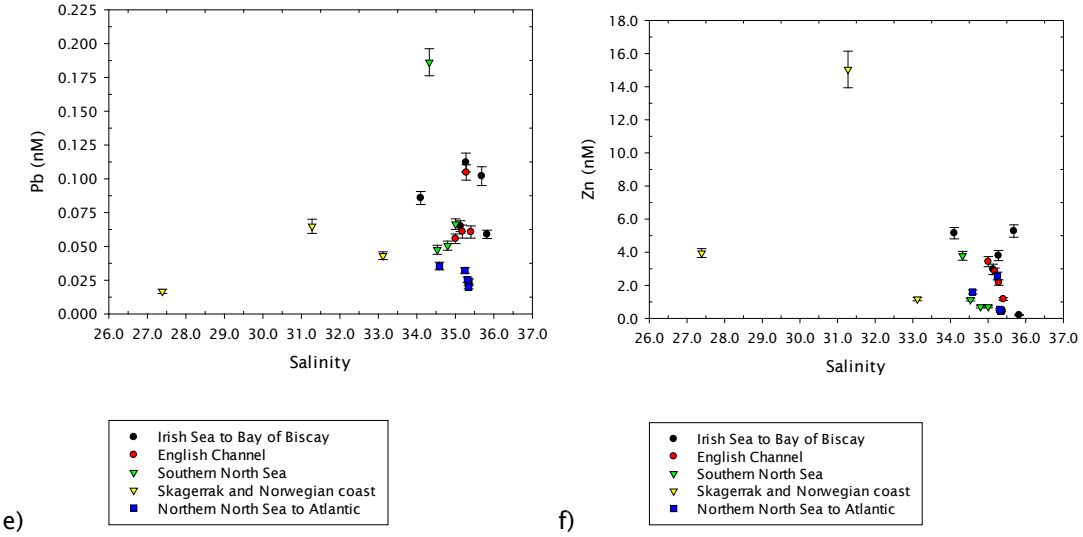

e) f)

Figure 5.10 Dissolved metal concentrations (nM) vs. salinity (n=21). a) Cd, b) Cu, c) Fe, d) Pb, e) Ni, f) Zn.

5.3.3.10 Dissolved metal concentrations in study areas

The description of metal concentrations per region are presented following the circulation pattern along the coast, starting at the Bay of Biscay and continuing north towards the Celtic and Irish Seas, meeting with Atlantic water in the north and then the North Sea, then moving in a southern direction meeting the Skagerrak outflow, and finally moving into the southern North Sea and the English Channel.

Region 1 Celtic and Irish Seas

High metal concentrations were observed at station 2. Dissolved Cu, Cd and Zn had some of their highest concentrations at this station located in the western Irish Sea (Figure 5.8). Achterberg and van den Berg (1996) showed that the river Mersey, which has its catchment area in the Liverpool Bay at the eastern Irish Sea, is an important source of Ni, Cu and Zn to this part of the Irish Sea. This river, along with the river Dee, carry industrial and domestic sewage into the Liverpool Bay (Achterberg and van den Berg, 1996).

The net anti-clockwise water movement in the eastern Irish Sea results in trace metal enhanced waters from the outflowing Mersey moving in a northerly direction along the eastern side of the Liverpool Bay (Achterberg and van den Berg, 1996).

Dissolved metals in the NW European shelf

Dissolved Cu levels between 5 and 7 nM were observed in the Irish Sea to the west of the Isle of Man by Kremling and Hydes (1988). Achterberg and van den Berg (1996) observed dCu levels between 7 and 9 nM in the western part of the Liverpool Bay. The dCu values observed during this study are similar to the ones observed by these authors for the Irish Sea.

Total dZn values observed by Achterberg and van den Berg (1996) ranged between 11 and 13 nM, in the western part of the Liverpool Bay, in the Irish Sea, which are higher than the values observed during this study for the Irish Sea stations (between 0.21 and 5.3 nM, Figure 5.8).

Achterberg and van den Berg (1996) found dissolved Ni levels ranging between 6 and 7 nM in western parts of the Liverpool Bay, while Kremling and Hydes (1988) observed dNi levels of 4 to 6.5 nM in surface waters of the western Irish Sea, which are both similar to the values observed during this study in the Irish Sea stations (between 2.7 and 4.8 nM).

Kremling and Hydes (1988) observed enhanced concentrations of dCd, dCu, dMn and dNi in the Irish Sea between 50-100% higher than in Scottish coastal waters or the central North Sea. They explained these enhanced concentrations by anthropogenic riverine inputs, as these high concentrations were associated with low salinity waters. Achterberg and van den Berg (1996) also found high dNi, dCu and dZn concentrations in the same area, related to decreasing salinity.

Region 2 Northern North Sea

Dissolved Ni concentrations observed by Achterberg *et al.* (1999) in coastal areas of the North Sea, away from the immediate vicinity of estuarine plumes, were between 3 and 6 nM, and between 4 and 8 nM for dCu. The dNi values were in good agreement with the values observed during this study for the North Sea (Figure 5.8). However, dCu values were higher than the ones observed during this study.

Region 3 Skagerrak

The Skagerrak was one of the areas with the lowest salinity values (27.4) and where the highest metal concentrations were observed during this study. Dissolved Cu, Cd, Ni and Fe presented some of their highest concentrations at

station 14 (Figure 5.8). Besides lowering the salinity of the Skagerrak area, the freshwater coming from the Baltic constitutes an important source of contaminant and nutrients into the North Sea (HELCOM, 2010), which can explain the highest metal concentrations during this study associated with the lowest salinities. During 1999-2007, the Hazardous Substances Assessment indicated that the Baltic Sea was highly contaminated with hazardous substances, amongst which were the heavy metals Cd and Pb (HELCOM, 2010).

Region 4 Southern North Sea

Station 10, localized in the southern North Sea, was also an area where high metal concentrations were observed. Dissolved Fe, Pb and Ni presented some of their highest concentrations at this station (Figure 5.8). One of the main inputs of trace metals into the North Sea is through the Dover Strait. The flow of water from the English Channel through the Strait transports a significant input of chemical substances in both dissolved and particulate forms (Statham *et al.*, 1993). Along with these inputs, the southern North Sea has significant riverine inputs, in particular the Elbe, Weser and Scheldt near station 10. Dissolved Cd, Co, Cu, Fe, Mn, Ni, Pb and Zn have been monitored across the Strait of Dover, presenting high metal concentrations (Statham *et al.*, 1993).

Region 5 English Channel

Dissolved Cu and Ni concentrations observed during this study in the English Channel were in good agreement with the summer values observed by Tappin *et al.* (1993) for the same area: dCu (3.0 $\pm$ 1.1), dNi (3.5 $\pm$ 0.5) nM. Dissolved Zn concentrations observed by these authors, however, were higher (7.3 $\pm$ 3.4) nM than the ones observed during this study for the English Channel area dZn ($\leq$ 4.0 nM).

Statham *et al.* (1993) reported dCu concentrations between 3.5 and 15.6 nM in the Strait of Dover, which is near to station 9 during this study. However, their sampling station was closer to the French coast and consequently the higher values could be explained by the influence of the river Seine, as observed by Achterberg *et al.* (1999) with similar high concentrations of dCu and dZn on a cruise station close to the French coast in the Strait of Dover (dZn ca. 18 nM).

Station 9 is near the Thames plume area (Figure 5.2). This area was used for disposal of sewage sludge in the past, containing high levels of nutrients,

metals and suspended matter (Achterberg *et al.*, 1999). However, station 9 during this study did not present high levels of metal concentrations, presumably as a result of the ceasing of sewage sludge dumping after 1998 (Try and Price, 1995). Achterberg *et al.* (1999) observed high dCu (21 nM), dNi (8 nM) and dZn (18 nM) values before the changes in UK legislation regarding the sewage dumping. Furthermore, salinity had a value of 35.0 at station 9, which may suggest that this study's sampling was made during a different tidal state compared to the Achterberg *et al.* (1999) study.

Even though similar dissolved metal concentration range can be observed by different authors, differences in exact sampling locations and seasons, as well as the employed analytical method, will have an important effect on the observed trace metal concentrations in coastal systems. These factors should be taken into account when data comparisons from different surveys are made.

5.3.3.11 Relation between dissolved metals and pH

The photosynthetic uptake of CO_2 and essential micronutrients to form organic matter (biological production) increases seawater pH. Photosynthesis decreases the concentration of dissolved inorganic carbon (DIC) and free protons, which lead to an increase in pH (Thomas *et al.*, 2005); whereas organic matter respiration and remineralisation lead to a decrease in pH, and to a release of essential trace metals such as Fe and Cu. Chlorophyll and pH levels in areas with high productivity therefore present a positive correlation, whereas chlorophyll levels and trace metal nutrients present a negative one.

On the other hand, terrestrial inputs, in particular from rivers, can inject significant loads of DIC and organic matter to coastal systems, consequently lowering the pH (Borges and Gypens, 2010). Lowest pH values were observed at the English Channel and southern North Sea, while the highest were observed at the northern North Sea and Atlantic. The southern North Sea is an area highly influenced by riverine inputs, which can explain the low pH values observed in this area. As mentioned before, highest chlorophyll levels were observed at the northern part of the cruise, e.g. the northern North Sea and Atlantic, hence related with the highest productivity in the area and consequently with the highest pH levels.

Due to the shallow depth in coastal areas, as in the case of the northwest European shelf, benthic processes can also affect significantly the pelagic carbon cycle and alkalinity (Thomas *et al.*, 2009). Spatial and temporal pH variabilities in shelf areas can be even higher than in the open ocean as a result of several simultaneous processes (Blackford and Gilbert, 2007).

Dissolved metals were plotted against pH in Figure 5.11. A significant negative correlation between Cd and pH was observed ($P < 0.05$, Pearson correlation). There was no significant correlation between pH and Zn, Pb, Ni, Cu or Fe ($P > 0.05$, Pearson correlation). However, during this study the highest Fe and Pb concentrations were observed at a station with one of the lowest pH values (station 10).

During this study, horizontal metal distributions do not appear to be controlled by surface seawater pH. A larger spatial and temporal scale may be needed in order to find significant relationships between pH and metal distributions in coastal systems.

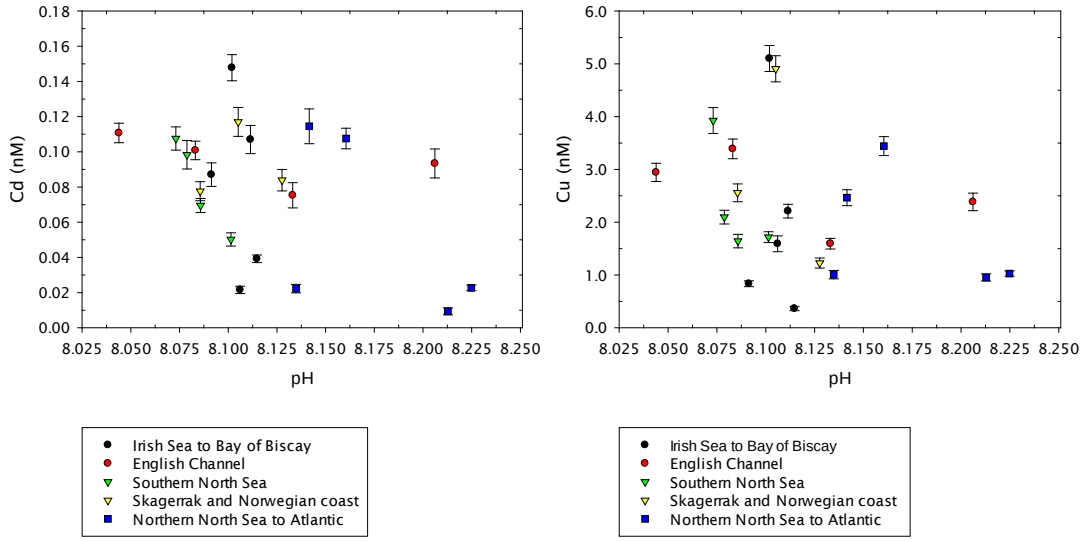

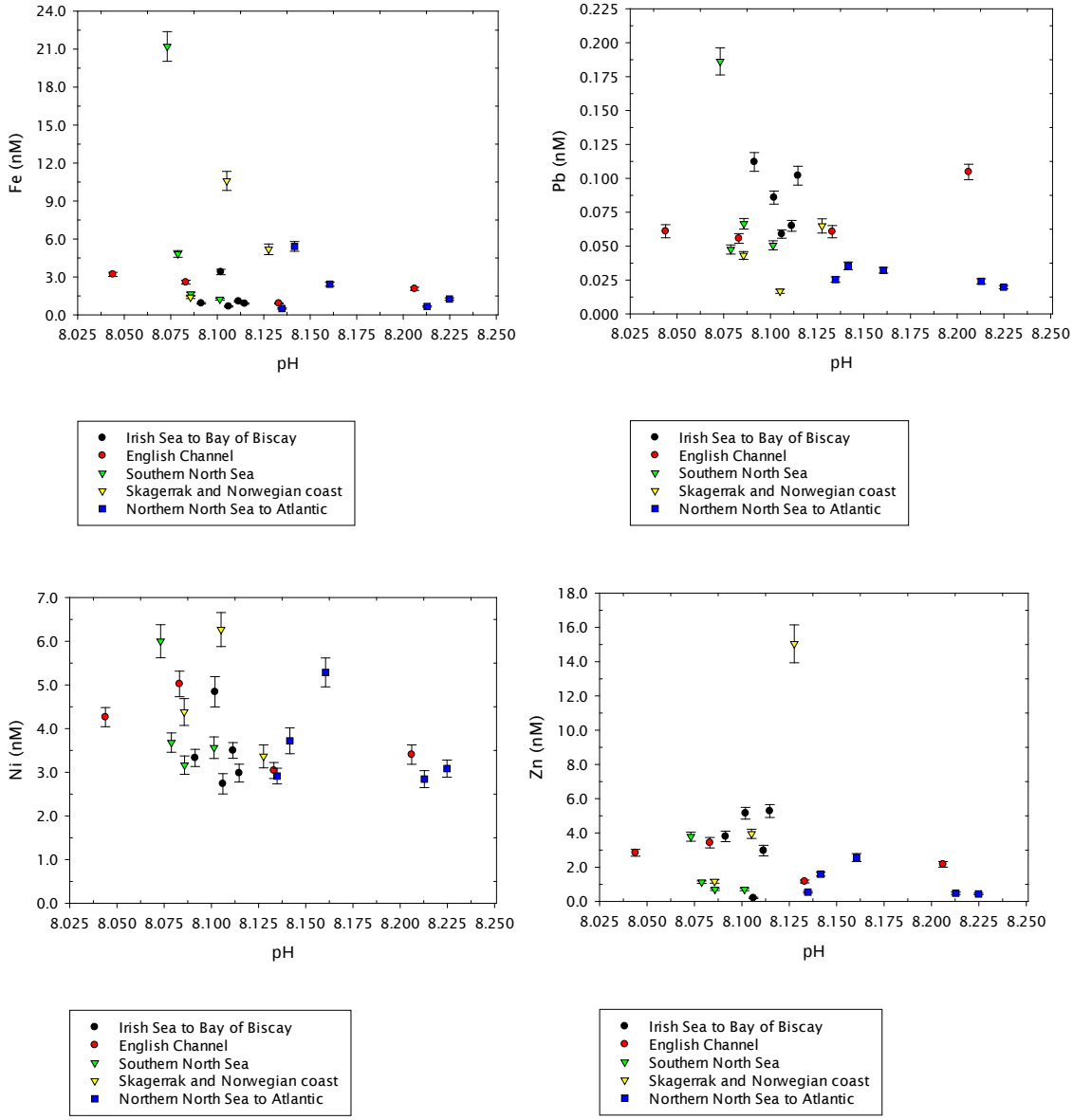

Figure 5.11 Dissolved metal concentrations (nM) vs. pH (n=21). a) Cd, b) Cu, c) Fe, d) Pb, e) Ni, f) Zn.

5.4 Conclusions

The northwest European continental shelf is strongly influenced by riverine freshwater inputs, especially in the North Sea. The catchment areas of the rivers draining into the North Sea are an important source of trace metals to the coastal system.

Highest metal concentrations were observed off the east coast of Ireland, in the Irish Sea (dissolved Cu, Cd and Zn), and in the southern North Sea (Fe, Pb

and Ni) where the Dover Strait is one of the main inputs of trace metals, along with significant riverine inputs. The Skagerrak area also presented high concentrations of dissolved Cu, Cd, Ni and Fe, as a result of the influence of waters from the Baltic Sea.

Surface dissolved metal distributions appear to be strongly influenced by riverine inputs. A negative correlation was observed (this is, metal concentrations tend to decrease when salinity increases) for all the metals except with Pb.

Surface trace metal distributions did not appear to be controlled by surface seawater pH during this study.

Chapter 6: Synthesis

This thesis has considered the influence of ocean acidification on the organic complexation of iron (Fe) and copper (Cu) in northwest European seas. In addition, the thesis considered organic Fe complexation in waters of the high latitude North Atlantic Ocean, at the current surface ocean pH. Furthermore, the horizontal distribution of several dissolved trace metals in the northwest European seas was determined. Understanding the changes in metal speciation as a result of changes in the ocean's carbonate system, forms the first step in the process to project the effects that a future decrease in seawater pH and increase in pCO_2 will have on the interactions of metals with marine biota. The changes in metal speciation will result in changes in the behaviour and fate of trace metals in marine waters. Future research considering the synergistic effects of changing temperature, pH and dissolved organic matter (DOM) content of seawater on metal bioavailability needs to follow this study. Furthermore, improvements in the accuracy and standardisation amongst research groups on the electrochemical techniques currently employed for the measurement of metal speciation are essential.

6.1 Conclusions of this project

Organic Fe complexation has been widely assessed in different regions of the world's oceans. The high latitude North Atlantic (HLNA) is a recent area of research interest due to its importance for the biological carbon cycle and the observed iron limitation of phytoplankton growth. However, little is known about the iron binding ligand characteristics in the HLNA. Organic Fe complexation measurements in waters of the HLNA showed that: (i) iron biogeochemistry in surface and subsurface waters in the study area is controlled by a combination of phytoplankton iron uptake and microbial ligand production, which can be concluded from the iron binding ligand concentrations measured; (ii) [L]/[dFe] ratios demonstrated to be a reliable approach to determine ligand saturation. High and variable [L]/[dFe] values were observed in surface and subsurface waters, while they decreased towards deep waters to more constant values and near saturation; and (iii) ligand saturation in deep waters of the HLNA, along with deep water mass formation, suggested that any additional Fe at these depths would tend to be removed by

precipitation and scavenging. Comparison of Fe binding ligand characteristics were in good agreement with a previous study conducted in the Iceland Basin and other waters of the HLNA.

Horizontal trace metal distributions have also been studied in different regions of the ocean. During this study, surface water trace metal distribution in the northwest European shelf seas was assessed. To our knowledge, it was the first time that dissolved metal concentrations were measured where a highly accurate pH level database was available. Highest dissolved metal concentrations were observed in the Irish Sea, the Skagerrak area and in the southern North Sea. Dissolved metal concentrations of Cd, Cu, Fe, Ni and Zn seemed to be strongly influenced by riverine inputs in the study area. Surface trace metal distributions did not appear to be controlled by surface seawater pH during this study.

The expected decrease in seawater pH from pre-industrial values (~ 8.25) to the ones projected for the end of this century (ca. 7.85), is projected to affect significantly the inorganic solubility of several trace metals, especially of the ones forming strong complexes with hydroxide and carbonate ions. However, the influence of ocean acidification on metal solubility is more complex than a direct influence of pH or temperature on solubility. Metal solubility is controlled by the interrelationship of inorganic solubility, organic complexation, redox chemistry, and phytoplankton-trace metal feedback mechanisms (Hoffmann *et al.*, 2012).

In the last decade, a great amount of published work on the impacts of ocean acidification on marine biota, and especially on the calcifying life-forms, has become available. However, studies concerning multifactor interactions such as seawater pH, temperature and trace metals are limited, although they emphasize the significance and importance of this approach. The present study gives an insight into one part of the whole system – the effect on the organic metal interactions. The northwest European shelf seas were the first of the regions studied under the NERC funded sea surface UK Ocean Acidification consortium programme. During this study, results for Fe (III) suggested that a decrease in surface ocean pH will potentially result in a reduction of the free and inorganic metal fraction (Fe'), and also in an increase in the organically complexed iron fraction. Conditional stability constants for the organic iron

complexes also appear to increase with a decrease in pH. These results may be explained by a reduced competition of the ambient ligands (with acidic binding groups that are not protonated in seawater) with OH^- for Fe chelation, with a decrease in pH. A decrease in Fe' uptake by phytoplankton from Fe-EDTA has been observed in previous studies (Shi *et al.*, 2010). However, these findings cannot lead alone to the conclusion of a decrease in iron bioavailability due to a decrease in pH, as Fe' uptake by phytoplankton is a simplistic scenario in which Fe' is the only bioavailable form of this micronutrient. Furthermore, it has to be considered that ambient Fe binding ligands possess a variety of metal binding sites (Barbeau *et al.*, 2003) with different H^+ stoichiometries (Breitbarth *et al.*, 2010).

Previous studies have shown a decrease in the organic Cu (II) complexation, when seawater pH decreases below 8.0. As a result, the inorganic Cu (Cu') fraction increased with a decrease in pH (Averyt, 2004; Louis *et al.*, 2009). During this study, no significant effects were observed of a decrease in pH on the organically complexed Cu (II) fraction, or on the overall free and inorganically bound fraction (Cu'). As inferred altogether from the present study and previous results, is still not clear whether Cu ligand production will be affected by ocean acidification, and what the effects on Cu toxicity will be. Intracellular Cu binding may not be directly affected by the surrounding seawater pH. However, Cu binding could possibly be affected indirectly via effects on phytoplankton physiology. Therefore, the diversity of the chemical and biological processes controlling Fe and Cu biogeochemistry, and the way in which they will be altered by ocean acidification, is likely to be complex (Figure 6.1).

Even slight changes in the bioavailability of Fe and Cu may have significant effects on marine ecosystems, as these metals are known to interact with each other (Hoffmann *et al.*, 2012). Cu is needed by a few phytoplankton species for sufficient Fe acquisition (Wells *et al.*, 2005; Maldonado *et al.*, 2006), and Cu requirements of natural phytoplankton communities increase under Fe limitation (Semeniuk *et al.*, 2009). Alternatively, Cu is a potentially toxic metal whose toxicity to marine phytoplankton is regulated by organic ligand complexation.

Phytoplankton uptake rates, along with other biological processes are needed in order to provide a better insight into the impact that these changes in metal speciation will have on the cycling of Fe and Cu in the ocean. The CLE-ACSV data interpretation, on the other hand, is subject to systematic errors on the calculation of ligand parameters, due to the inherent limitations of the method. A holistic understanding is needed on the impacts of a decreasing ocean pH and rising temperatures on trace metals and marine biota. Furthermore, direct or indirect effects of ocean acidification on marine biota will affect trace metal biogeochemistry via alteration of biological trace metal uptake rates and metal binding to organic ligands.

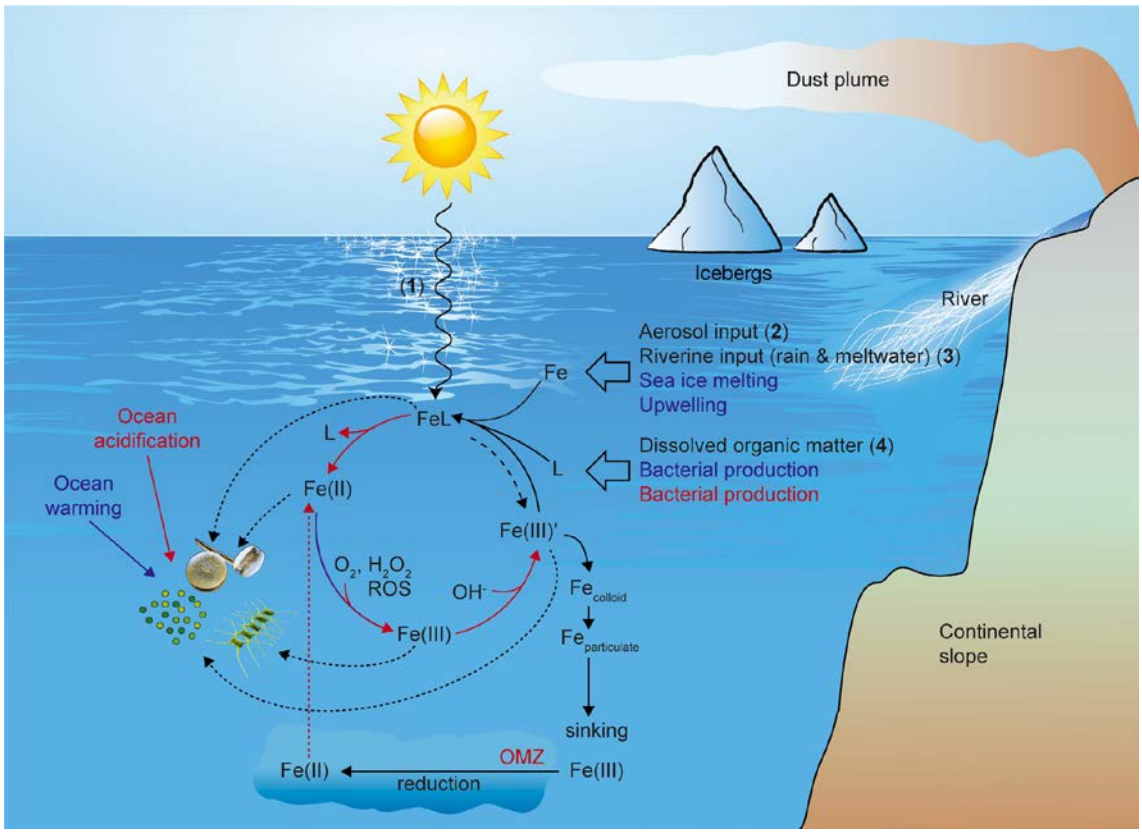

Figure 6.1 Direct effects of ocean acidification (red) and ocean warming (blue) on Fe chemistry in seawater. Ocean acidification and ocean warming both influence phytoplankton and bacterial physiology with possible effects for biological Fe uptake and ligand production. Source: Hoffmann *et al.* (2012).

6.2 Future work

Future studies on iron and copper organic complexation should couple trace metal clean size fractionation approaches, CLE-ACSV, and HPLC-MS techniques (Gledhill and Buck, 2012), along with phytoplankton incubations and other

biological process studies, in order to provide a better insight into the nature and cycling of Fe and Cu binding ligands in the contemporary and future ocean. The biogeochemical role of each of the natural ligand types requires further investigation also.

Ocean surface pH is decreasing, thus the behaviour of trace metals in the ocean is likely to change. It is necessary to improve our understanding of the broader implications that the changes in metal biogeochemistry will bring in the future for marine ecosystems. Moreover, the way in which marine biota will react to changes in the speciation of biologically mediated metals, e.g., effects on phytoplankton uptake rates, is not well known. Therefore, a multidisciplinary approach is needed in order to provide a better understanding of these future changes.

Trace metal clean experimental protocols for ocean acidification work is essential, as the effects of ocean acidification can be biased by contamination artefacts associated with the experimental setup. Automated analytical systems for voltammetric measurements would be desirable for metal speciation work in future research involving ocean acidification, in order to reduce possible artefacts associated with changes in temperature and in the chemical nature of the natural ligands as a result of sample storage and manipulation.

In order to allow for intercomparisons between different research groups when assessing the influence of a decrease in pH on metal speciation, and in particular in the organic complexation, standardisation in the determination of side reaction coefficients for the binding between added ligands (AL) and trace metals (Me) at different pH and salinity levels would be most useful, as different research groups currently use different experimental procedures and/or modelling approaches. The election of specific added ligands amongst all the research groups would be also desirable, in addition to the utilisation of the same detection windows.

Moreover, metal speciation models have to improve with the insertion of all of the different chemical, biological and physical processes that affect trace metal biogeochemistry in the ocean. Future research is recommended in order to assess the capacity of metal speciation models to represent realistic changes in inorganic/organic metal complexation, so they can be used accurately to project future changes under different seawater acidification scenarios.

Conclusions

Temperature and Fe have been observed to have synergistic effects on phytoplankton growth rates (Rose *et al.*, 2009). Furthermore, the interaction between vitamins and pCO_2 has been observed to affect the uptake and metal net use efficiency of Fe, Co, Zn and Cd (King *et al.*, 2011). These studies demonstrate the need of considering multiple factors when trying to assess the influence of ocean acidification and warming on the marine ecosystem.

The knowledge of the influence of ocean acidification on trace metal speciation should continue to improve. In the short term, the combination of this work's experimental approach with the application of a speciation model will improve the understanding in future research of any changes related to a decrease in seawater pH, when the modelling of iron and copper speciation is performed with accuracy.

Appendix A

Certified Reference materials (SAFe surface and SAFe D2 data) used for the dissolved iron analysis (D354 surface and water column samples) for the organic complexation of Fe in the HLNA (Chapter 3). Analyses were performed by Dr. Sebastian Steigenberger, NOC, with the ID-ICPMS technique.

CRM	Fe (nM)	s.d.	recovery
SAFe S-171	0.094	0.008	157%
consensus	0.148	0.023	
SAFe D2-441	0.923	0.029	116%
consensus	1.067	0.188	
Detection limits	50-60 pM		
Blanks	18 pM		

Appendix B

Steps to obtain the [Fe $^{3+}$]/[FeL] plot equation during the CLE-AdCSV linear analysis:

$$K'_{FeL} = [FeL]/[Fe^{3+}][L'] \quad (3.2)$$

$$C_L = [L'] + [FeL] \quad (3.3)$$

By substituting [L'] from equation (3.3) into equation (3.2), the following relationship is obtained following the steps:

$[L'] = C_L - [FeL]$, then substituting:

$K'_{FeL} = \frac{[FeL]}{[Fe^{3+}][C_L - [FeL]]}$, and taking the inverse:

$\frac{1}{K'_{FeL}} = \frac{[Fe^{3+}][C_L - [FeL]]}{[FeL]}$,

$\frac{1}{K'_{FeL}} = \frac{\left[[Fe^{3+}]C_L\right]}{[FeL]} - \frac{\left[[Fe^{3+}][FeL]\right]}{[FeL]}$,

$\frac{1}{K'_{FeL}} = \frac{\left[[Fe^{3+}]C_L\right]}{[FeL]} - [Fe^{3+}]$,

$\frac{1}{K'_{FeL}} + [Fe^{3+}] = \frac{\left[[Fe^{3+}]C_L\right]}{[FeL]}$,

$\frac{1}{C_L}\left(\frac{1}{K'_{FeL}} + [Fe^{3+}]\right) = \frac{[Fe^{3+}]}{[FeL]}$, and rearranging:

$$\frac{[Fe^{3+}]}{[FeL]} = \frac{[Fe^{3+}]}{C_L} + \frac{[1]}{K'_{FeL}C_L} \quad (3.4)$$

Appendix C

Examples of linear and non-linear graphic results obtained with a code in the R programming language for the determination of the ligand characteristics throughout this PhD work.

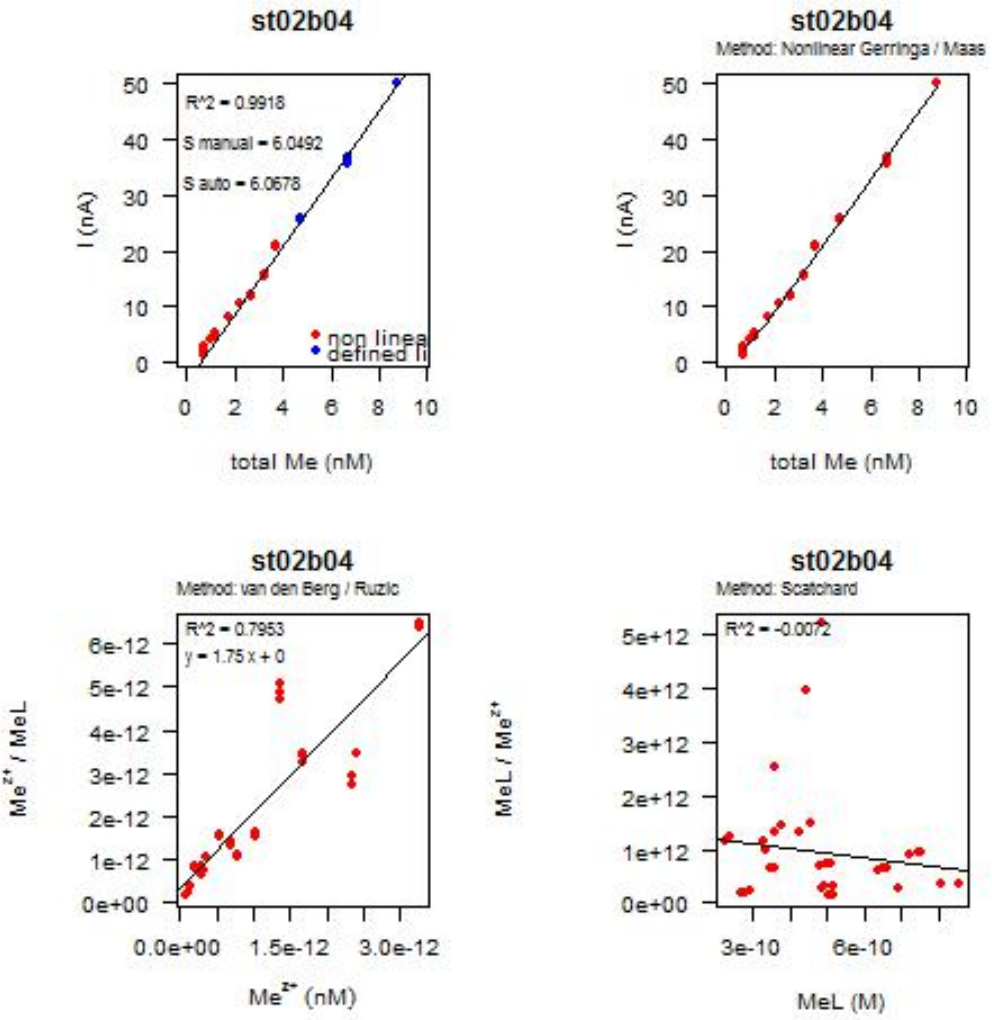

Appendix C

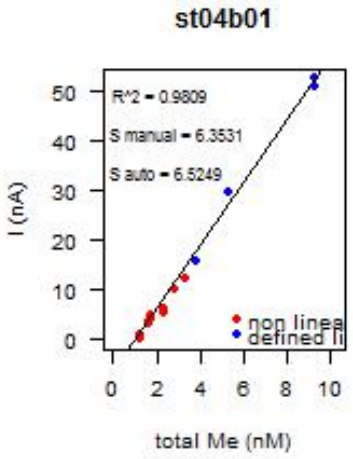
st04b01
R^2 = 0.9809
S manual = 6.3531
S auto = 6.5249
non linea
defined li
I (nA)
total Me (nM)

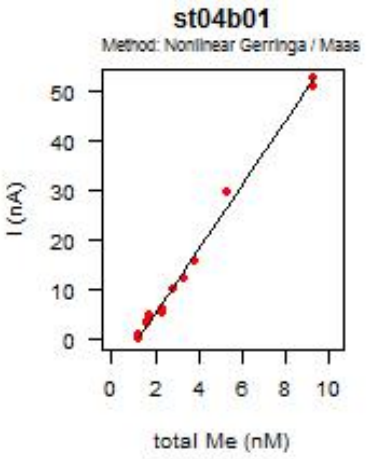
st04b01
Method: Nonlinear Gerringa / Maas
I (nA)
total Me (nM)

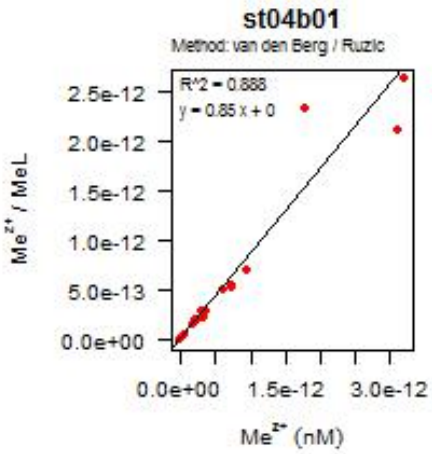
st04b01
Method: van den Berg / Ruzic
R^2 = 0.888
y = 0.85 x + 0
Me^z+ / MeL
Me^z+ (nM)

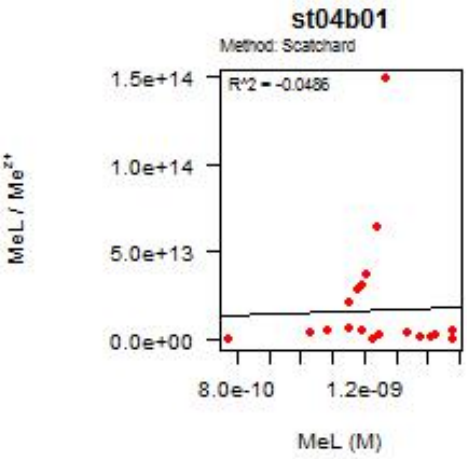
st04b01
Method: Scatchard
R^2 = -0.0486
MeL / Me^z+
MeL (M)

Appendix D

Certified Reference materials (SAFe surface data) used for the dissolved metal analysis (D366 surface seawater samples) for the organic complexation of Fe and Cu (Chapter 4) and for the spatial distribution of dissolved metals in the western European shelf seas (Chapter 5). Analyses were performed by Dr. Christian Schloesser, NOC.

CRM	Cd (pmol kg-1)	s.d.	Pb (pmol kg-1)	s.d.	Fe (nmol kg-1)	s.d.
SAFe S	**7.24**	**1.57**	**48.42**	**6.08**	**0.09**	**0.03**
consensus	1.00	0.20	47.60	2.40	0.09	0.01
n=	25		27		15	
Detection Limit	**3.877**		**3.287**		**0.133**	
Blanks	**0.716**		**1.809**		**0.061**	

CRM	Ni (nmol kg-1)	s.d.	Cu (nmol kg-1)	s.d.	Zn (nmol kg-1)	s.d.
SAFe S	**2.56**	**0.55**	**0.55**	**0.06**	**0.07**	**0.06**
consensus	2.31	0.10	0.51	0.05	0.06	0.02
n=	25		30		10	
Detection Limit	**0.075**		**0.054**		**0.129**	
Blanks	**0.040**		**0.019**		**0.129**	

Method:

* Multielement isotope dilution method (Milne *et al.*, 2010).

* UV digestion for 3 hours

* Off-line preconcentration using a WAKO resin (similar to NOBIAS Chelate PA1) (Kagaya *et al.*, 2009).

* Analysis on an Element XR ICP-MS

Bibliography

Achterberg, E. P., C. Colombo and C. M. G. van den Berg (1999). The distribution of dissolved Cu, Zn, Ni, Co and Cr in English coastal surface waters. Continental Shelf Research 19(4): 537-558.

Achterberg, E. P., T. W. Holland, A. R. Bowie, R. Fauzi, C. Mantoura and P. J. Worsfold (2001). Determination of iron in seawater. Analytica Chimica Acta 442(1): 1-14.

Achterberg, E. P., C. M. Moore, S. A. Henson, S. Steigenberger, A. Stohl, S. Eckhardt, L. C. Avendano, M. Cassidy, D. Hembury, J. K. Klar, M. I. Lucas, A. I. Macey, C. M. Marsay and T. J. Ryan-Keogh (2013). Natural iron fertilization by the Eyjafjallajokull volcanic eruption. Geophysical Research Letters 40(5): 921-926.

Achterberg, E. P. and C. M. G. van den Berg (1996). Automated monitoring of Ni, Cu and Zn in the Irish Sea. Marine Pollution Bulletin 32(6): 471-479.

Albrecht-Gary, A. M. and A. L. Crumbliss (1998). Coordination chemistry of siderophores: Thermodynamics and kinetics of iron chelation and release. Metal Ions in Biological Systems, Vol 35 35: 239-327.

Averyt, K. B., J. P. Kim and K. A. Hunter (2004). Effect of pH on measurement of strong copper binding ligands in lakes. Limnology and Oceanography 49(1): 20-27.

Averyt, K. B., Kim, J. P., and Hunter, K. A. (2004). Effect of pH on measurement of strong copper binding ligands in lakes. Limnol. Oceanography (49): 20–27.

Baars, O., W. Abouchami, S. J. G. Galer, M. Boye and P. L. Croot (2014). Dissolved cadmium in the Southern Ocean: Distribution, speciation, and relation to phosphate. Limnology and Oceanography 59(2): 385-399.

Barbeau, K., J. W. Moffett, D. A. Caron, P. L. Croot and D. L. Erdner (1996). Role of protozoan grazing in relieving iron limitation of phytoplankton. Nature 380(6569): 61-64.

Barbeau, K., E. L. Rue, K. W. Bruland and A. Butler (2001). Photochemical cycling of iron in the surface ocean mediated by microbial iron(III)-binding ligands. Nature 413(6854): 409-413.

Barbeau, K., E. L. Rue, C. G. Trick, K. T. Bruland and A. Butler (2003). Photochemical reactivity of siderophores produced by marine heterotrophic bacteria and cyanobacteria based on characteristic Fe(III) binding groups. Limnology and Oceanography 48(3): 1069-1078.

Batchelli, S., F. L. L. Muller, M. Baalousha and J. R. Lead (2009). Size fractionation and optical properties of colloids in an organic-rich estuary (Thurso, UK). Marine Chemistry 113(3-4): 227-237.

Bennett, S. A., E. P. Achterberg, D. P. Connelly, P. J. Statham, G. R. Fones and C. R. German (2008). The distribution and stabilisation of dissolved Fe in deep-

sea hydrothermal plumes. Earth and Planetary Science Letters 270(3-4): 157-167.

Bergquist, B. A., J. Wu and E. A. Boyle (2007). Variability in oceanic dissolved iron is dominated by the colloidal fraction. Geochimica Et Cosmochimica Acta 71(12): 2960-2974.

Blackford, J. C. and F. J. Gilbert (2007). pH variability and CO2 induced acidification in the North Sea. Journal of Marine Systems 64(1-4): 229-241.

Blain, S., G. Sarthou and P. Laan (2008). Distribution of dissolved iron during the natural iron-fertilization experiment KEOPS (Kerguelen Plateau, Southern Ocean). Deep-Sea Research Part Ii-Topical Studies in Oceanography 55(5-7): 594-605.

Borges, A. V. and N. Gypens (2010). Carbonate chemistry in the coastal zone responds more strongly to eutrophication than to ocean acidification. Limnology and Oceanography 55(1): 346-353.

Boukhalfa, H. and A. L. Crumbliss (2002). Chemical aspects of siderophore mediated iron transport. Biometals 15(4): 325-339.

Bown, J., M. Boye, A. Baker, E. Duvieilbourg, F. Lacan, F. Le Moigne, F. Planchon, S. Speich and D. M. Nelson (2011). The biogeochemical cycle of dissolved cobalt in the Atlantic and the Southern Ocean south off the coast of South Africa. Marine Chemistry 126(1-4): 193-206.

Boyd, P. W. and M. J. Ellwood (2010). The biogeochemical cycle of iron in the ocean. Nature Geoscience 3(10): 675-682.

Boyd, P. W., T. Jickells, C. S. Law, S. Blain, E. A. Boyle, K. O. Buesseler, K. H. Coale, J. J. Cullen, H. J. W. de Baar, M. Follows, M. Harvey, C. Lancelot, M. Levasseur, N. P. J. Owens, R. Pollard, R. B. Rivkin, J. Sarmiento, V. Schoemann, V. Smetacek, S. Takeda, A. Tsuda, S. Turner and A. J. Watson (2007). Mesoscale iron enrichment experiments 1993-2005: Synthesis and future directions. Science 315(5812): 612-617.

Boyd, P. W., A. J. Watson, C. S. Law, E. R. Abraham, T. Trull, R. Murdoch, D. C. E. Bakker, A. R. Bowie, K. O. Buesseler, H. Chang, M. Charette, P. Croot, K. Downing, R. Frew, M. Gall, M. Hadfield, J. Hall, M. Harvey, G. Jameson, J. LaRoche, M. Liddicoat, R. Ling, M. T. Maldonado, R. M. McKay, S. Nodder, S. Pickmere, R. Pridmore, S. Rintoul, K. Safi, P. Sutton, R. Strzepek, K. Tanneberger, S. Turner, A. Waite and J. Zeldis (2000). A mesoscale phytoplankton bloom in the polar Southern Ocean stimulated by iron fertilization. Nature 407(6805): 695-702.

Boye, M., A. Aldrich, C. M. G. van den Berg, J. T. M. de Jong, H. Nirmaier, M. Veldhuis, K. R. Timmermans and H. J. W. de Baar (2006). The chemical speciation of iron in the north-east Atlantic Ocean. Deep-Sea Research Part I-Oceanographic Research Papers 53(4): 667-683.

Boye, M., A. P. Aldrich, C. M. G. van den Berg, J. T. M. de Jong, M. Veldhuis and H. J. W. de Baar (2003). Horizontal gradient of the chemical speciation of iron

in surface waters of the northeast Atlantic Ocean. Marine Chemistry 80(2-3): 129-143.

Boye, M., J. Nishioka, P. Croot, P. Laan, K. R. Timmermans, V. H. Strass, S. Takeda and H. J. W. de Baar (2010). Significant portion of dissolved organic Fe complexes in fact is Fe colloids. Marine Chemistry 122(1-4): 20-27.

Boye, M., J. Nishioka, P. L. Croot, P. Laan, K. R. Timmermans and H. J. W. de Baar (2005). Major deviations of iron complexation during 22 days of a mesoscale iron enrichment in the open Southern Ocean. Marine Chemistry 96(3-4): 257-271.

Boye, M., C. M. G. van den Berg, J. T. M. de Jong, H. Leach, P. Croot and H. J. W. de Baar (2001). Organic complexation of iron in the Southern Ocean. Deep-Sea Research Part I-Oceanographic Research Papers 48(6): 1477-1497.

Boye, M., B. D. Wake, P. L. Garcia, J. Bown, A. R. Baker and E. P. Achterberg (2012). Distributions of dissolved trace metals (Cd, Cu, Mn, Pb, Ag) in the southeastern Atlantic and the Southern Ocean. Biogeosciences 9(8): 3231-3246.

Boyle, E. A. (1988). Cadmium: Chemical Tracer of Deepwater Paleoceanography. Paleoceanography 3(4): 471-489.

Brand, L. E. (1991). Minimum Iron Requirements of Marine-Phytoplankton and the Implications for the Biogeochemical Control of New Production. Limnology and Oceanography 36(8): 1756-1771.

Brand, L. E., W. G. Sunda and R. R. L. Guillard (1983). Limitation of Marine-Phytoplankton Reproductive Rates by Zinc, Manganese, and Iron. Limnology and Oceanography 28(6): 1182-1198.

Brand, L. E., W. G. Sunda and R. R. L. Guillard (1986). Reduction of Marine-Phytoplankton Reproduction Rates by Copper and Cadmium. Journal of Experimental Marine Biology and Ecology 96(3): 225-250.

Breitbarth, E., E. P. Achterberg, M. V. Ardelan, A. R. Baker, E. Bucciarelli, F. Chever, P. L. Croot, S. Duggen, M. Gledhill, M. Hassellov, C. Hassler, L. J. Hoffmann, K. A. Hunter, D. A. Hutchins, J. Ingri, T. Jickells, M. C. Lohan, M. C. Nielsdottir, G. Sarthou, V. Schoemann, J. M. Trapp, D. R. Turner and Y. Ye (2010). Iron biogeochemistry across marine systems - progress from the past decade. Biogeosciences 7(3): 1075-1097.

Brewer, P. G. (1997). Ocean chemistry of the fossil fuel CO2 signal: The haline signal of "business as usual". Geophysical Research Letters 24(11): 1367-1369.

Bruland, K. W. (1980). Oceanographic Distributions of Cadmium, Zinc, Nickel, and Copper in the North Pacific. Earth and Planetary Science Letters 47(2): 176-198.

Bruland, K. W. (1989). Complexation of Zinc by Natural Organic-Ligands in the Central North Pacific. Limnology and Oceanography 34(2): 269-285.

Bibliography

Bruland, K. W., J. R. Donat and D. A. Hutchins (1991). Interactive Influences of Bioactive Trace-Metals on Biological Production in Oceanic Waters. Limnology and Oceanography 36(8): 1555-1577.

Bruland, K. W. and R. P. Franks (1983). Mn, Ni, Cd, Cu and Zn in the Western North Atlantic. Trace Metals in Sea Water. C. S. Wong, E. Boyle, K. W. Bruland, J. S. Burton and E. D. Gotdberg. New York, Plenum Press: 395--414.

Bruland, K. W., G. A. Knauer and J. H. Martin (1978a). Cadmium in Northeast Pacific Waters. Limnology and Oceanography 23(4): 618-625.

Bruland, K. W., G. A. Knauer and J. H. Martin (1978b). Zinc in Northeast Pacific Water. Nature 271(5647): 741-743.

Bruland, K. W. and M. C. Lohan (2004). Controls on trace metals in seawater. The Oceans and Marine Geochemistry. H. Elderfield. London, Elsevier. 6: 23-49.

Bruland, K. W., K. J. Orians and J. P. Cowen (1994). Reactive Trace-Metals in the Stratified Central North Pacific. Geochimica Et Cosmochimica Acta 58(15): 3171-3182.

Bruland, K. W., E. L. Rue, J. R. Donat, S. A. Skrabal and J. W. Moffett (2000). Intercomparison of voltammetric techniques to determine the chemical speciation of dissolved copper in a coastal seawater sample. Analytica Chimica Acta 405(1-2): 99-113.

Bruland, K. W., E. L. Rue and G. J. Smith (2001). Iron and macronutrients in California coastal upwelling regimes: Implications for diatom blooms. Limnology and Oceanography 46(7): 1661-1674.

Bruland, K. W. a. E. L. R. (2001). Chapter 6: Iron: Analytical methods for the determination of concentrations and speciation. SCOR - IUPAC Working Group on Iron in the Oceans.

Buck, K. N. and K. W. Bruland (2007). The physicochemical speciation of dissolved iron in the Bering Sea, Alaska. Limnology and Oceanography 52(5): 1800-1808.

Buck, K. N., M. C. Lohan, C. J. M. Berger and K. W. Bruland (2007). Dissolved iron speciation in two distinct river plumes and an estuary: Implications for riverine iron supply. Limnology and Oceanography 52(2): 843-855.

Buck, K. N., J. Moffett, K. A. Barbeau, R. M. Bundy, Y. Kondo and J. F. Wu (2012). The organic complexation of iron and copper: an intercomparison of competitive ligand exchange-adsorptive cathodic stripping voltammetry (CLE-ACSV) techniques. Limnology and Oceanography-Methods 10: 496-515.

Buck, K. N., K. E. Selph and K. A. Barbeau (2010). Iron-binding ligand production and copper speciation in an incubation experiment of Antarctic Peninsula shelf waters from the Bransfield Strait, Southern Ocean. Marine Chemistry 122(1-4): 148-159.

Burton, J. D., M. Althaus, G. E. Millward, A. W. Morris, P. J. Statham, A. D. Tappin and A. Turner (1993). Processes Influencing the Fate of Trace-Metals in

the North-Sea. Philosophical Transactions of the Royal Society of London Series a-Mathematical Physical and Engineering Sciences 343(1669): 557-568.

Byrne, R. H. (2002). Inorganic speciation of dissolved elements in seawater: the influence of pH on concentration ratios. Geochemical Transactions 3: 11-16.

Byrne, R. H., L. R. Kump and K. J. Cantrell (1988). The Influence of Temperature and Ph on Trace-Metal Speciation in Seawater. Marine Chemistry 25(2): 163-181.

Caldeira, K. and M. E. Wickett (2003). Anthropogenic carbon and ocean pH. Nature 425(6956): 365-365.

Caldeira, K. and M. E. Wickett (2005). Ocean model predictions of chemistry changes from carbon dioxide emissions to the atmosphere and ocean. Journal of Geophysical Research-Oceans 110(C9).

Campbell, A. L., S. Mangan, R. P. Ellis and C. Lewis (2014). Ocean Acidification Increases Copper Toxicity to the Early Life History Stages of the Polychaete Arenicola marina in Artificial Seawater. Environmental Science & Technology 48(16): 9745-9753.

Campos, M. L. A. M. and C. M. G. Van Den Berg (1994). Determination of Copper Complexation in Sea-Water by Cathodic Stripping Voltammetry and Ligand Competition with Salicylaldoxime. Analytica Chimica Acta 284(3): 481-496.

Chester, R. and T. D. Jickells (2012). Marine geochemistry. Hoboken, NJ, John Wiley & Sons.

Coale, K. H. and K. W. Bruland (1988). Copper Complexation in the Northeast Pacific. Limnology and Oceanography 33(5): 1084-1101.

Croot, P. L., O. Baars and P. Streu (2011). The distribution of dissolved zinc in the Atlantic sector of the Southern Ocean. Deep-Sea Research Part Ii-Topical Studies in Oceanography 58(25-26): 2707-2719.

Croot, P. L. and M. Johansson (2000). Determination of iron speciation by cathodic stripping voltammetry in seawater using the competing ligand 2-(2-thiazolylazo)-p-cresol (TAC). Electroanalysis 12(8): 565-576.

Croot, P. L., J. W. Moffett and L. E. Brand (2000). Production of extracellular Cu complexing ligands by eucaryotic phytoplankton in response to Cu stress. Limnology and Oceanography 45(3): 619-627.

Cullen, J. T., B. A. Bergquist and J. W. Moffett (2006). Thermodynamic characterization of the partitioning of iron between soluble and colloidal species in the Atlantic Ocean. Marine Chemistry 98(2-4): 295-303.

Curry, R. and C. Mauritzen (2005). Dilution of the northern North Atlantic Ocean in recent decades. Science 308(5729): 1772-1774.

de Baar, H., L. Gerringa and C. E. Thuroczy (2008). Effects of changes in carbonate chemistry on nutrient and metal speciation. EPOCA. Geotraces.

de Baar, H. J. W., P. W. Boyd, K. H. Coale, M. R. Landry, A. Tsuda, P. Assmy, D. C. E. Bakker, Y. Bozec, R. T. Barber, M. A. Brzezinski, K. O. Buesseler, M. Boye, P. L. Croot, F. Gervais, M. Y. Gorbunov, P. J. Harrison, W. T. Hiscock, P. Laan, C. Lancelot, C. S. Law, M. Levasseur, A. Marchetti, F. J. Millero, J. Nishioka, Y. Nojiri, T. van Oijen, U. Riebesell, M. J. A. Rijkenberg, H. Saito, S. Takeda, K. R. Timmermans, M. J. W. Veldhuis, A. M. Waite and C. S. Wong (2005). Synthesis of iron fertilization experiments: From the iron age in the age of enlightenment. Journal of Geophysical Research-Oceans 110(C9): 1-24.

de Baar, H. J. W., P. M. Saager, R. F. Nolting and J. Vandermeer (1994). Cadmium Versus Phosphate in the World Ocean. Marine Chemistry 46(3): 261-281.

De La Rocha, C. L., D. A. Hutchins, M. A. Brzezinski and Y. H. Zhang (2000). Effects of iron and zinc deficiency on elemental composition and silica production by diatoms. Marine Ecology Progress Series 195: 71-79.

Donat, J. R., K. A. Lao and K. W. Bruland (1994). Speciation of Dissolved Copper and Nickel in South San-Francisco Bay - a Multimethod Approach. Analytica Chimica Acta 284(3): 547-571.

Donat, J. R. and C. M. G. van den Berg (1992). A New Cathodic Stripping Voltammetric Method for Determining Organic Copper Complexation in Seawater. Marine Chemistry 38(1-2): 69-90.

Doney, S. C. (2006). The dangers of ocean acidification. Scientific American 294(3): 58-65.

Doney, S. C., V. J. Fabry, R. A. Feely and J. A. Kleypas (2009). Ocean Acidification: The Other CO2 Problem. Annual Review of Marine Science 1: 169-192.

Duinker, J. C. and R. F. Nolting (1982). Dissolved Copper, Zinc and Cadmium in the Southern Bight of the North-Sea. Marine Pollution Bulletin 13(3): 93-96.

Dupont, C. L., J. W. Moffett, R. R. Bidigare and B. A. Ahner (2006). Distributions of dissolved and particulate biogenic thiols in the subartic Pacific Ocean. Deep-Sea Research Part I-Oceanographic Research Papers 53(12): 1961-1974.

Ellwood, M. J. (2008). Wintertime trace metal (Zn, Cu, Ni, Cd, Pb and Co) and nutrient distributions in the Subantarctic Zone between 40-52 degrees S; 155-160 degrees E. Marine Chemistry 112(1-2): 107-117.

Ellwood, M. J. and C. M. G. van den Berg (2000). Zinc speciation in the Northeastern Atlantic Ocean. Marine Chemistry 68(4): 295-306.

Feely, R. A., S. C. Doney and S. R. Cooley (2009). Ocean Acidification: Present Conditions and Future Changes in a High-CO2 World. Oceanography 22(4): 36-47.

Feely, R. A., C. L. Sabine, K. Lee, W. Berelson, J. Kleypas, V. J. Fabry and F. J. Millero (2004). Impact of anthropogenic CO2 on the CaCO3 system in the oceans. Science 305(5682): 362-366.

Fitter, A. H. and D. Raffaelli (1999). Advances in ecological research, Academic Press.

Flegal, A. R. and C. C. Patterson (1983). Vertical Concentration Profiles of Lead in the Central Pacific at 15-Degrees-N and 20-Degrees-S. Earth and Planetary Science Letters 64(1): 19-32.

Fogelqvist, E., J. Blindheim, T. Tanhua, S. Osterhus, E. Buch and F. Rey (2003). Greenland-Scotland overflow studied by hydro-chemical multivariate analysis. Deep-Sea Research Part I-Oceanographic Research Papers 50(1): 73-102.

Frants, M., S. T. Gille, M. Hatta, W. T. Hiscock, M. Kahru, C. I. Measures, B. G. Mitchell and M. Zhou (2013). Analysis of horizontal and vertical processes contributing to natural iron supply in the mixed layer in southern Drake Passage. Deep-Sea Research Part Ii-Topical Studies in Oceanography 90: 68-76.

Geider, R. J., J. Laroche, R. M. Greene and M. Olaizola (1993). Response of the Photosynthetic Apparatus of Phaeodactylum-Tricornutum (Bacillariophyceae) to Nitrate, Phosphate, or Iron Starvation. Journal of Phycology 29(6): 755-766.

Gerringa, L. J. A., S. Blain, P. Laan, G. Sarthou, M. J. W. Veldhuis, C. P. D. Brussaard, E. Viollier and K. R. Timmermans (2008). Fe-binding dissolved organic ligands near the Kerguelen Archipelago in the Southern Ocean (Indian sector). Deep-Sea Research Part II-Topical Studies in Oceanography 55(5-7): 606-621.

Gerringa, L. J. A., P. M. J. Herman and T. C. W. Poortvliet (1995). Comparison of the Linear Vandenberg Ruzic Transformation and a Nonlinear Fit of the Langmuir Isotherm Applied to Cu Speciation Data in the Estuarine Environment. Marine Chemistry 48(2): 131-142.

Gerringa, L. J. A., M. J. A. Rijkenberg, C. E. Thuroczy and L. R. M. Maas (2014). A critical look at the calculation of the binding characteristics and concentration of iron complexing ligands in seawater with suggested improvements. Environmental Chemistry 11(2): 114-136.

Gerringa, L. J. A., M. J. W. Veldhuis, K. R. Timmermans, G. Sarthou and H. J. W. de Baar (2006). Co-variance of dissolved Fe-binding ligands with phytoplankton characteristics in the Canary Basin. Marine Chemistry 102(3-4): 276-290.

Gledhill, M., E. P. Achterberg, L. Keqiang, K. N. Mohamed and M. Rijkenberg (submitted). Influence of ocean acidification on the complexation of iron and copper to organic ligands. Marine Chemistry: 35.

Gledhill, M. and K. N. Buck (2012). The organic complexation of iron in the marine environment: a review. Front Microbiol 3: 69.

Gledhill, M., P. McCormack, S. Ussher, E. P. Achterberg, R. F. C. Mantoura and P. J. Worsfold (2004). Production of siderophore type chelates by mixed bacterioplankton populations in nutrient enriched seawater incubations. Marine Chemistry 88(1-2): 75-83.

Gledhill, M. and C. M. G. van den Berg (1994). Determination of Complexation of Iron(Iii) with Natural Organic Complexing Ligands in Seawater Using Cathodic Stripping Voltammetry. Marine Chemistry 47(1): 41-54.

Gledhill, M., C. M. G. van den Berg, R. F. Nolting and K. R. Timmermans (1998). Variability in the speciation of iron in the northern North Sea. Marine Chemistry 59(3-4): 283-300.

Gledhill, M. and C. M. G. Vandenberg (1995). Measurement of the Redox Speciation of Iron in Seawater by Catalytic Cathodic Stripping Voltammetry. Marine Chemistry 50(1-4): 51-61.

Gordon, A. S., J. R. Donat, R. A. Kango, B. J. Dyer and L. M. Stuart (2000). Dissolved copper-complexing ligands in cultures of marine bacteria and estuarine water. Marine Chemistry 70(1-3): 149-160.

Granger, J. and N. M. Price (1999). The importance of siderophores in iron nutrition of heterotrophic marine bacteria. Limnology and Oceanography 44(3): 541-555.

Grasshoff, K., M. Ehrhardt, K. Kremling and L. G. Anderson (1999). Methods of seawater analysis. Weinheim ; New York, Wiley-VCH.

Hassler, C. S., V. Schoemann, C. M. Nichols, E. C. V. Butler and P. W. Boyd (2011). Saccharides enhance iron bioavailability to Southern Ocean phytoplankton. Proceedings of the National Academy of Sciences of the United States of America 108(3): 1076-1081.

Hawkes, J. A., D. P. Connelly, M. Gledhill and E. P. Achterberg (2013). The stabilisation and transportation of dissolved iron from high temperature hydrothermal vent systems. Earth and Planetary Science Letters 375: 280-290.

HELCOM (2010). Ecosystem Health of the Baltic Sea 2003-2007: HELCOM Initial Holistic Assessment.

Henderson, C. (2006). Ocean acidification: the other CO2 problem. New Scientist.

Hering, J. G., W. G. Sunda, R. L. Ferguson and F. M. M. Morel (1987). A Field Comparison of 2 Methods for the Determination of Copper Complexation - Bacterial Bioassay and Fixed-Potential Amperometry. Marine Chemistry 20(4): 299-312.

Hertkorn, N., R. Benner, M. Frommberger, P. Schmitt-Kopplin, M. Witt, K. Kaiser, A. Kettrup and J. I. Hedges (2006). Characterization of a major refractory component of marine dissolved organic matter. Geochimica Et Cosmochimica Acta 70(12): 2990-3010.

Hoffmann, L. J., E. Breitbarth, P. W. Boyd and K. A. Hunter (2012). Influence of ocean warming and acidification on trace metal biogeochemistry. Marine Ecology Progress Series 470: 191-205.

Holt, J., S. Wakelin and J. Huthnance (2009). Down- welling circulation of the northwest European continental shelf: A driving mechanism for the continental shelf carbon pump. Geophys. Res. Lett.(L14602): 36.

Houghton, R. A. (2001). Counting terrestrial sources and sinks of carbon. Climatic Change 48(4): 525-534.

Hudson, R. J. M., D. T. Covault and F. M. M. Morel (1992). Investigations of Iron Coordination and Redox Reactions in Seawater Using Fe-59 Radiometry and Ion-Pair Solvent-Extraction of Amphiphilic Iron Complexes. Marine Chemistry 38(3-4): 209-235.

Hudson, R. J. M. and F. M. M. Morel (1990). Iron Transport in Marine-Phytoplankton - Kinetics of Cellular and Medium Coordination Reactions. Limnology and Oceanography 35(5): 1002-1020.

Hudson, R. J. M., E. L. Rue and K. W. Bruland (2003). Modeling complexometric titrations of natnral water samples. Environmental Science & Technology 37(8): 1553-1562.

Hunter, K. A. and P. W. Boyd (2007). Iron-binding ligands and their role in the ocean biogeochemistry of iron. Environmental Chemistry 4(4): 221-232.

Hutchins, D. A. and K. W. Bruland (1994). Grazer-Mediated Regeneration and Assimilation of Fe, Zn and Mn from Planktonic Prey. Marine Ecology-Progress Series 110(2-3): 259-269.

Hutchins, D. A., G. R. DiTullio, Y. Zhang and K. W. Bruland (1998). An iron limitation mosaic in the California upwelling regime. Limnology and Oceanography 43(6): 1037-1054.

Hutchins, D. A., A. E. Witter, A. Butler and G. W. Luther (1999). Competition among marine phytoplankton for different chelated iron species. Nature 400(6747): 858-861.

Jacquot, J. E., Y. Kondo, A. N. Knapp and J. W. Moffett (2013). The speciation of copper across active gradients in nitrogen-cycle processes in the eastern tropical South Pacific. Limnology and Oceanography 58(4): 1387-1394.

Jickells, T. D., L.J. Spokes (2001). Atmospheric iron inputs to the Oceans. In: The biogeochemistry of iron. D. R. T. a. K. A. Hunter. Chichester-Wiley: 85-121.

Johnson, K. S., R. M. Gordon and K. H. Coale (1997). What controls dissolved iron concentrations in the world ocean? Marine Chemistry 57(3-4): 137-161.

Kagaya, S., E. Maeba, Y. Inoue, W. Kamichatani, T. Kajiwara, H. Yanai, M. Saito and K. Tohda (2009). A solid phase extraction using a chelate resin immobilizing carboxymethylated pentaethylenehexamine for separation and preconcentration of trace elements in water samples. Talanta 79(2): 146-152.

King, A. L., S. A. Sanudo-Wilhelmy, K. Leblanc, D. A. Hutchins and F. X. Fu (2011). CO2 and vitamin B-12 interactions determine bioactive trace metal requirements of a subarctic Pacific diatom. Isme Journal 5(8): 1388-1396.

Klar, J. (2010). Dissolved iron and aluminum distribution in the Iceland and Irminger Basin during D354. In: RRS Discovery D350 and D354 cruise reports, University of Southampton, National Oceanography Centre 304.

Kleypas, J. A., R. W. Buddemeier, D. Archer, J. P. Gattuso, C. Langdon and B. N. Opdyke (1999). Geochemical consequences of increased atmospheric carbon dioxide on coral reefs. Science 284(5411): 118-120.

Klunder, M. B., P. Laan, R. Middag, H. J. W. De Baar and J. C. van Ooijen (2011). Dissolved iron in the Southern Ocean (Atlantic sector). Deep-Sea Research Part Ii-Topical Studies in Oceanography 58(25-26): 2678-2694.

Kondo, Y., S. Takeda, et al. (2012). Distinct trends in dissolved Fe speciation between shallow and deep waters in the Pacific Ocean. Marine Chemistry 134-145: 18-28.

Kondo, Y., S. Takeda and K. Furuya (2007). Distribution and speciation of dissolved iron in the Sulu Sea and its adjacent waters. Deep-Sea Research Part II-Topical Studies in Oceanography 54(1-2): 60-80.

Kondo, Y., S. Takeda, J. Nishioka, H. Obata, K. Furuya, W. K. Johnson and C. S. Wong (2008). Organic iron(III) complexing ligands during an iron enrichment experiment in the western subarctic North Pacific. Geophysical Research Letters 35(12).

Krauss, W. (1995). Mixing in the Irminger Sea and in the Iceland Basin. Journal of Geophysical Research-Oceans 100(C6): 10851-10871.

Kremling, K. (1983). Trace-Metal Fronts in European Shelf Waters. Nature 303(5914): 225-227.

Kremling, K. (1985). The Distribution of Cadmium, Copper, Nickel, Manganese, and Aluminum in Surface Waters of the Open Atlantic and European Shelf Area. Deep-Sea Research Part a-Oceanographic Research Papers 32(5): 531-555.

Kremling, K. and D. Hydes (1988). Summer Distribution of Dissolved Al, Cd, Co, Cu, Mn and Ni in Surface Waters around the British-Isles. Continental Shelf Research 8(1): 89-105.

Kremling, K. and P. Streu (2001). The behaviour of dissolved Cd, Co, Zn, and Pb in North Atlantic near-surface waters (30 degrees N/60 degrees W-60 degrees N/2 degrees W). Deep-Sea Research Part I-Oceanographic Research Papers 48(12): 2541-2567.

Kuma, K. and K. Matsunaga (1995). Availability of Colloidal Ferric Oxides to Coastal Marine-Phytoplankton. Marine Biology 122(1): 1-11.

Kuma, K., J. Nishioka and K. Matsunaga (1996). Controls on iron(III) hydroxide solubility in seawater: The influence of pH and natural organic chelators. Limnology and Oceanography 41(3): 396-407.

Kustka, A. B., A. E. Allen and F. M. M. Morel (2007). Sequence analysis and transcriptional regulation of iron acquisition genes in two marine diatoms. Journal of Phycology 43(4): 715-729.

Laes, A., S. Blain, P. Laan, S. J. Ussher, E. P. Achterberg, P. Treguer and H. J. W. de Baar (2007). Sources and transport of dissolved iron and manganese along the continental margin of the Bay of Biscay. Biogeosciences 4(2): 181-194.

Laglera, L. M., G. Battaglia and C. M. G. van den Berg (2007). Determination of humic substances in natural waters by cathodic stripping voltammetry of their complexes with iron. Analytica Chimica Acta 599(1): 58-66.

Laglera, L. M., G. Battaglia and C. M. G. van den Berg (2011). Effect of humic substances on the iron speciation in natural waters by CLE/CSV. Marine Chemistry 127(1-4): 134-143.

Laglera, L. M. and C. M. G. van den Berg (2003). Copper complexation by thiol compounds in estuarine waters. Marine Chemistry 82(1-2): 71-89.

Laglera, L. M. and C. M. G. van den Berg (2009). Evidence for geochemical control of iron by humic substances in seawater. Limnology and Oceanography 54(2): 610-619.

Langdon, C., W. S. Broecker, D. E. Hammond, E. Glenn, K. Fitzsimmons, S. G. Nelson, T. H. Peng, I. Hajdas and G. Bonani (2003). Effect of elevated CO2 on the community metabolism of an experimental coral reef. Global Biogeochemical Cycles 17(1).

Leal, M. F. C. and C. M. G. van den Berg (1998). Evidence for strong copper(I) complexation by organic ligands in seawater. Aquatic Geochemistry 4(1): 49-75.

Lenhart, H. J., J. Patsch, W. Kuhn, A. Moll and T. Pohlmann (2004). Investigation on the trophic state of the North Sea for three years (1994–1996) simulated with the ecosystem model ERSEM – the role of a sharp NAOI decline. Biogeosciences Discussions 1: 725-754.

Liu, X. W. and F. J. Millero (1999). The solubility of iron hydroxide in sodium chloride solutions. Geochimica Et Cosmochimica Acta 63(19-20): 3487-3497.

Liu, X. W. and F. J. Millero (2002). The solubility of iron in seawater. Marine Chemistry 77(1): 43-54.

Lohan, M. C., D. W. Crawford, D. A. Purdie and P. J. Statham (2005). Iron and zinc enrichments in the northeastern subarctic Pacific: Ligand production and zinc availability in response to phytoplankton growth. Limnology and Oceanography 50(5): 1427-1437.

Louis, Y., C. Garnier, V. Lenoble, D. Omanovic, S. Mounier and I. Pizeta (2009). Characterisation and modelling of marine dissolved organic matter interactions with major and trace cations. Marine Environmental Research 67(2): 100-107.

Macrellis, H. M., C. G. Trick, E. L. Rue, G. Smith and K. W. Bruland (2001). Collection and detection of natural iron-binding ligands from seawater. Marine Chemistry 76(3): 175-187.

Maldonado, M. T., A. E. Allen, J. S. Chong, K. Lin, D. Leus, N. Karpenko and S. L. Harris (2006). Copper-dependent iron transport in coastal and oceanic diatoms. Limnology and Oceanography 51(4): 1729-1743.

Maldonado, M. T. and N. M. Price (1999). Utilization of iron bound to strong organic ligands by plankton communities in the subarctic Pacific Ocean. Deep-Sea Research Part II-Topical Studies in Oceanography 46(11-12): 2447-2473.

Maldonado, M. T. and N. M. Price (2001). Reduction and transport of organically bound iron by Thalassiosira oceanica (Bacillariophyceae). Journal of Phycology 37(2): 298-309.

Maldonado, M. T., R. F. Strzepek, S. Sander and P. W. Boyd (2005). Acquisition of iron bound to strong organic complexes, with different Fe binding groups and photochemical reactivities, by plankton communities in Fe-limited subantarctic waters. Global Biogeochemical Cycles 19(4).

Maranger, R., D. F. Bird and N. M. Price (1998). Iron acquisition by photosynthetic marine phytoplankton from ingested bacteria. Nature 396(6708): 248-251.

Martin, J. H. and S. E. Fitzwater (1988). Iron-Deficiency Limits Phytoplankton Growth in the Northeast Pacific Subarctic. Nature 331(6154): 341-343.

Martin, J. H., S. E. Fitzwater, R. M. Gordon, C. N. Hunter and S. J. Tanner (1993). Iron, Primary Production and Carbon Nitrogen Flux Studies during the Jgofs North-Atlantic Bloom Experiment. Deep-Sea Research Part Ii-Topical Studies in Oceanography 40(1-2): 115-134.

Martin, J. H. and R. M. Gordon (1988). Northeast Pacific Iron Distributions in Relation to Phytoplankton Productivity. Deep-Sea Research Part a-Oceanographic Research Papers 35(2): 177-196.

Martin, J. M. and H. L. Windom (1991). Present and Future Roles of Ocean Margins in Regulating Marine Biogeochemical Cycles of Trace-Elements. Ocean Margin Processes in Global Change: 45-67.

Mawji, E., M. Gledhill, J. A. Milton, G. A. Tarran, S. Ussher, A. Thompson, G. A. Wolff, P. J. Worsfold and E. P. Achterberg (2008). Hydroxamate Siderophores: Occurrence and Importance in the Atlantic Ocean. Environmental Science & Technology 42(23): 8675-8680.

Mawji, E., M. Gledhill, J. A. Milton, M. V. Zubkov, A. Thompson, G. A. Wolff and E. P. Achterberg (2011). Production of siderophore type chelates in Atlantic Ocean waters enriched with different carbon and nitrogen sources. Marine Chemistry 124(1-4): 90-99.

Measures, C. I., W. M. Landing, M. T. Brown and C. S. Buck (2008). High-resolution Al and Fe data from the Atlantic Ocean CLIVAR-CO(2) repeat hydrography A16N transect: Extensive linkages between atmospheric dust and upper ocean geochemistry. Global Biogeochemical Cycles 22(1).

Millero, F. J. (1998). Solubility of Fe(III) in seawater. Earth and Planetary Science Letters 154(1-4): 323-329.

Millero, F. J. (2001). Speciation of metals in natural waters. Abstracts of Papers of the American Chemical Society 221: U533-U533.

Millero, F. J., R. Woosley, B. Ditrolio and J. Waters (2009). Effect of Ocean Acidification on the Speciation of Metals in Seawater. Oceanography 22(4): 72-85.

Millero, F. J., W. S. Yao and J. Aicher (1995). The Speciation of Fe(II) and Fe(III) in Natural-Waters. Marine Chemistry 50(1-4): 21-39.

Milne, A., W. Landing, M. Bizimis and P. Morton (2010). Determination of Mn, Fe, Co, Ni, Cu, Zn, Cd and Pb in seawater using high resolution magnetic sector inductively coupled mass spectrometry (HR-ICP-MS). Analytica Chimica Acta 665(2): 200-207.

Moffett, J. W. and L. E. Brand (1996). Production of strong, extracellular Cu chelators by marine cyanobacteria in response to Cu stress. Limnology and Oceanography 41(3): 388-395.

Moffett, J. W. and C. Dupont (2007). Cu complexation by organic ligands in the sub-arctic NW Pacific and Bering Sea. Deep-Sea Research Part I-Oceanographic Research Papers 54(4): 586-595.

Mohamed, K. N., S. Steigenberger, M. C. Nielsdottir, M. Gledhill and E. P. Achterberg (2011). Dissolved iron(III) speciation in the high latitude North Atlantic Ocean. Deep-Sea Research Part I-Oceanographic Research Papers 58(11): 1049-1059.

Moore, C. M., M. I. Lucas, R. Sanders and R. Davidson (2005). Basin-scale variability of phytoplankton bio-optical characteristics in relation to bloom state and community structure in the Northeast Atlantic. Deep-Sea Research Part I-Oceanographic Research Papers 52(3): 401-419.

Moore, C. M., M. M. Mills, E. P. Achterberg, R. J. Geider, J. LaRoche, M. I. Lucas, E. L. McDonagh, X. Pan, A. J. Poulton, M. J. A. Rijkenberg, D. J. Suggett, S. J. Ussher and E. M. S. Woodward (2009). Large-scale distribution of Atlantic nitrogen fixation controlled by iron availability. Nature Geoscience 2(12): 867-871.

Morel, F. M. M., R. J. M. Hudson and N. M. Price (1991). Limitation of Productivity by Trace-Metals in the Sea. Limnology and Oceanography 36(8): 1742-1755.

Morel, F. M. M. and N. M. Price (2003). The biogeochemical cycles of trace metals in the oceans. Science 300(5621): 944-947.

Morel, F. M. M., J. R. Reinfelder, S. B. Roberts, C. P. Chamberlain, J. G. Lee and D. Yee (1994). Zinc and Carbon Co-Limitation of Marine-Phytoplankton. Nature 369(6483): 740-742.

Nielsdottir, M. C., C. M. Moore, R. Sanders, D. J. Hinz and E. P. Achterberg (2009). Iron limitation of the postbloom phytoplankton communities in the Iceland Basin. Global Biogeochemical Cycles 23.

Officer, C. B. (1979). Discussion of the Behavior of Non-Conservative Dissolved Constituents in Estuaries. Estuarine and Coastal Marine Science 9(1): 91-94.

Orr, J. C., V. J. Fabry, O. Aumont, L. Bopp, S. C. Doney, R. A. Feely, A. Gnanadesikan, N. Gruber, A. Ishida, F. Joos, R. M. Key, K. Lindsay, E. Maier-Reimer, R. Matear, P. Monfray, A. Mouchet, R. G. Najjar, G. K. Plattner, K. B. Rodgers, C. L. Sabine, J. L. Sarmiento, R. Schlitzer, R. D. Slater, I. J. Totterdell,

M. F. Weirig, Y. Yamanaka and A. Yool (2005a). Anthropogenic ocean acidification over the twenty-first century and its impact on calcifying organisms. Nature 437(7059): 681-686.

Orr, J. C., S. Pantoja and H. O. Portner (2005b). Introduction to special section: The ocean in a high-CO2 world. Journal of Geophysical Research-Oceans 110(C9): -.

OSPAR Commission (2000). Quality Status Report 2000, Region II Greater North Sea, Region III Celtic Seas. OSPAR Commission(London): 149

Pan, K. and W. X. Wang (2012). Trace metal contamination in estuarine and coastal environments in China. Science of the Total Environment 421: 3-16.

Patterson, C. C. and D. M. Settle (1987). Review of Data on Eolian Fluxes of Industrial and Natural Lead to the Lands and Seas in Remote Regions on a Global Scale. Marine Chemistry 22(2-4): 137-162.

Peers, G., S. A. Quesnel and N. M. Price (2005). Copper requirements for iron acquisition and growth of coastal and oceanic diatoms. Limnology and Oceanography 50(4): 1149-1158.

Pickart, R. S., F. Straneo and G. W. K. Moore (2003). Is Labrador Sea Water formed in the Irminger basin? Deep-Sea Research Part I-Oceanographic Research Papers 50(1): 23-52.

Poulton, A. J., A. Charalampopoulou, J. R. Young, G. A. Tarran, M. I. Lucas and G. D. Quartly (2010). Coccolithophore dynamics in non-bloom conditions during late summer in the central Iceland Basin (July-August 2007). Limnology and Oceanography 55(4): 1601-1613.

Price, N. M., B. A. Ahner and F. M. M. Morel (1994). The Equatorial Pacific-Ocean - Grazer-Controlled Phytoplankton Populations in an Iron-Limited Ecosystem. Limnology and Oceanography 39(3): 520-534.

Price, N. M. and F. M. M. Morel (1990). Cadmium and Cobalt Substitution for Zinc in a Marine Diatom. Nature 344(6267): 658-660.

Price, N. M. and F. M. M. Morel (1998). Biological cycling of iron in the ocean. Metal Ions in Biological Systems, Vol 35 35: 1-36.

Raven, J. A., M. C. W. Evans and R. E. Korb (1999). The role of trace metals in photosynthetic electron transport in O(2)-evolving organisms. Photosynthesis Research 60(2-3): 111-149.

Raymond, K. N., G. Muller and B. F. Matzanke (1984). Complexation of Iron by Siderophores - a Review of Their Solution and Structural Chemistry and Biological Function. Topics in Current Chemistry 123: 49-102.

Read, J. F. (2001). CONVEX-91: water masses and circulation of the Northeast Atlantic subpolar gyre. Progress in Oceanography 48(4): 461-510.

Rérolle, V. M. C., C. F. A. Floquet, M. C. Mowlem, R. R. G. J. Bellerby, D. P. Connelly and E. P. Achterberg (2012). Seawater-pH measurements for ocean-acidification observations. Trac-Trends in Analytical Chemistry 40: 146-157.

Rérolle, V. M. C., M. Ribas-Ribas, V. Kitidis, I. Brown, D. C. E. Bakker, G. A. Lee, T. Shi, M. C. Mowlem and E. P. Achterberg (2014). Controls on pH in surface waters of northwestern European shelf seas. Biogeosciences Discussions 11: 943–974.

Riebesell, U., I. Zondervan, B. Rost, P. D. Tortell, R. E. Zeebe and F. M. M. Morel (2000). Reduced calcification of marine plankton in response to increased atmospheric CO2. Nature 407(6802): 364-367.

Rijkenberg, M. J. A., C. F. Powell, M. Dall'Osto, M. C. Nielsdottir, M. D. Patey, P. G. Hill, A. R. Baker, T. D. Jickells, R. M. Harrison and E. P. Achterberg (2008). Changes in iron speciation following a Saharan dust event in the tropical North Atlantic Ocean. Marine Chemistry 110(1-2): 56-67.

Ringbom, A. and E. Still (1972). Calculation and Use of Alpha-Coefficients. Analytica Chimica Acta 59(1): 143-&.

Rose, J. M., Y. Feng, G. R. DiTullio, R. B. Dunbar, C. E. Hare, P. A. Lee, M. Lohan, M. Long, W. O. Smith, B. Sohst, S. Tozzi, Y. Zhang and D. A. Hutchins (2009). Synergistic effects of iron and temperature on Antarctic phytoplankton and microzooplankton assemblages. Biogeosciences 6(12): 3131-3147.

Ross, A. R. S., M. G. Ikonomou and K. J. Orians (2003). Characterization of copper-complexing ligands in seawater using immobilized copper(II)-ion affinity chromatography and electrospray ionization mass spectrometry. Marine Chemistry 83(1-2): 47-58.

Rost, B., U. Riebesell, S. Burkhardt and D. Sultemeyer (2003). Carbon acquisition of bloom-forming marine phytoplankton. Limnology and Oceanography 48(1): 55-67.

Roy, E. G., M. L. Wells and D. W. King (2008). Persistence of iron(II) in surface waters of the western subarctic Pacific. Limnology and Oceanography 53(1): 89-98.

Royal Society, T. (2005). Ocean acidification due to increasing atmospheric carbon dioxide. I. 2. 6-9 Carlton House Terrace London SW1Y 5AG: 60.

Rue, E. L. and K. W. Bruland (1995). Complexation of Iron(Iii) by Natural Organic-Ligands in the Central North Pacific as Determined by a New Competitive Ligand Equilibration Adsorptive Cathodic Stripping Voltammetric Method. Marine Chemistry 50(1-4): 117-138.

Rue, E. L. and K. W. Bruland (1997). The role of organic complexation on ambient iron chemistry in the equatorial Pacific Ocean and the response of a mesoscale iron addition experiment. Limnology and Oceanography 42(5): 901-910.

Ruzic, I. (1982). Theoretical Aspects of the Direct Titration of Natural-Waters and Its Information Yield for Trace-Metal Speciation. Analytica Chimica Acta 140(1): 99-113.

Ryan-Keogh, T. J., A. I. Macey, M. C. Nielsdottir, M. I. Lucas, S. S. Steigenberger, M. C. Stinchcombe, E. P. Achterberg, T. S. Bibby and C. M. Moore (2013).

Spatial and temporal development of phytoplankton iron stress in relation to bloom dynamics in the high-latitude North Atlantic Ocean. Limnology and Oceanography 58(2): 533-545.

Sabine, C. L., R. A. Feely, N. Gruber, R. M. Key, K. Lee, J. L. Bullister, R. Wanninkhof, C. S. Wong, D. W. R. Wallace, B. Tilbrook, F. J. Millero, T. H. Peng, A. Kozyr, T. Ono and A. F. Rios (2004). The oceanic sink for anthropogenic CO2. Science 305(5682): 367-371.

Sanders, R., L. Brown, S. Henson and M. Lucas (2005). New production in the Irminger Basin during 2002. Journal of Marine Systems 55(3-4): 291-310.

Sarmiento, J. L. and J. R. Toggweiler (1984). A New Model for the Role of the Oceans in Determining Atmospheric Pco2. Nature 308(5960): 621-624.

Sarthou, G., E. Bucciarelli, F. Chever, S. P. Hansard, M. Gonzalez-Davila, J. M. Santana-Casiano, F. Planchon and S. Speich (2011). Labile Fe(II) concentrations in the Atlantic sector of the Southern Ocean along a transect from the subtropical domain to the Weddell Sea Gyre. Biogeosciences 8(9): 2461-2479.

Sato, M., S. Takeda and K. Furuya (2007). Iron regeneration and organic iron(III)-binding ligand production during in situ zooplankton grazing experiment. Marine Chemistry 106(3-4): 471-488.

Schlosser, C. and P. L. Croot (2008). Application of cross-flow filtration for determining the solubility of iron species in open ocean seawater. Limnology and Oceanography-Methods 6: 630-642.

Semeniuk, D. M., R. M. Bundy, C. D. Payne, K. A. Barbeau and M. T. Maldonado (2015). Acquisition of organically complexed copper by marine phytoplankton and bacteria in the northeast subarctic Pacific Ocean. Marine Chemistry.

Semeniuk, D. M., J. T. Cullen, W. K. Johnson, K. Gagnon, T. J. Ruth and M. T. Maldonado (2009). Plankton copper requirements and uptake in the subarctic Northeast Pacific Ocean. Deep-Sea Research Part I-Oceanographic Research Papers 56(7): 1130-1142.

Shaked, Y., A. B. Kustka and F. M. M. Morel (2005). A general kinetic model for iron acquisition by eukaryotic phytoplankton. Limnology and Oceanography 50(3): 872-882.

Shaked, Y. and H. Lis (2012). Disassembling iron availability to phytoplankton. Frontiers in Microbiology 3.

Shi, D. L., Y. Xu, B. M. Hopkinson and F. M. M. Morel (2010). Effect of Ocean Acidification on Iron Availability to Marine Phytoplankton. Science 327(5966): 676-679.

Soria-Dengg, S., R. Reissbrodt and U. Horstmann (2001). Siderophores in marine, coastal waters and their relevance for iron uptake by phytoplankton: experiments with the diatom Phaeodactylum tricornutum. Marine Ecology Progress Series 220: 73-82.

Spokes, L., T. Jickells and K. Jarvis (2001). Atmospheric inputs of trace metals to the northeast Atlantic Ocean: the importance of southeasterly flow. Marine Chemistry 76(4): 319-330.

Statham, P. J., Y. Auger, J. D. Burton, P. Choisy, J. C. Fischer, R. H. James, N. H. Morley, B. Ouddane, E. Puskaric and M. Wartel (1993). Fluxes of Cd, Co, Cu, Fe, Mn, Ni, Pb, and Zn through the Strait of Dover into the Southern North-Sea. Oceanologica Acta 16(5-6): 541-552.

Steigenberger, S., J. Klar et al. (2010). Dissolved iron and aluminium distribution in the Iceland and Iminger Basin during D354. In: RRS Discovery D350 and D354 cruise reports. S. Steingenberger. Southampton, University of Southampton, National Oceanography Centre Southampton: 304.

Stinchcombe, M. (2010). Inorganic nutrient analysis during D354. In: RRS Discovery D350 and D354 cruise reports. S. Steigenberger. Southampton, University of Southampton, National Oceanography Centre Southampton: 304.

Stolpe, B., L. D. Guo, A. M. Shiller and M. Hassellov (2010). Size and composition of colloidal organic matter and trace elements in the Mississippi River, Pearl River and the northern Gulf of Mexico, as characterized by flow field-flow fractionation. Marine Chemistry 118(3-4): 119-128.

Stolpe, B. and M. Hassellov (2010). Nanofibrils and other colloidal biopolymers binding trace elements in coastal seawater: Significance for variations in element size distributions. Limnology and Oceanography 55(1): 187-202.

Stumm, W. and J. J. Morgan (1981). Aquatic chemistry : an introduction emphasizing chemical equilibria in natural waters. New York, Wiley.

Sunda, W. and S. Huntsman (2003). Effect of pH, light, and temperature on Fe-EDTA chelation and Fe hydrolysis in seawater. Marine Chemistry 84(1-2): 35-47.

Sunda, W. G. (2010). Iron and the Carbon Pump. Science 327(5966): 654-655.

Sunda, W. G. and A. K. Hanson (1987). Measurement of Free Cupric Ion Concentration in Seawater by a Ligand Competition Technique Involving Copper Sorption onto C-18 Sep-Pak Cartridges. Limnology and Oceanography 32(3): 537-551.

Sunda, W. G. and S. A. Huntsman (1992). Feedback Interactions between Zinc and Phytoplankton in Seawater. Limnology and Oceanography 37(1): 25-40.

Sunda, W. G. and S. A. Huntsman (1995a). Cobalt and zinc interreplacement in marine phytoplankton: Biological and geochemical implications. Limnology and Oceanography 40(8): 1404-1417.

Sunda, W. G. and S. A. Huntsman (1995b). Iron Uptake and Growth Limitation in Oceanic and Coastal Phytoplankton. Marine Chemistry 50(1-4): 189-206.

Sy, A. (1988). Investigation of Large-Scale Circulation Patterns in the Central North-Atlantic - the North-Atlantic Current, the Azores Current, and the Mediterranean Water Plume in the Area of the Mid-Atlantic Ridge. Deep-Sea Research Part a-Oceanographic Research Papers 35(3): 383-413.

Tagliabue, A., L. Bopp, J. C. Dutay, A. R. Bowie, F. Chever, P. Jean-Baptiste, E. Bucciarelli, D. Lannuzel, T. Remenyi, G. Sarthou, O. Aumont, M. Gehlen and C. Jeandel (2010). Hydrothermal contribution to the oceanic dissolved iron inventory. Nature Geoscience 3(4): 252-256.

Talley, L. D. and M. S. Mccartney (1982). Distribution and Circulation of Labrador Sea-Water. Journal of Physical Oceanography 12(11): 1189-1205.

Tang, D. G., M. M. Shafer, D. A. Karner, J. Overdier and D. E. Armstrong (2004). Factors affecting the presence of dissolved glutathione in estuarine waters. Environmental Science & Technology 38(16): 4247-4253.

Tappin, A. D., D. J. Hydes, J. D. Burton and P. J. Statham (1993). Concentrations, Distributions and Seasonal Variability of Dissolved Cd, Co, Cu, Mn, Ni, Pb and Zn in the English-Channel. Continental Shelf Research 13(8-9): 941-969.

Tappin, A. D., G. E. Millward, P. J. Statham, J. D. Burton and A. W. Morris (1995). Trace-Metals in the Central and Southern North-Sea. Estuarine Coastal and Shelf Science 41(3): 275-323.

Thomas, H., Y. Bozec, H. J. W. de Baar, K. Elkalay, M. Frankignoulle, L. S. Schiettecatte, G. Kattner and A. V. Borges (2005). The carbon budget of the North Sea. Biogeosciences 2(1): 87-96.

Thomas, H., L. S. Schiettecatte, K. Suykens, Y. J. M. Kone, E. H. Shadwick, A. E. F. Prowe, Y. Bozec, H. J. W. de Baar and A. V. Borges (2009). Enhanced ocean carbon storage from anaerobic alkalinity generation in coastal sediments. Biogeosciences 6(2): 267-274.

Thuroczy, C. E., L. J. A. Gerringa, M. B. Klunder, P. Laan and H. J. W. de Baar (2011). Observation of consistent trends in the organic complexation of dissolved iron in the Atlantic sector of the Southern Ocean. Deep-Sea Research Part Ii-Topical Studies in Oceanography 58(25-26): 2695-2706.

Thuroczy, C. E., L. J. A. Gerringa, M. B. Klunder, R. Middag, P. Laan, K. R. Timmermans and H. J. W. de Baar (2010). Speciation of Fe in the Eastern North Atlantic Ocean. Deep-Sea Research Part I-Oceanographic Research Papers 57(11): 1444-1453.

Tian, F., R. D. Frew, S. Sander, K. A. Hunter and M. J. Ellwood (2006). Organic iron(III) speciation in surface transects across a frontal zone: the Chatham Rise, New Zealand. Marine and Freshwater Research 57(5): 533-544.

Tortell, P. D., M. T. Maldonado and N. M. Price (1996). The role of heterotrophic bacteria in iron-limited ocean ecosystems. Nature 383(6598): 330-332.

Try, P. M. and G. J. Price (1995). Sewage and industrial effluents. Waste Treatment and Disposal. R. E. Hester and R. M. Harrison. Letchworth, The Royal Society of Chemistry 17-41.

Turner, A., G. E. Millward, A. J. Bale and A. W. Morris (1992). The Solid-Solution Partitioning of Trace-Metals in the Southern North-Sea - Insitu Radiochemical Experiments. Continental Shelf Research 12(11): 1311-1329.

Turner, D. R., M. Whitfield and A. G. Dickson (1981). The Equilibrium Speciation of Dissolved Components in Fresh-Water and Seawater at 25-Degrees-C and 1 Atm Pressure. Geochimica Et Cosmochimica Acta 45(6): 855-881.

Ussher, S. J., E. P. Achterberg and P. J. Worsfold (2004). Marine Biogeochemistry of Iron. Environmental Chemistry 1(2): 67-80.

Ussher, S. J., P. J. Worsfold, E. P. Achterberg, A. Laes, S. Blain, P. Laan and H. J. W. de Baar (2007). Distribution and redox speciation of dissolved iron on the European continental margin. Limnology and Oceanography 52(6): 2530-2539.

van den Berg, C. M. G. (1982a). Determination of Copper Complexation with Natural Organic-Ligands in Sea-Water by Equilibration with Mno2 .1. Theory. Marine Chemistry 11(4): 307-322.

van den Berg, C. M. G. (1982b). Determination of Copper Complexation with Natural Organic-Ligands in Sea-Water by Equilibration with Mno2 .2. Experimental Procedures and Application to Surface Sea-Water. Marine Chemistry 11(4): 323-342.

van den Berg, C. M. G. (1995). Evidence for Organic Complexation of Iron in Seawater. Marine Chemistry 50(1-4): 139-157.

van den Berg, C. M. G. and J. R. Kramer (1979). Determination of Complexing Capacities of Ligands in Natural-Waters and Conditional Stability-Constants of the Copper-Complexes by Means of Manganese-Dioxide. Analytica Chimica Acta 106(1): 113-120.

Waeles, M., R. D. Riso, J. F. Maguer and P. Le Corre (2004). Distribution and chemical speciation of dissolved cadmium and copper in the Loire estuary and North Biscay continental shelf, France. Estuarine Coastal and Shelf Science 59(1): 49-57.

Wagener, T., E. Pulido-Villena and C. Guieu (2008). Dust iron dissolution in seawater: Results from a one-year time-series in the Mediterranean Sea. Geophysical Research Letters 35(16).

Waite, T. D. (2001). Thermodynamics of Fe in seawater. Biogeochemistry of Iron in Seawater. IUPAC Series on Analytical and Physical Chemistry of Environmental Systems. K. Hunter and D. Turner, Wiley. 7: 250-284.

Wells, M. L., N. M. Price and K. W. Bruland (1995). Iron Chemistry in Seawater and Its Relationship to Phytoplankton - a Workshop Report. Marine Chemistry 48(2): 157-182.

Wells, M. L., C. G. Trick, W. P. Cochlan, M. P. Hughes and V. L. Trainer (2005). Domoic acid: The synergy of iron, copper, and the toxicity of diatoms. Limnology and Oceanography 50(6): 1908-1917.

Witter, A. E., D. A. Hutchins, A. Butler and G. W. Luther (2000). Determination of conditional stability constants and kinetic constants for strong model Fe-binding ligands in seawater. Marine Chemistry 69(1-2): 1-17.

Witter, A. E. and G. W. Luther (1998). Variation in Fe-organic complexation with depth in the Northwestern Atlantic Ocean as determined using a kinetic approach. Marine Chemistry 62(3-4): 241-258.

Wolf-Gladrow, D. A., U. Riebesell, S. Burkhardt and J. Bijma (1999). Direct effects of CO2 concentration on growth and isotopic composition of marine plankton. Tellus Series B-Chemical and Physical Meteorology 51(2): 461-476.

Wu, J. F., E. Boyle, W. Sunda and L. S. Wen (2001). Soluble and colloidal iron in the olgotrophic North Atlantic and North Pacific. Science 293(5531): 847-849.

Wu, J. F. and M. B. Jin (2009). Competitive ligand exchange voltammetric determination of iron organic complexation in seawater in two-ligand case: Examination of accuracy using computer simulation and elimination of artifacts using iterative non-linear multiple regression. Marine Chemistry 114(1-2): 1-10.

Wu, J. F. and G. W. Luther (1995). Complexation of Fe(Iii) by Natural Organic-Ligands in the Northwest Atlantic-Ocean by a Competitive Ligand Equilibration Method and a Kinetic Approach. Marine Chemistry 50(1-4): 159-177.

Wu, J. F. and G. W. Luther (1996). Spatial and temporal distribution of iron in the surface water of the northwestern Atlantic Ocean. Geochimica Et Cosmochimica Acta 60(15): 2729-2741.

Wyatt, N. J., A. Milne, E. M. S. Woodward, A. P. Rees, T. J. Browning, H. A. Bouman, P. J. Worsfold and M. C. Lohan (2014). Biogeochemical cycling of dissolved zinc along the GEOTRACES South Atlantic transect GA10 at 40 S. Global Biogeochemical Cycles 28(1): 44-56.

Yang, R. J. and C. M. G. van den Berg (2009). Metal Complexation by Humic Substances in Seawater. Environmental Science & Technology 43(19): 7192-7197.

Young, J. R., A. J. Poulton and T. Tyrrell (2014). Morphology of Emiliania huxleyi coccoliths on the northwestern European shelf - is there an influence of carbonate chemistry? Biogeosciences 11(17): 4771-4782.

Zeebe, R. E. and D. A. Wolf-Gladrow (2001). CO b2 s in seawater : equilibrium, kinetics, isotopes. Amsterdam ; New York, Elsevier.

Zirino, A. and S. Yamamoto (1972). Ph-Dependent Model for Chemical Speciation of Copper, Zinc, Cadmium, and Lead in Seawater. Limnology and Oceanography 17(5): 661-671.

Zondervan, I., R. E. Zeebe, B. Rost and U. Riebesell (2001). Decreasing marine biogenic calcification: A negative feedback on rising atmospheric pCO(2). Global Biogeochemical Cycles 15(2): 507-516.